



University  
of Glasgow

<https://theses.gla.ac.uk/>

Theses Digitisation:

<https://www.gla.ac.uk/myglasgow/research/enlighten/theses/digitisation/>

This is a digitised version of the original print thesis.

Copyright and moral rights for this work are retained by the author

A copy can be downloaded for personal non-commercial research or study,  
without prior permission or charge

This work cannot be reproduced or quoted extensively from without first  
obtaining permission in writing from the author

The content must not be changed in any way or sold commercially in any  
format or medium without the formal permission of the author

When referring to this work, full bibliographic details including the author,  
title, awarding institution and date of the thesis must be given

Enlighten: Theses

<https://theses.gla.ac.uk/>  
[research-enlighten@glasgow.ac.uk](mailto:research-enlighten@glasgow.ac.uk)

SOME PHOTOCHEMICAL PROPERTIES OF  
FERRIC IRON SOLUTIONS.

ProQuest Number: 10656266

All rights reserved

INFORMATION TO ALL USERS

The quality of this reproduction is dependent upon the quality of the copy submitted.

In the unlikely event that the author did not send a complete manuscript and there are missing pages, these will be noted. Also, if material had to be removed, a note will indicate the deletion.



ProQuest 10656266

Published by ProQuest LLC (2017). Copyright of the Dissertation is held by the Author.

All rights reserved.

This work is protected against unauthorized copying under Title 17, United States Code  
Microform Edition © ProQuest LLC.

ProQuest LLC.  
789 East Eisenhower Parkway  
P.O. Box 1346  
Ann Arbor, MI 48106 – 1346

A THESIS

submitted to

THE UNIVERSITY OF GLASGOW

in fulfilment of the

requirements for the

DEGREE OF DOCTOR OF PHILOSOPHY

by

MALCOLM H. MILLOY

November, 1959.

ACKNOWLEDGMENTS.

The author wishes to express his most sincere thanks to Dr. William Good for his keen interest and valuable guidance throughout this investigation and to acknowledge with gratitude the receipt of a Research Studentship from the Department of Scientific and Industrial Research.

## SUMMARY.

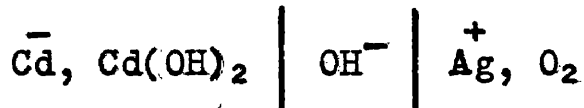
The concentrations of the species  $\text{Fe}^{3+}$ ,  $\text{FeOH}^{2+}$ ,  $\text{Fe(OH)}_2^+$ ,  $\text{Fe}_2(\text{OH})_2^{4+}$ ,  $\text{FeCl}_2^{2+}$  and  $\text{FeCl}_2^+$  in  $1.3 \times 10^{-3}$  M ferric chloride solutions of pH between 2.20 and 2.94 at 20°C have been calculated. These solutions were found to be photo-active and absorption of light in the region 300 to 400  $\mu\text{m}$  is attributed to the species  $\text{FeOH}^{2+}$  and  $\text{Fe(OH)}_2^+$ . The molar extinction coefficients and absorption fractions of the absorbing species were calculated from optical density measurements, the absorption fraction of the species  $\text{FeOH}^{2+}$  being of the order of 0.8.

Experimental evidence is given to show that in the absence of added substrate, the ferric iron is photochemically reduced to ferrous while water is oxidised to oxygen in accordance with the stoichiometry of the equation



The oxygen was estimated quantitatively

(a) in the gas phase employing the sensitive Hersch galvanic cell



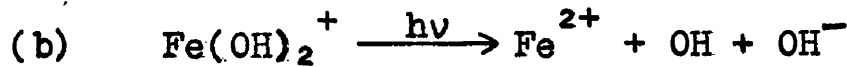
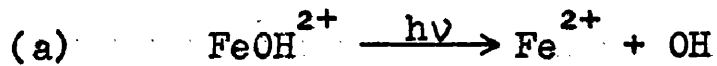
the oxygen being first removed from solution to the gas phase by nitrogen. The potential drop across this cell is proportional to the concentration of oxygen in the gas surrounding the silver electrode.

(b) in the liquid phase polarographically using a Tinsley MK 19 pen-recording polarograph in conjunction with a dropping mercury electrode at which the oxygen was reduced. The photoproduced oxygen was identified by its characteristic double wave polarogram.

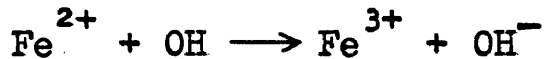
The ferrous ion was estimated colorimetrically by 2-2' dipyridyl, the ferrous-dipyridyl complex having a peak absorption in the region of 520 m $\mu$ .

The following reaction scheme is proposed to account for the experimental results :-

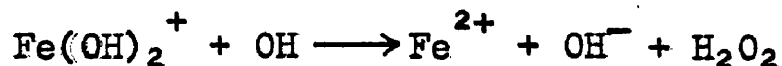
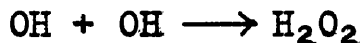
Primary reactions :



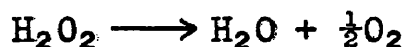
followed by the back reaction :



Formation of hydrogen peroxide by one or more of the following steps :



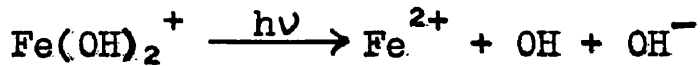
Decomposition of the hydrogen peroxide by iron catalysis :



The quantum yield of ferrous ion formation is  $\phi_{\text{max}} = 0.05$ .

The effect of light intensity and pH on the initial rate of ferrous ion formation was investigated.  $\frac{d\text{Fe}^{2+}}{dt} \propto I^n$  where n increases from 0.32 at pH 2.20 to 0.73 at pH 2.94. For a fixed light intensity,  $\frac{d\text{Fe}^{2+}}{dt}$  increases steadily with increasing pH in the pH range 2.10 to 2.90, and then much more rapidly to reach a maximum between 2.94 and 2.98; thereafter, the reduction rate decreases as the pH is increased from 2.98 to 3.70. The quantum yield  $\phi_{\text{Fe}^{2+}}$  increases with increasing pH in the range 2.10 to 2.94 and at any particular pH, increases with decreasing light intensity.

Light was observed to initiate and accelerate the process of secondary hydrolysis of the iron to  $\text{Fe(OH)}_3$  as compared with the dark hydrolysis. It is proposed that the reaction



is mainly responsible for the phenomenon. The effect of hydrogen peroxide and glucose on the light and dark hydrolysis was studied. Hydrogen peroxide was found strongly to diminish the acceleration of the hydrolysis produced by light.

The decomposition of hydrogen peroxide in  $1.3 \times 10^{-3} \text{ M}$  solutions of ferric chloride and ferric nitrate was investigated. The peroxide decomposed slightly faster in the

ferric chloride than in the ferric nitrate solution, and in both cases the decomposition appeared to take place in a sequence of first order steps.

---

## I N D E X

---

	<u>Page.</u>
General Introduction.....	1
Part 1. The Photo-active Species in $1.3 \times 10^{-3}$ M..... Ferric Chloride Solutions.	22
Part 2. The Detection and Quantitative Determination.. of Photochemically Produced Oxygen	44
Section A. Estimation of Oxygen using the..... Hersch Galvanic Cell.	47
Section B. The Polarographic Estimation of..... Photochemically Produced Oxygen.	65
Part 3. The Variation with Light Intensity and..... pH, of the Initial Rate of Photochemical Reduction of Ferric Chloride Solutions. The Quantum Yield of the Reaction.	98
Part 4. The Effect of Light on the Hydrolysis.....	122
Part 5. The Decomposition of Hydrogen Peroxide..... in $1.3 \times 10^{-3}$ M Ferric Chloride Solutions.	147
Bibliography.....	157

---

GENERAL INTRODUCTION.

Free Radicals.

As a result of investigations of line and band spectra, the transitory existence, under suitable conditions, of free atoms and radicals such as H, Cl, OH, CH, etc., has been recognized for some time. The short life of these radicals is not due to instability but rather to their high reactivity which results in their rapid reaction with themselves or other substances present.

The possibility that free atoms might take part in chemical reactions was first realized when chain mechanisms were postulated to account for the large quantum yields of certain photochemical reactions e.g. of that between hydrogen and chlorine. Free radical mechanisms were similarly introduced when Taylor<sup>1</sup> proposed a chain mechanism involving ethyl free radicals for the mercury photosensitized hydrogenation of ethylene. Since then, the vast amount of work that has been done on reaction kinetics has shown that many thermal and most photochemical reactions proceed to some extent by free radical mechanisms. The existence of free radicals is generally deduced from kinetic measurements, spectroscopy, electrical conductivity, magnetic susceptibility, etc.

The monographs of Steacie<sup>2</sup> and Waters<sup>3</sup> are mainly concerned with organic free radicals. The review by Uri<sup>4</sup>,

"Inorganic Free Radicals in Solution", deals with reactions which involve inorganic ions or radicals in the primary steps. A Special Publication<sup>5</sup> by the Chemical Society gives an account of many free radical reactions in the gas phase, while the monograph by Semenov<sup>6</sup> includes a wealth of structural and thermodynamic numerical data relating to free radicals. Free radicals and their reactions which are relevant to the present work are discussed below followed by a general survey of the photochemistry of ferric iron solutions.

The OH and HO<sub>2</sub> radicals and the O<sub>2</sub><sup>-</sup> radical-ion.

Bonhoeffer and Haber<sup>7</sup>, Farkas, Goldfinger and Haber<sup>8</sup>, and Haber<sup>9</sup> postulated the OH radical in the reaction between hydrogen and oxygen. In the decomposition of water vapour, its occurrence was assumed by Bonhoeffer and Reichardt<sup>10</sup>.

Urey, Dawsey and Rice<sup>11</sup> postulated the OH radical in a study of the absorption spectrum of hydrogen peroxide in the gas phase and in solution. That OH radicals have quite long lives was shown by Oldenberg<sup>12</sup> who used a spectrophotometric method of determining the rate of disappearance in discharge tubes. The absorption spectrum of OH radicals in the gas phase was further investigated by Oldenberg and Reike.<sup>13</sup>

Since Haber<sup>9</sup> first suggested that the HO<sub>2</sub> radical might be involved in the reaction between hydrogen and oxygen, HO<sub>2</sub>

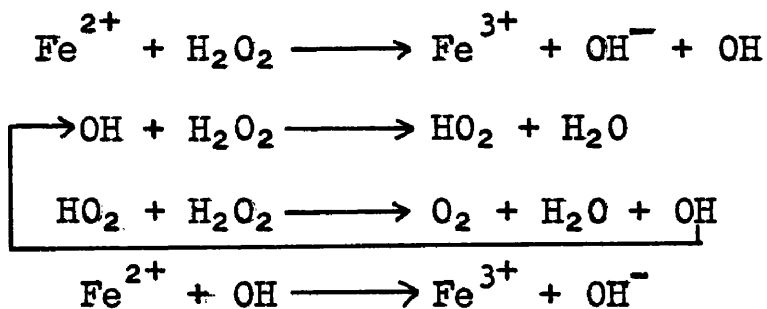
has been postulated as an intermediate in many reactions. The existence of the radical is supported by considerable chemical evidence and theoretical discussion<sup>14</sup>. The photochemical formation of hydrogen peroxide from hydrogen and oxygen (whether sensitized by mercury or not) was claimed by Bates and Salley<sup>15</sup> to involve HO<sub>2</sub> radicals. The gas phase reaction of hydrogen and oxygen above 400°C provided stronger evidence for the existence of HO<sub>2</sub><sup>16</sup>. Geib and Harteck<sup>17</sup> included HO<sub>2</sub> radicals in a mechanism for the reaction of atomic hydrogen and molecular oxygen at low temperatures and pressures. Bodenstein and Schenk<sup>18</sup> suggested that the inhibition of the hydrogen - chlorine reaction by oxygen is due to the formation of HO<sub>2</sub> radicals which react with hydrogen and chlorine. This theory was supported by the work of Farkas and Sachsse<sup>19</sup> on the recombination of hydrogen atoms; they found that at pressures above 200 mm., hydrogen atoms react with oxygen to give HO<sub>2</sub> in termolecular collisions. Minkoff<sup>20</sup> has reviewed the evidence for the existence of the HO<sub>2</sub> radical in the gas phase and, more recently, Gray<sup>21</sup> has reviewed and re-evaluated much of the thermochemical data relating to OH and HO<sub>2</sub> radicals.

The O<sub>2</sub><sup>-</sup> ion is the anion of MO<sub>2</sub>. Potassium superoxide which was originally given the structure M<sub>2</sub>O<sub>4</sub>, is paramagnetic and the X-ray study of its crystal structure by Helms and

Klemm<sup>22</sup> revealed that the correct formula is  $M\text{O}_2$  ( $M$  = potassium, rubidium, or caesium). This was confirmed by Kassatochkin<sup>23</sup> who with Kotov<sup>24</sup> had previously suggested the structure  $\text{MO}_2$ . In aqueous solution the  $\text{HO}_2$  radical is dissociated into  $\text{H}^+$  and  $\text{O}_2^-$  ions.

### The Catalytic Decomposition of Hydrogen Peroxide.

The work of Haber and Weiss<sup>25</sup> on the catalytic decomposition of hydrogen peroxide by ferrous and ferric ion was the first in which a complete reaction mechanism was based on OH and  $\text{HO}_2$  radicals in solution as intermediate entities. Their original scheme for the reaction of ferrous ion and hydrogen peroxide is as follows :-

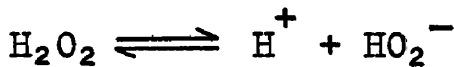


The catalytic decomposition of hydrogen peroxide is thus a chain reaction with OH and  $\text{HO}_2$  radicals acting as chain carriers, accompanied by the oxidation of ferrous ion. In the ferric ion catalysis, the primary step proposed by Haber and Weiss is :-

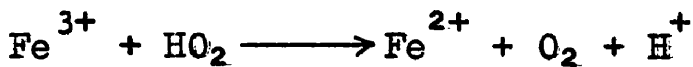


in which the reactive state of the hydrogen peroxide is the

anion  $\text{HO}_2^-$  the concentration of which is related to that of the peroxide by

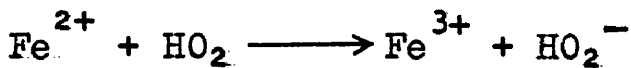


This was supported by the observation that the rate constant was proportional to the concentration of ferric ion and hydrogen peroxide and inversely proportional to the acidity. Subsequently oxygen would be evolved either by a chain reaction as in the ferrous ion catalysis or a reaction of ferric ion with the  $\text{HO}_2$  radical:

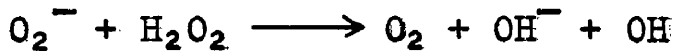


Later it was suggested by Weiss<sup>26</sup> that the  $\text{HO}_2$  radical is dissociated in aqueous solution into  $\text{H}^+$  and  $\text{O}_2^-$  ions and that it is the latter which reacts with the hydrogen peroxide rather than the  $\text{HO}_2$  radical.

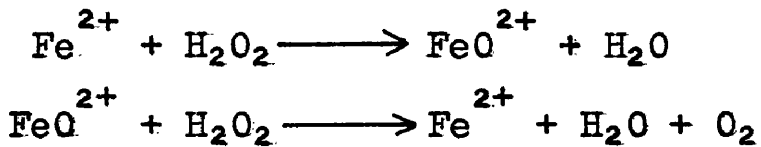
Evans, Hush and Uri<sup>27</sup> suggested a pK value of ~2 for the dissociation of  $\text{HO}_2$  in aqueous solution, so that in slightly acid solution both species  $\text{HO}_2$  and  $\text{O}_2^-$  will be present.  $\text{HO}_2^-$  reacts as an oxidising agent, the reduction product being  $\text{HO}_2^-$



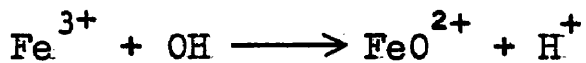
and  $\text{O}_2^-$  as a reducing agent, the oxidation product being  $\text{O}_2$



Bray and Gorin<sup>28</sup> suggested an alternative chain mechanism to that of Haber and Weiss, involving the formation of ferryl ion (tetravalent iron):



This mechanism was later revived by Medalia and Kolthoff<sup>29</sup> but it was pointed out by Uri<sup>30</sup> that it was unlikely on the principle that reactions for which no simple mechanism involving only bond breaking and electron transfer can be devised are less probable. The formation of ferryl ion by a different mechanism was suggested by Barb, Baxendale, George and Hargrave<sup>31, 32</sup> :-



but these authors are not convinced that the experimental evidence for its occurrence is conclusive.

George<sup>33</sup> investigated the reaction of potassium super-oxide,  $\text{KO}_2$  (the salt of the  $\text{HO}_2$  radical) in hydrogen peroxide solution but did not observe any chain reaction even with 99% hydrogen peroxide, which seemed to indicate that there was no reaction of the  $\text{HO}_2$  radical or  $\text{O}_2^-$  ion with hydrogen peroxide as proposed by Haber and Weiss. Agar and Dainton<sup>34</sup> however, consider that George's conclusions are invalid since the high alkalinity at the  $\text{KO}_2$ /solution interface would tend to inhibit the reaction between peroxide and  $\text{O}_2^-$  ions and the latter could disappear by a different mechanism before their diffusion into the bulk of the solution.

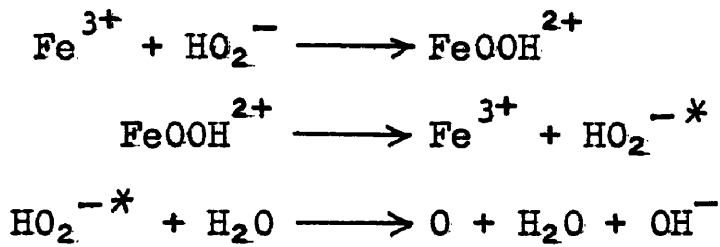
An important modification of the original Haber-Weiss

mechanism was put forward almost simultaneously by Barb et al.<sup>35</sup>, Weiss and Humphrey<sup>36</sup>, and Medalia and Kolthoff<sup>29</sup>. It was shown by these authors that the main step leading to oxygen evolution is not that of  $\text{HO}_2$  with hydrogen peroxide, but  $\text{HO}_2^-$  or  $\text{O}_2^-$  with ferric ion :



This applies not only to the slow decomposition of hydrogen peroxide by ferric ion, for which Haber and Weiss have already suggested the above reaction, but also to the oxygen burst in the reaction of ferrous ion and hydrogen peroxide.

Andersen<sup>37</sup> observed that with lower peroxide/ferric ion concentration ratios, deviations from first order decomposition occur and proposed a mechanism later revised by Christiansen and Andersen<sup>38</sup>, to explain it :



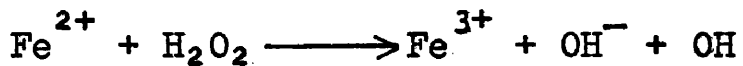
Uri<sup>4</sup> claims that this scheme is unacceptable since the formation of an excited  $\text{HO}_2^{-*}$  ion in a thermal reaction seems improbable while the formation of oxygen atoms in the reaction between ferric ion and  $\text{HO}_2^-$  ion is energetically impossible. However, Barb et al.<sup>31, 32</sup>, and Weiss<sup>39</sup> show that Andersen's results can be accounted for by assuming that the catalytic

decomposition of hydrogen peroxide by ferric ion is a chain reaction produced by the small but measurable stationary concentration of ferrous ion.

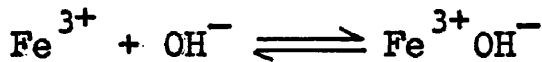
Uri<sup>40</sup> suggested that an important reaction in the Haber-Weiss mechanism had been overlooked viz.



This is the back reaction of the primary step of the Haber-Weiss mechanism and is analogous to the reaction  $\text{Ce}^{4+} \text{OH}^- + \text{OH}$  postulated by Evans and Uri<sup>41</sup> in the photo-oxidation of water by ceric ions. Haber and Weiss had formulated the forward reaction as



so that the back reaction would have involved termolecular collisions since the equilibrium



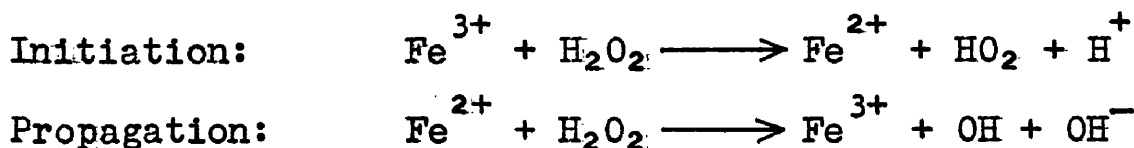
was not visualised at that time. By modifying the results of Barb et al. and Weiss to include this reaction, Uri was able, more satisfactorily, to account for Andersen's results.

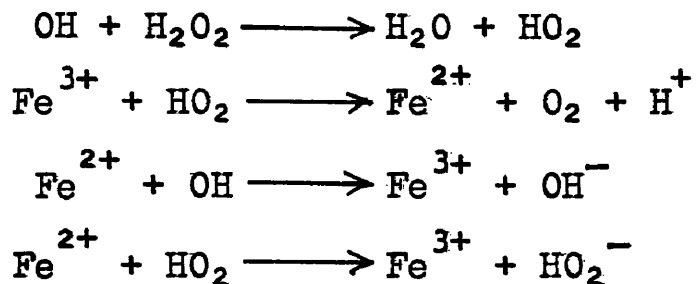
More recently, Cahill and Taube<sup>42</sup>, from experiments with heavy oxygen O<sup>18</sup>, have established that in the ferric ion - hydrogen peroxide reaction, the oxygen formed is derived only from the hydrogen peroxide. They proposed a reaction scheme involving tetravalent iron and the complexes  $\text{FeO}_2\text{H}^{3+}$  and  $\text{FeO}_2\text{H}^{2+}$ . Abel<sup>43</sup> postulates a mechanism involving an  $\text{FeO}_2\text{H}^+$

complex while Koefoed<sup>44</sup> suggests the existence of the complex  $\text{Fe}_2\text{O}_2\text{H}^{4+}$ .

Jones et al<sup>45</sup>, working on the ferric ion catalysed hydrogen peroxide decomposition, propose a scheme in which the water molecules in the solvation shell of the ferric ion are replaced by molecules of hydrogen peroxide to give ferric-peroxy complexes of the type  $[\text{Fe}(\text{H}_2\text{O})_5(\text{H}_2\text{O}_2)]^{3+}$ . The kinetic of the reaction are compared and are found to be consistent with the radical mechanism originally proposed by Haber and Weiss for the reaction in dilute solution. Finally, Kremer and Stein<sup>46</sup>, also working on the ferric ion reaction, claim to have proved the presence of a complex composed of ferric and  $\text{HO}_2^-$  ions but are unable to decide whether the actual decomposition of hydrogen peroxide proceeds through this complex or whether the latter is simply in equilibrium with ferric ion and hydrogen peroxide.

It is evident from the foregoing diversity of opinion, that the mechanism of the decomposition of hydrogen peroxide catalysed by ferric ion is, as yet, far from understood. However, the following scheme, developed by Barb et al<sup>32</sup>., probably includes the more important reactions in the ferric ion catalysed decomposition.





### Termination:

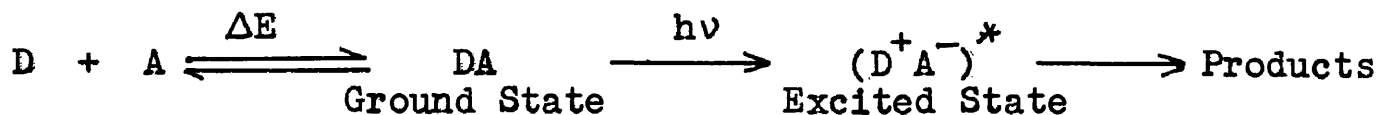
## Charge-Transfer Spectra and Photochemical Oxidation-

## Reduction Reactions.

When an isolated molecule absorbs visible or ultra-violet radiation, an electronic transition occurs which may result in a considerable intramolecular redistribution of charge.

In the review by Orgel<sup>47</sup> transitions involving intermolecular or interionic charge transfer are discussed. These transitions are in fact photochemical oxidation-reduction reactions and it is from this that their importance in chemistry arises.

On absorption of a quantum of light energy, the resulting electronic excitation occurs in a time which is too short to permit any relative movement of particles of atomic dimensions. It therefore follows that before any photochemically stimulated electron transfer can occur, the electron donor D and acceptor A must previously exist in close association. The process can be written:



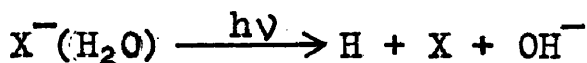
The consequences of the absorption of light will depend upon the nature of D and A.  $D^+$  and  $A^-$  may separate with considerable initial energy which, however, may be lost to solvent molecules so that  $D^+$  and  $A^-$  may return to the ground state without emission of energy and no reaction will be detected. On the other hand,  $D^+$  and  $A^-$  may separate sufficiently to prevent this primary recombination occurring and any subsequent recombination will therefore be in competition with reactions of  $D^+$  and  $A^-$  with added solute, with solvent molecules or with themselves.

Photo-excited electron transfer reactions of inorganic ions in solution are described below.

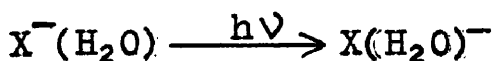
#### (1) Anions.

A characteristic feature of the spectra of anions in aqueous solution is the occurrence of a very strong absorption band in the ultra-violet around 2,000 - 2,500 Å, e.g. the spectra of chloride, bromide and iodide ions show maxima at 1,800, 2,000 and 2,300 Å respectively, with molar extinction coefficients in the range 5,000 - 12,000. Franck and Scheibe<sup>48</sup> were the first to interpret these spectra as charge-transfer bands and suggested that the absorption of light by a hydrated negative ion was accompanied by the formation of a free radical and a hydrated electron which escaped into the bulk of the solution.

Franck and Haber<sup>49</sup> revised this scheme and postulated the primary process



Farkas and Farkas<sup>50</sup>, however, were the first to point out that the primary photochemical process consists of a mere electron transfer from the anion to one of the molecules in the hydration layer :-



The electron could then return to its original orbit or alternatively some permanent chemical change could take place.

## (2) Cations.

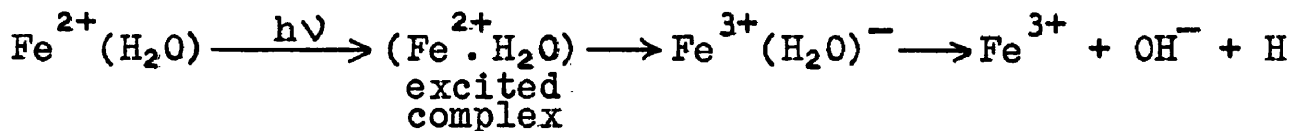
Many cations absorb strongly in the ultra-violet, the main exceptions being the stable alkali metal ions and alkaline earth metal ions which show no charge transfer bands below the limit of observation. The hydrated ions of other metals have been studied by a number of workers, particularly Fromherz and his school<sup>51</sup>.

The nature of the charge transfer process responsible for the cation bands is not as obvious as in the case of anions. In suitable circumstances charge transfer may be expected either from cation to the solvent or vice versa.

It was suggested by Rabinowitch<sup>52</sup>, that with easily oxidised cations the charge transfer absorption of longest wavelength is from the ion to the solvent while with easily reduced

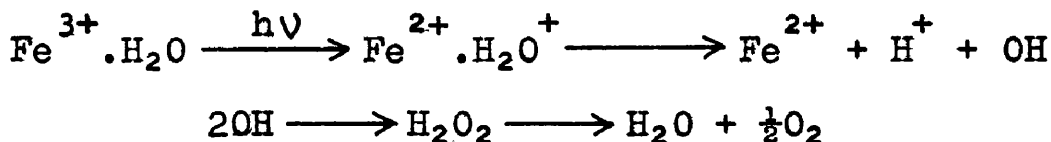
cations it is in the opposite direction.

Potterill, Walker and Weiss<sup>53</sup> observed that water is photoreduced by ferrous ion and represented the primary process by

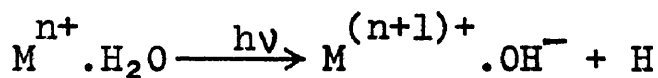


followed by  $2\text{H} \longrightarrow \text{H}_2$

The photo-oxidation of water was reported by Dain and Kachan<sup>54</sup>. The reaction may be written :



The photochemical formation of hydrogen atoms in aqueous solution was extensively studied by Dainton and James<sup>55</sup>. It was shown that the hydrogen atoms formed by photoreduction of water :



initiate the polymerization of vinyl compounds. It seems certain that with these ions the charge transfer process is from bivalent ion to solvent.

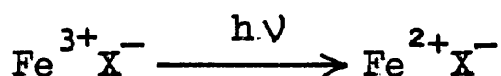
### (3) Cation-Anion Complexes.

Certain cation-anion complexes absorb in the visible or near ultra-violet region and it has been established that the transitions are associated with charge transfer processes.

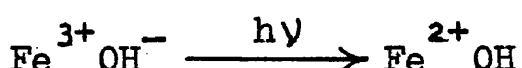
Fromherz<sup>51</sup> determined the spectra of simple binary complexes such as Pb<sup>2+</sup>Cl<sup>-</sup>, Pb<sup>2+</sup>Br<sup>-</sup> and Pb<sup>2+</sup>I<sup>-</sup> by means of the variation of the absorption spectrum with the concentration of the halide ion. The general behaviour agrees well with that predicted for charge transfer spectra, the maximum occurring at the longest wavelengths for the iodides and shortest for the chlorides.

The most widely studied of the inner complexes of transition metals are those of the ferric ion. In a study of the visible spectra of ferric chloride, bromide and hydroxide, Rabinowitch and Stockmayer<sup>56</sup> succeeded in isolating the spectra of each of the Fe<sup>3+</sup>X<sup>-</sup> ions and also those of more complex ions such as FeCl<sub>2</sub><sup>+</sup> and FeCl<sub>3</sub>. The chloride spectra were found to the short wavelength side of those of the bromides, in agreement with the work of Fromherz, while the thiocyanate spectrum measured by Kiss, Abraham and Hegedus<sup>57</sup> was to the longer wavelength side of the bromide.

Rabinowitch<sup>52</sup> proposed that the absorption spectra of ion-pair complexes in general and of ferric ion in particular be interpreted as electron transfer spectra. i.e.



Evans and Uri<sup>58,59</sup>, from work on the energetics of the process



have shown that the repulsion energy between the nuclei in

the complex  $\text{Fe}^{2+}\text{OH}$  is  $\sim 50$  kcal. This value does not vary appreciably from anion to anion so that dissociation of the complex  $\text{Fe}^{2+}\text{X}$  into  $\text{Fe}^{2+} + \text{X}$  would be expected to be a rapid reaction. This was shown from kinetic results later obtained from photopolymerization work. Evans and Uri<sup>59,60</sup> have shown that atoms or radicals produced photochemically from ion-pair complexes can lead to (a) polymerization of vinyl compounds, (b) the oxidation of organic substrates and (c) the photo-oxidation of water. The photochemistry of ferric iron solutions will be discussed under these headings.

(a) The initiation of vinyl polymerization.

Polymerization by photosensitizers based on electron transfer excitation was first described by Evans and Uri<sup>59,60</sup> and later by Evans, Santappa and Uri<sup>61</sup>. These workers, using acrylonitrile, methyl methacrylate and methacrylic acid as monomers, showed that the following ion-pairs are active photosensitizers:-  $\text{Fe}^{3+}\text{OH}^-$ ,  $\text{Fe}^{3+}\text{Cl}^-$ ,  $\text{Fe}^{3+}\text{F}^-$ ,  $\text{Fe}^{3+}\text{N}_3^-$ ,  $\text{Fe}^{3+}\text{C}_2\text{O}_4^{2-}$ ,  $\text{Fe}^{3+}\text{HCitr}^{2-}$ ,  $\text{Pb}^{2+}\text{Cl}^-$  and  $\text{Ce}^{4+}\text{OH}^-$ . In the case of  $\text{Fe}^{3+}\text{Cl}^-$  and  $\text{Fe}^{3+}\text{F}^-$ , the polymers were found to contain Cl and F end-groups respectively. The dependence of the quantum yield on the light intensity, light absorption fraction, and the concentration of vinyl monomer and ferrous ion added initially was investigated. It was observed that with regard to

$dFe^{2+}/dt$ , the quantum yield is dependent on the species used as initiator: the maximum values obtained at 25°C were:- 0.05 for  $Fe^{3+}OH^-$ , 0.13 for  $Fe^{3+}Cl^-$ , and 0.5 for  $Fe^{3+}N_3^-$ . A complete mechanism both with regard to the formation of free radicals and the polymerization reaction was evolved.

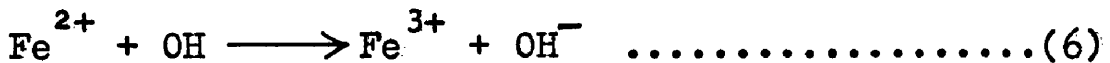
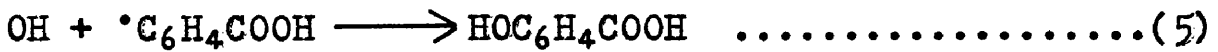
More recently, Dainton and Tordoff<sup>62</sup> studied in detail the polymerization of acrylamide photosensitized by the ion-pair  $\text{Fe}^{3+}\text{OH}^-$  and calculated the quantum yield for the primary reaction to be 0.19 which is considerably higher than the corresponding value calculated by Evans, Santappa and Uri.

(b) Oxidation of organic substrates.

It has been known since the middle of last century that photoreduction of ferric ion takes place in the presence of organic substrates. These were organic acids e.g. oxalic<sup>63</sup>, glycollic<sup>64</sup>, etc., sugars<sup>65</sup> and a variety of alcohols<sup>66</sup>.

More recently, Bates, Evans and Uri<sup>67</sup> have investigated the photo-oxidation of benzoic acid to salicylic acid by the ion-pair  $\text{Fe}^{3+}\text{OH}^-$  with light of  $3650 \text{ \AA}$ . A mechanism was postulated which is, in principle, similar to that adopted for the initiation of polymerization reactions:-



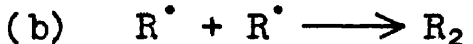
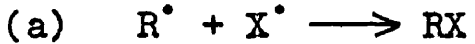


The primary quantum yield was evaluated as  $\sim 0.05$ .

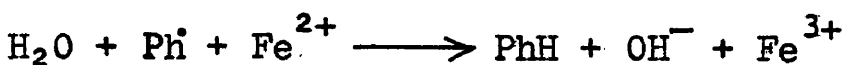
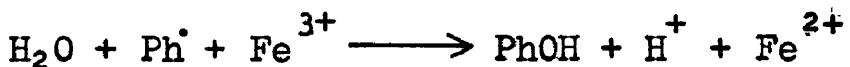
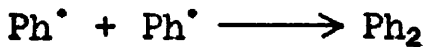
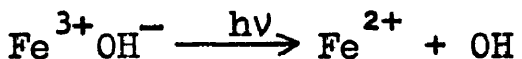
This scheme was later modified by Bates and Uri<sup>68</sup> as a result of work on the photo-oxidation of a number of aromatic substrates by ferric iron complexes. They proposed that the formation of salicylic acid by reaction (5) should be replaced by a reaction of the type



Termination at very low ferric ion concentrations takes place by (a)  $R^\bullet + X^\bullet \longrightarrow RX$



The photo-oxidation of benzene by ferric ion in aqueous solution was investigated by Baxendale and Magee<sup>69</sup> with light of 313 m $\mu$ , the products of the reaction being phenol, diphenyl and ferrous ion. Their observations were found to be in quantitative agreement with the mechanism :

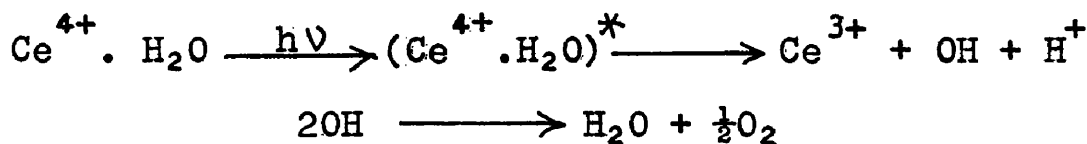


The primary quantum efficiency is 0.13 In similar work on the photo-oxidation of benzene in aqueous ferric chloride

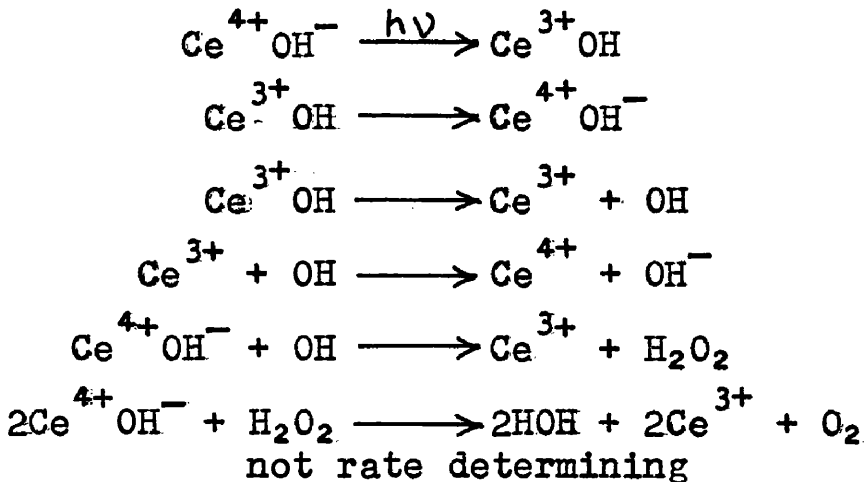
solutions, Korsunovskii<sup>70</sup> calculated a quantum yield of 0.05 for the formation of phenol with light of 366 m $\mu$ .

(c) The photo-oxidation of water.

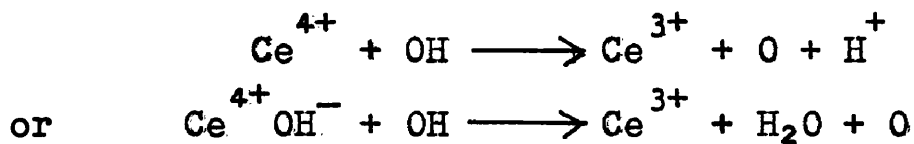
The photo-oxidation of water by ceric ions was studied by Weiss and Porret<sup>71</sup> who proposed a mechanism involving an excited Ce<sup>4+\*</sup> ion.



After carefully re-investigating this reaction, Heidt and Smith<sup>72</sup> attributed the photochemical activity to ceric dimers. Evans and Uri<sup>73</sup>, however, found no evidence of dimerization and suggested that their own results and those of Heidt and Smith are best explained by the following mechanism :

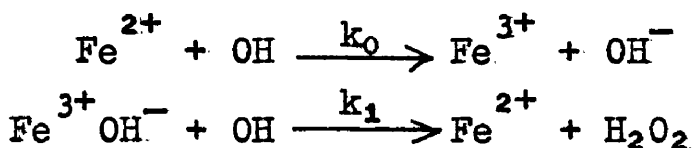


Weiss<sup>74</sup> claimed that it is possible that ceric ions (and other ions of a sufficiently high oxidation potential) could react directly with OH radicals according to



i.e. hydrogen peroxide may not be formed as an intermediate.

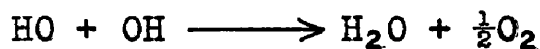
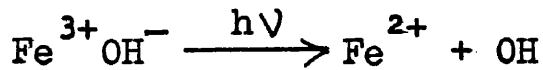
By analogy with the ceric system, Uri<sup>4</sup> considers that in the photo-oxidation of water by ferric ion, the two competing reactions would be



In view of the considerably lower ionization potential of ferrous iron in aqueous solution,  $k_0/k_1$  will be much larger than in the ceric-cerous system. Furthermore, any hydrogen peroxide formed will partially re-oxidise the ferrous ion. Uri is therefore of the opinion that extremely high light intensities and also large  $\text{Fe}^{3+} \text{OH}^-$  concentrations would be required to obtain measurable oxygen yields.

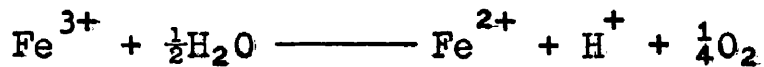
Dain and Kachan<sup>54</sup> however, have measured oxygen evolution from irradiated solutions of ferric perchlorate, quantum yields of the order of  $10^{-3}$  being found. They attributed the photo-activity to the hydrated ferric ion  $\text{Fe}^{3+} \cdot \text{H}_2\text{O}$ . In the course of recent investigations on polymerization<sup>59,61</sup> and oxidation of organic substrates<sup>68,69</sup> initiated by the ion-pair  $\text{Fe}^{3+} \text{OH}^-$ , a small amount of photoreduction of ferric to ferrous ion was found in the absence of added substrate. At first it was suggested by Evans and Uri<sup>59</sup> that this

indicated photo-oxidation of the water to oxygen.

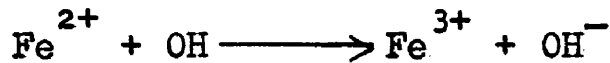
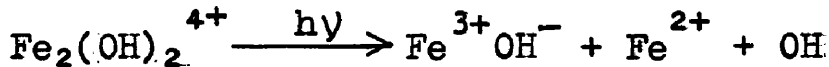


However these workers now attribute this ferrous ion formation to oxidisable organic impurities in the distilled water, presumably because no oxygen was found.

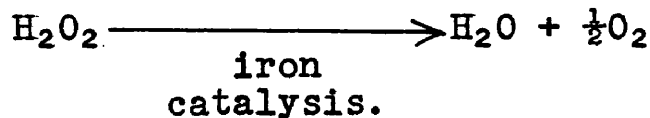
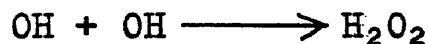
More recently Purdon<sup>75</sup> has shown that with dilute ferric chloride solutions ( $\sim 10^{-3}$  M, pH 2.0 - 3.05) in the absence of added substrate, the water can be photo-oxidised to oxygen by the ferric ion which is reduced to ferrous. The photo-activity is attributed to the dimer  $\text{Fe}_2(\text{OH})_2^{4+}$  and possibly also to the species  $\text{Fe}^{3+}\text{OH}^-$ . The gas evolved was identified as pure oxygen by (a) the phosphor method of Kautsky and Hirsch and (b) sparking with hydrogen, resulting in a 2 - 1 combination. The amount of oxygen was found to accord with the stoichiometry of the equation



The following reaction scheme is proposed :



or



The quantum yield with respect to ferrous ion is 0.026. Purdon also found that light initiates and accelerates the process of secondary hydrolysis of the iron to  $\text{Fe(OH)}_3$ , compared with the dark hydrolysis and suggested that the reaction  $\text{Fe}^{2+} + \text{H}_2\text{O}_2$  is basically responsible for this phenomenon.

The Present Investigation.

The present work is a further investigation of some of the photochemical and associated properties of ferric iron solutions. Since the detection of oxygen and its quantitative relationship to the amount of ferrous ion produced is of major importance in establishing the photo-oxidation of water by ferric ion, it was decided to estimate the oxygen evolved by two entirely independent methods and to determine the primary quantum yield and its variation with pH and light intensity. Experiments were also carried out on the initiation by light of the secondary hydrolysis of ferric ion and on the catalytic decomposition of hydrogen peroxide which is believed to be formed as an intermediate in the photo-oxidation of water.

PART 1.

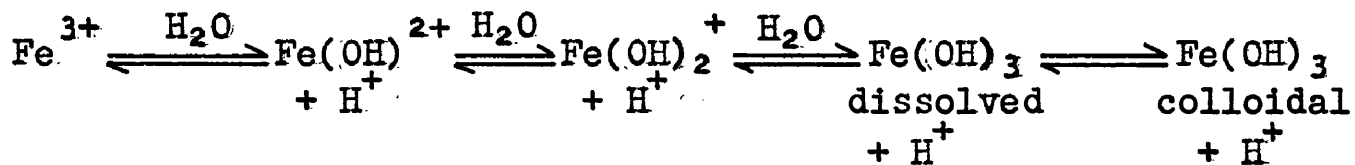
THE PHOTO-ACTIVE SPECIES IN  $1.3 \times 10^{-3}$  M FERRIC CHLORIDE

SOLUTIONS.

## INTRODUCTION.

In solutions of ions which readily form complexes, it is sometimes difficult to decide which species are present and of these which, if any, are photo-active. The relative concentrations of the species will be dependent on many factors, e.g., temperature, ionic strength, pH, etc. The present investigations were carried out with  $1.3 \times 10^{-3}$  M ferric chloride solutions at 20°C and pH 2.94 (a lower pH being obtained by the addition of hydrochloric acid). It is therefore proposed in this section, to calculate from data available in the literature, the quantities of various species which are present (and photo-active) in these solutions.

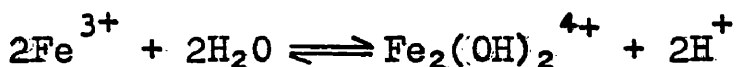
Ferric chloride when dissolved in water, is subject to instantaneous hydrolysis characteristic of the salt of a strong acid and a weak base, the equilibria being represented as follows :



It should be noted that, henceforth, species will generally be given their net charge e.g.  $\text{Fe}^{3+}\text{OH}^-$  will be written  $\text{FeOH}^{2+}$ .

The hydroxy complexes of ferric ion in particular have been studied by a number of workers.<sup>56, 76-80</sup> The existence

of the dimer  $\text{Fe}_2(\text{OH})_2^{4+}$  was first suggested by Hedstrom<sup>81</sup> following an investigation on the hydrolysis products of ferric ion by new e.m.f. methods developed by Biedermann and Sillen<sup>82</sup> for studying complex equilibria. The dimer formation can be represented by :-



Further evidence of dimer formation was subsequently reported by Milburn and Vosburgh<sup>83</sup> and Mulay and Selwood<sup>84</sup> from magnetic and spectrophotometric studies on ferric perchlorate solutions.

With aqueous ferric chloride solutions, the existence of ferric-chloro complexes must also be considered. Rabinowitch and Stockmayer<sup>56</sup> suggested that a solution of ferric chloride could contain all the species  $\text{Fe}^{3+}$ ,  $\text{FeCl}^{2+}$ ,  $\text{FeCl}_2^+$ ,  $\text{FeCl}_3$ ,  $\text{FeCl}_4^-$ ,  $\text{FeCl}_5^{2-}$ , and  $\text{FeCl}_6^{3-}$ , and from an extensive spectrophotometric study of the spectra of ferric perchlorate solutions containing hydrochloric acid, obtained values for the stability constants of  $\text{FeCl}^{2+}$ ,  $\text{FeCl}_2^+$ , and  $\text{FeCl}_3$ .

Olerup<sup>85</sup>, from a similar study but in the ultra-violet region of the spectrum, obtained values which were in good agreement with those of Rabinowitch and Stockmayer. Gamlan and Jordan<sup>86</sup>, from a consideration of previous data and from their own results, conclude that the highest chloro-complex formed has the formula  $\text{FeCl}_4^-$ . Consideration of the data given by

them indicates that under the conditions applying in the present investigations, only the complexes  $\text{FeCl}_2^{2+}$  and  $\text{FeCl}_3^+$  need be considered.

A knowledge of the equilibrium constants of reactions in which the complexes mentioned above are formed, is necessary for a calculation of their concentrations in the solutions at present under investigation. For aqueous solutions, equilibrium constants in general vary principally with the temperature and with the ionic strength  $I$  of the solution where

$$I = 0.5 \sum c_i z_i^2$$

where  $c_i$  is the ionic concentration in mole/litre of solution and  $z_i$  is the valency of the ion concerned. The ionic strength of a  $1.3 \times 10^{-3}$  M ferric chloride solution is thus given by

$$\begin{aligned} I &= 0.5(0.0013 \times 3^2 + 0.0039 \times 1^2) \\ &= \underline{\underline{0.0078}} \end{aligned}$$

The conditions of the present study are therefore :-  
temperature  $20^\circ\text{C}$  and ionic strength 0.0078 .

Equilibrium constants are reported in the literature at a variety of ionic strengths. Bray and Hershey<sup>77</sup> however, have deduced the following relationship from Debye-Hückel theory, for the variation of equilibrium constant with ionic strength:

$$\log_{10} K = \log_{10} K^\circ - \Delta z^2 \cdot f(\gamma)$$

where  $K^o$  and  $K$  are the equilibrium constants at ionic strengths 0 and I respectively.

Z is the charge on each ion in the reaction.

$f(\gamma)$  is a function of the activity coefficients of the ions and at  $25^\circ C$  approaches the limit  $-0.5I^{\frac{1}{2}}$  as  $I^{\frac{1}{2}}$  approaches 0. Bray and Hershey give values of  $f(\gamma)$  at various ionic strengths. It follows that if  $K_1$  and  $K_2$  are the equilibrium constants at ionic strengths corresponding to the functions  $f(\gamma)_1$  and  $f(\gamma)_2$  :-

$$\log_{10}K_1 = \log_{10}K_2 + \Delta Z^2 [f(\gamma)_2 - f(\gamma)_1]$$

and, for example, for a  $1.3 \times 10^{-3}$  M ferric chloride solution where  $I = 0.0078$  and  $f(\gamma)_1 = -0.04$

$$\log_{10}K_1 = \log_{10}K_2 + \Delta Z^2 [f(\gamma)_2 + 0.04]$$

Since this calculation is concerned with a  $1.3 \times 10^{-3}$  M ferric chloride solution, the above equation is used throughout to re-evaluate equilibrium constants for an ionic strength of 0.0078 .

#### Evaluation of Equilibrium Constants.

##### (a) $K_1$ for the complex $\text{FeOH}^{2+}$ .



from which 
$$K_1 = \frac{[\text{FeOH}^{2+}][\text{H}^+]}{[\text{Fe}^{3+}]}$$

$\Delta Z^2$  for this reaction is given by  $2^2 + 1^2 - 3^2 = -4$

showing that  $K_1$  decreases as the ionic strength of the solution increases.

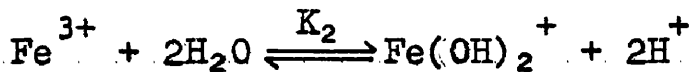
A number of published values of  $K_1$  for  $\text{FeOH}^{2+}$  between 15 and 25°C at various ionic strengths up to 1 are given in Table 1. Only those values which are reported at a definite ionic strength and are based on sound experimental evidence are included. Column 4 in the table gives the values of  $K_1$  recalculated for ionic strength 0.0078 by Bray and Hershey's equation.

TABLE 1

Temp. °C	Ionic Strength	$K_1 \times 10^3$	$K_1 \times 10^3$ recalculated for $I = 0.0078$	Literature Ref. No.
15	0.5	1.18	2.63	87
15	0.5	1.18	2.63	88
18	0.012	2.83	2.95	89
20	1.0	1.80	4.37	90
25	0	6.03	4.17	77
25	0.53	1.74	3.98	91,78,92
25	0.046	2.82	4.07	79
25	0	6.46	4.47	80
25	0	6.76	4.68	83
25	0.5	1.91	4.27	88
25	0.012	4.25	4.57	89

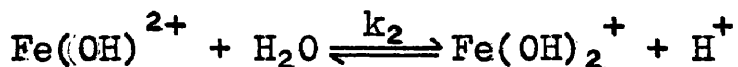
The values calculated for  $K_1$  at  $25^\circ\text{C}$  and  $I = 0.0078$  are seen to be in good agreement. Assuming therefore, that the average value of  $4.32 \times 10^{-3}$  for  $K_1$  at  $25^\circ\text{C}$  is correct, the values  $2.63 \times 10^{-3}$  and  $2.95 \times 10^{-3}$  at  $15^\circ$  and  $18^\circ\text{C}$  are of the right order since  $K_1$  increases with temperature. The value  $4.37 \times 10^{-3}$  for  $K_1$  at  $20^\circ\text{C}$  calculated from Perrin's<sup>90</sup> results is probably slightly high. From a consideration therefore, of the values of  $K_1$  at  $15^\circ$ ,  $18^\circ$ , and  $25^\circ\text{C}$ , a reasonable value for  $K_1$  at  $20^\circ\text{C}$  is  $3.5 \times 10^{-3}$ .

(b)  $K_2$  for the complex  $\text{Fe}(\text{OH})_2^+$



where 
$$K_2 = \frac{[\text{Fe}(\text{OH})_2^+] [\text{H}^+]^2}{[\text{Fe}^{3+}]}$$

$\Delta Z^2$  has the value -6 indicating that  $K_2$  also decreases as the ionic strength increases. In the literature, values are generally reported for  $k_2$  for the reaction



for which  $\Delta Z^2 = -2$ .  $K_2$  can be calculated from the relation

$$K_2 = k_2 \times K_1$$

Published values of  $k_2$  are not as numerous as those of  $K_1$ , but in Table 2 are listed three reliable values, two of which are given at a definite ionic strength.

TABLE 2

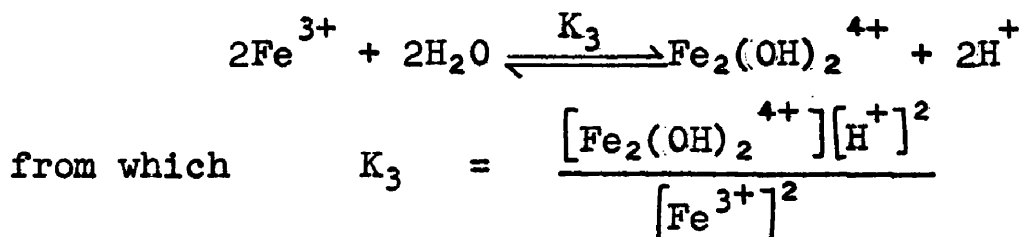
Temp. °C	Ionic Strength	$k_2 \times 10^4$	$k_2 \times 10^4$ recalculated for $I = 0.0078$	Literature Ref. No.
20	1.0	4.95	7.59	90
25	3.0	5.50	8.91	81
25	$\text{SO}_4^{2-}$ various	4.17		93

The three uncorrected values of  $k_2$  are in good agreement, while the corrected value at 25°C is slightly greater than that at 20°C as would be expected. The value of  $k_2$  at 20°C will therefore be taken as  $7.6 \times 10^{-4}$ . Since  $K_1 = 3.5 \times 10^{-3}$  at 20°C (from the previous section),  $K_2$  is obtained from

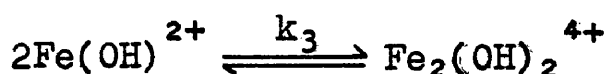
$$K_2 = K_1 \cdot k_2 = 3.5 \times 10^{-3} \times 7.6 \times 10^{-4}$$

i.e.  $\underline{\underline{K_2 = 2.7 \times 10^{-6}}}$

(c)  $K_3$  for the complex  $\text{Fe}_2(\text{OH})_2^{4+}$



$\Delta Z^2 = 0$  showing that for this reaction  $K_3$  is independent of ionic strength. There are a number of results reported for the formation of the dimer according to



for which  $\Delta Z^2 = +8$  indicating that this equilibrium is

strongly dependent on ionic strength, increase in which increases  $k_3$ . If  $k_3$  is known,  $K_3$  can be evaluated from the relation

$$K_3 = (K_1)^2 \cdot k_3$$

Table 3 shows values of  $k_3$  at various temperatures and ionic strengths.

TABLE 3

Temp. °C	Ionic Strength	$k_3$	$k_3$ recalculated for $I = 0.0078$	Literature Ref. No.
20	1.0	431	76	90
25	0	29	60	83
25	3.0	1549	219	81
18	0.1	270	91	89
25	0.1	220	74	89
32	0.1	170	58	89

The last set of results at temperatures 18°, 25° and 32°C indicate that  $k_3$  decreases quite markedly with increase in temperature. However, the increase in  $K_1$  with increase in temperature and the occurrence of  $(K_1)^2$  in the relation

$$K_3 = (K_1)^2 \cdot k_3$$

makes the rate of change of  $K_3$  with temperature, positive.

This is in accordance with the results of Mulay and Selwood.<sup>84</sup>

The value 219 calculated for  $k_3$  from Hedstrom's results is of a higher order than the others. It is suggested that

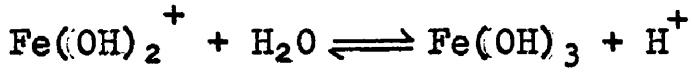
the Bray and Hershey relationship may become less reliable at values of  $\Delta Z^2$  as high as 8, which would account for the (apparently) high value of 219. Since the other three sets of results indicate that  $k_3$  lies between 91 (at  $18^\circ\text{C}$ ) and 60 (at  $25^\circ\text{C}$ ), the value of  $k_3$  at  $20^\circ\text{C}$  will be taken as 80.  $K_3$  can now be evaluated :

$$\begin{aligned} K_3 &= (K_1)^2 \cdot k_3 \\ &= (3.5 \times 10^{-3})^2 \times 80 \\ &= \underline{\underline{9.8 \times 10^{-4}}} \end{aligned}$$

(d) K for the complex  $\text{Fe(OH)}_3$  (dissolved).

There do not appear to be any values of the equilibrium constant for the formation of  $\text{Fe(OH)}_3$  reported in the literature.

By assuming a value of  $4 \times 10^{-7}$  for the equilibrium constant of the reaction



Lamb and Jacques<sup>76</sup>, working on the hydrolysis of  $10^{-2}$  to  $10^{-3}\text{ M}$  ferric chloride solutions, have shown that  $\text{Fe(OH)}_3$  is practically insoluble and as soon as its concentration exceeds about  $2 \times 10^{-9}\text{ M}$ , the original molecular solution transforms itself more or less rapidly into a colloidal solution or suspension. The species  $\text{Fe(OH)}_3$  will therefore be ignored in the present study.

(e)  $K_4$  for the complex  $\text{FeCl}^{2+}$



where  $K_4 = \frac{[\text{FeCl}^{2+}]}{[\text{Fe}^{3+}][\text{Cl}^-]}$

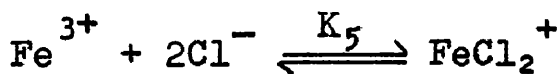
$\Delta Z^2 = -6$  showing that  $K_4$  decreases with increase of ionic strength. Values of  $K_4$  are recorded in Table 4.

TABLE 4

Temp. C	Ionic Strength	$K_4$	$K_4$ recalculated for $I = 0.0078$	Literature Ref. No.
16	0	28.2	16.2	94
20	0	25.7	14.8	95
20	2.0	5.8	23.2	85
25	0	20.0	11.5	77
25	0	30.2	17.4	56
25	0.53	2.3	7.8	91,78,92
25	1.2	4.1	10.0	96

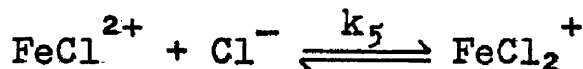
The diversity of values within the range 7.8 to 23.2 suggest that  $K_4$  is not markedly temperature dependent. The average of all the corrected values of  $K_4$  is 14.4, so that of the two values at  $20^\circ\text{C}$ , 14.8 is in line with the others while 23.2 is rather high. The value of  $K_4$  at  $20^\circ\text{C}$  will therefore be taken as 15.0.

(f)  $K_5$  for the complex  $\text{FeCl}_2^+$



where  $K_5 = \frac{[\text{FeCl}_2^+]}{[\text{Fe}^{3+}][\text{Cl}^-]^2}$

In Table 5 are listed values of  $k_5$  for the reaction



for which  $\Delta Z^2 = -4$ .  $K_5$  can be calculated from the relation

$$K_5 = K_4 \cdot k_5$$

TABLE 5

Temp. °C	Ionic Strength	$k_5$	$k_5$ recalculated for $I = 0.0078$	Literature Ref. No.
20	2.0	2.0	5.0	85
25	0	4.5	3.1	56
25	1.2	1.5	3.7	96

The value 5.0 calculated for  $k_5$  at  $20^\circ\text{C}$  from Olerup's<sup>85</sup> results is possibly slightly high (as also was the value for  $K_4$  calculated from his results), since a value nearer 3.0 would be more in line with the values of  $k_5$  at  $25^\circ\text{C}$ . The value of  $k_5$  at  $20^\circ\text{C}$  will therefore be taken as 3.0, whence

$$\begin{aligned} K_5 &= K_4 \cdot k_5 \\ &= 15 \times 3 \\ &= \underline{\underline{45}} \end{aligned}$$

The values of the equilibrium constants which have been evaluated for ionic strength 0.0078 and temperature 20°C are shown together in Table 6, below.

TABLE 6

Equilibrium	Equilibrium Constant
$\text{Fe}^{3+} + \text{H}_2\text{O} \rightleftharpoons \text{FeOH}^{2+} + \text{H}^+$	$K_1 = 3.5 \times 10^{-3}$
$\text{Fe}^{3+} + 2\text{H}_2\text{O} \rightleftharpoons \text{Fe(OH)}_2^+ + 2\text{H}^+$	$K_2 = 2.7 \times 10^{-6}$
$2\text{Fe}^{3+} + 2\text{H}_2\text{O} \rightleftharpoons \text{Fe}_2(\text{OH})_2^{4+} + 2\text{H}^+$	$K_3 = 9.8 \times 10^{-4}$
$\text{Fe}^{3+} + \text{Cl}^- \rightleftharpoons \text{FeCl}^{2+}$	$K_4 = 15.0$
$\text{Fe}^{3+} + 2\text{Cl}^- \rightleftharpoons \text{FeCl}_2^+$	$K_5 = 45.0$

The Concentrations of the Species Present in  $1.3 \times 10^{-3}$  M

Ferric Chloride Solutions at 20°C

pH = 2.94

$$\text{Let total iron} = [\text{Fe}^{3+}]_0 = 1.3 \times 10^{-3} \text{M}$$

$$\text{total chloride} = [\text{Cl}^-]_0 = 3.9 \times 10^{-3} \text{M}$$

$$[\text{H}^+] = 1.1 \times 10^{-3} \text{M}$$

From Table 6, the concentrations of the species to be considered are given by :-

$$[\text{FeOH}^{2+}] = \frac{K_1 [\text{Fe}^{3+}]}{[\text{H}^+]} \quad \dots \dots \dots \quad (1)$$

$$[\text{Fe(OH)}_2^+] = \frac{K_2 [\text{Fe}^{3+}]}{[\text{H}^+]^2} \dots \dots \dots (2)$$

$$[\text{Fe}_2(\text{OH})_2^{4+}] = \frac{K_3 [\text{Fe}^{3+}]^2}{[\text{H}^+]^2} \dots \dots \dots (3)$$

$$[\text{FeCl}_2^{2+}] = K_4 [\text{Fe}^{3+}][\text{Cl}^-] \dots\dots\dots(4)$$

$$[\text{FeCl}_2^+] = K_5 [\text{Fe}^{3+}] [\text{Cl}^-]^2 \dots\dots\dots(5)$$

$$\begin{aligned}
 \text{Now, } [\text{Cl}^-]_0 &= [\text{Cl}^-] + [\text{FeCl}_2^{2+}] + 2[\text{FeCl}_2^+] \\
 &= [\text{Cl}^-] + K_4 [\text{Fe}^{3+}] [\text{Cl}^-] + 2K_5 [\text{Fe}^{3+}] [\text{Cl}^-]^2 \\
 &= [\text{Cl}^-] \left( 1 + K_4 [\text{Fe}^{3+}] + 2K_5 [\text{Fe}^{3+}] [\text{Cl}^-] \right)
 \end{aligned}$$

Since,  $[Fe^{3+}] > 1.3 \times 10^{-3}$  and  $[Cl^-] > 3.9 \times 10^{-3}$

$$K_4[Fe^{3+}] + 2K_5[Fe^{3+}][Cl^-] > 15 \times 1.3 \times 10^{-3} + \\ 2 \times 45 \times 1.3 \times 10^{-3} \times 3.9 \times 10^{-3} \\ > \underline{0.02}$$

$$\therefore 1 + K_4[\text{Fe}^{3+}] + 2K_5[\text{Fe}^{3+}][\text{Cl}^-] \doteq 1$$

$$\therefore [Cl^-]_o \doteq [Cl^-]$$

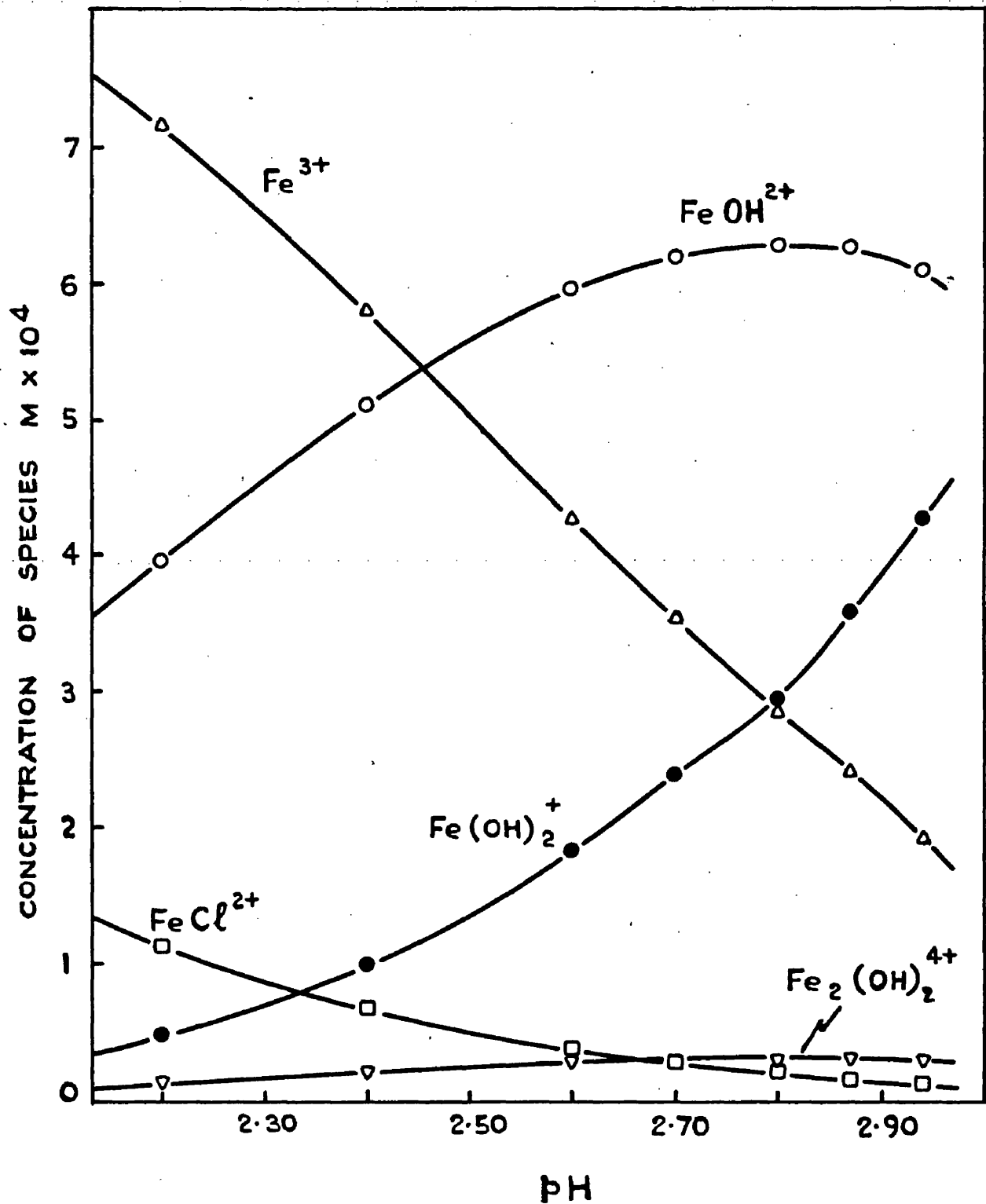
$$[\text{Fe}^{3+}] + [\text{FeOH}^{2+}] + [\text{Fe(OH)}_2^+] + 2[\text{Fe}_2(\text{OH})_2^{4+}] + [\text{FeCl}^{2+}]$$

$$+ [\text{FeCl}_2^+] = [\text{Fe}^{3+}]_0$$

$$\therefore \left[ \text{Fe}^{3+} \right] + \frac{K_1 \left[ \text{Fe}^{3+} \right]}{\left[ \text{H}^+ \right]} + \frac{K_2 \left[ \text{Fe}^{3+} \right]}{\left[ \text{H}^+ \right]^2} + \frac{2K_3 \left[ \text{Fe}^{3+} \right]^2}{\left[ \text{H}^+ \right]^2}$$

$$+ K_4 [Fe^{3+}][Cl^-] + K_5 [Fe^{3+}][Cl^-]^2 = [Fe^{3+}]_a$$

FIG. I



$$\therefore [\text{Fe}^{3+}] + \frac{3.5 \times 10^{-3} [\text{Fe}^{3+}]}{1.1 \times 10^{-3}} + \frac{2.7 \times 10^{-6} [\text{Fe}^{3+}]}{(1.1 \times 10^{-3})^2}$$

$$+ \frac{2 \times 9.8 \times 10^{-4} [\text{Fe}^{3+}]^2}{(1.1 \times 10^{-3})^2} + 15 \times 3.9 \times 10^{-3} [\text{Fe}^{3+}]$$

$$+ 45 \times (3.9 \times 10^{-3})^2 [\text{Fe}^{3+}] = 1.3 \times 10^{-3}$$

$$\therefore 1.62 \times 10^3 [\text{Fe}^{3+}]^2 + 6.472 [\text{Fe}^{3+}] - 1.3 \times 10^{-3} = 0$$

Solving this quadratic gives  $[\text{Fe}^{3+}] = 1.91 \times 10^{-4} \text{ M}$

Substitution for  $[\text{Fe}^{3+}]$  in equations (1), (2), (3), (4) and (5) gives :-

$$[\text{FeOH}^{2+}] = 6.08 \times 10^{-4} \quad [\text{Fe(OH)}_2^+] = 4.26 \times 10^{-4}$$

$$[\text{Fe}_2(\text{OH})_2^{4+}] = 0.30 \times 10^{-4} \quad [\text{FeCl}^{2+}] = 0.11 \times 10^{-4}$$

$$[\text{FeCl}_2^+] = 1 \times 10^{-7}$$

Concentrations of the species at 20°C calculated, as above, for various pH's in the range 2.20 to 2.94 are summarised in Table 7 and shown graphically in Fig. 1. The lower pH's were achieved by the addition of hydrochloric acid (see page 103). The values of the constants are assumed to remain unchanged between pH 2.94 and 2.20 since the ionic strengths of the solutions only change from 0.0078 to 0.014.

TABLE 7

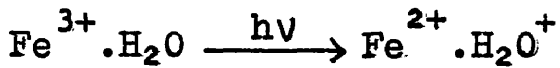
pH	$\text{Fe}^{3+}$	$\text{FeOH}^{2+}$	$\text{Fe(OH)}_2^+$	$\text{Fe}_2(\text{OH})_2^{4+}$	$\text{FeCl}^{2+}$	$\text{FeCl}_2^+$
2.94	1.91	6.08	4.26	0.30	0.11	0
2.87	2.41	6.25	3.57	0.31	0.15	0
2.80	2.85	6.27	2.94	0.32	0.20	0
2.70	3.52	6.18	2.39	0.31	0.27	0
2.60	4.26	5.95	1.83	0.28	0.37	0.01
2.40	5.80	5.10	0.99	0.21	0.67	0.02
2.20	7.15	3.96	0.48	0.13	1.12	0.03

The Photo - active Species in the Present System.

Previous spectrophotometric work on ferric iron solutions has been carried out at such widely varying conditions of ferric iron concentration, pH, temperature, ionic strength, etc., that it is almost impossible to deduce directly from published data, which is the absorbing species in the present system.

According to the spectrophotometric studies of a number of workers<sup>56, 97, 84</sup>, the hydrated ferric ion  $\text{Fe}^{3+} \cdot (\text{H}_2\text{O})_6$  will be inactive with wavelengths greater than 300  $\mu\text{m}$ . On the

other hand, Dain and Kachan<sup>54</sup> working with high light intensities, have shown that if sufficient energy is supplied for the primary process



the hydrated ferric ion may be photo-active. It has been shown by Purdon<sup>75</sup> and also in the present work (page 117), that with light of wavelength above 300 m $\mu$ , the photoreduction of  $1.3 \times 10^{-3}$  M ferric chloride solutions decreases rapidly as the pH is lowered from 2.94 to 2.20. This is contrary to what would be expected if  $\text{Fe}^{3+}(\text{H}_2\text{O})_6$  or any free (hydrated) ferric ion is the photo-active species since Fig. 1 shows that the concentration of ferric ion increases rapidly as the pH is similarly lowered. It therefore seems likely that some ferric iron complex and not  $\text{Fe}^{3+}$  aq. is the photo-active species at 300 m $\mu$  and above.

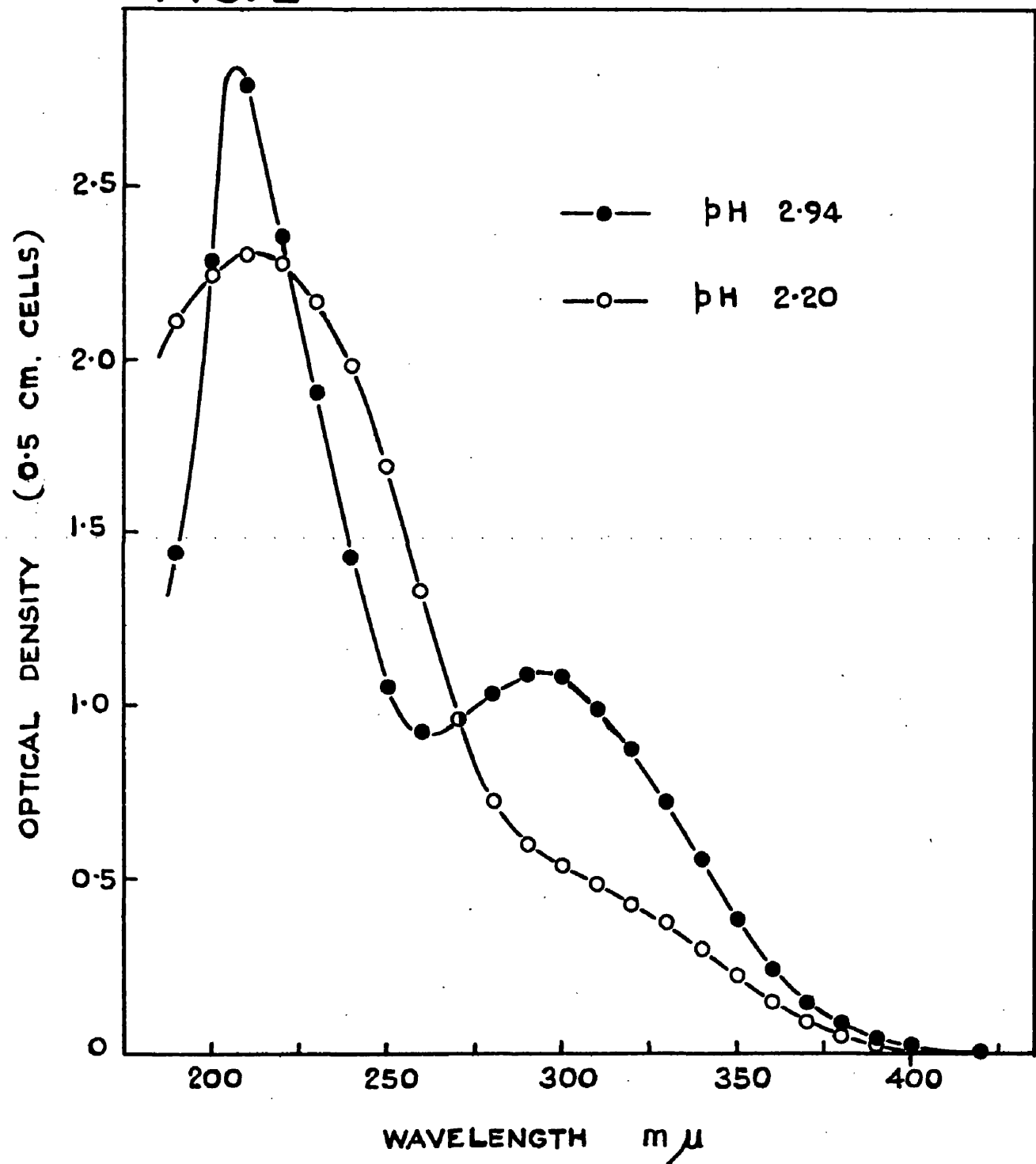
Mulay and Selwood<sup>84</sup>, from spectrophotometric studies on 0.04 M ferric perchlorate and 3 M sodium perchlorate solutions, claim that the absorption band at 240 m $\mu$  obtained with solutions of high acidity ( $\text{pH} < 0$ ) is due solely to  $\text{Fe}^{3+}$ . Solutions within the pH range 0.1 to 1.8 at the same temperature show an additional maximum at 335 m $\mu$  which is claimed to be due almost entirely to the dimer  $\text{Fe}_2(\text{OH})_2^{4+}$ , while the band at 240 m $\mu$  is due to contributions both from  $\text{Fe}^{3+}$  and  $\text{FeOH}^{2+}$ .

It has been shown however, by Milburn and Vosburgh<sup>83</sup> working with light of wavelength 340 m $\mu$ , that absorption by the dimer is significant only in solutions of total ferric concentration greater than  $10^{-3}$  M. It is therefore suggested that in the present system where the total  $[Fe^{3+}] = 1.3 \times 10^{-3}$  M and the molar concentration of  $Fe_2(OH)_2^{4+}$  does not exceed 2.5%, the latter species will make a negligible contribution to the photo-activity of the solutions.

It has been widely accepted by a number of authors<sup>59, 61, 62, 69</sup> that the species  $FeOH^{2+}$  is photo-active in ferric ion solutions of concentration below  $10^{-2}$  M at various pH's. Rabinowitch and Stockmayer<sup>56</sup> have shown that  $FeOH^{2+}$  has a maximum absorption in the region of 325 m $\mu$ , while Olson and Simonson<sup>79</sup> have ascribed the photo-activity of solutions of  $[Fe^{3+}] = 5 \times 10^{-4}$  at pH 2 to 3 in the range 270 to 360 m $\mu$ , to the species  $Fe^{3+}$  and  $FeOH^{2+}$ . Sutton<sup>98</sup> claims that  $FeOH^{2+}$  has a peak absorption at 300 m $\mu$ .

A review of spectrophotometric investigations<sup>95, 56, 85, 86</sup> on ferric-chloro complexes indicates that the species  $FeCl^{2+}$  and  $FeCl_2^+$  have an absorption maximum at 340 m $\mu$ , but that neither of these species is likely to contribute to the photo-activity of the present systems in which their combined concentrations do not exceed 9% at pH 2.20. This is supported by the observation that for the spectral region

**FIG. 2**



300 to 600  $\mu\text{m}$ , the photo-activity of the ferric chloride solutions employed in this work falls off rapidly as the pH is lowered i.e. as the concentrations of  $\text{FeCl}_3^{2+}$  and  $\text{FeCl}_2^+$  increase.

Fig. 2 shows spectral curves for the present system,  $1.3 \times 10^{-3}$  M ferric chloride solution in 0.5 cm. cells at pH's 2.94 and 2.20. Both curves show absorption peaks at 210  $\mu\text{m}$  which are probably due to the species  $\text{Fe}^{3+}$  and  $\text{FeOH}^{2+}$  as proposed by Mulay and Selwood. At 300  $\mu\text{m}$ , the curve for pH 2.94 shows a pronounced maximum while that for pH 2.20 has a point of inflexion. There is no indication of any band at 340  $\mu\text{m}$  at either pH, showing that neither  $\text{FeCl}_3^{2+}$  nor  $\text{FeCl}_2^+$  are absorbing to any significant extent. Further strong evidence that ferric-chloro complexes show no absorption in the solution of pH 2.94 is provided by the fact that the spectral curves for  $1.3 \times 10^{-3}$  M solutions of ferric chloride and ferric nitrate (containing no ferric-chloro complexes) are almost identical over the spectral range 200 to 400  $\mu\text{m}$ .

Since it has been shown that none of the species  $\text{Fe}^{3+}$ ,  $\text{Fe}_2(\text{OH})_2^{4+}$ ,  $\text{FeCl}^{2+}$ ,  $\text{FeCl}_2^+$  absorb in the region 300 - 400  $\mu\text{m}$ , the absorption band at 300  $\mu\text{m}$  must be due to either or both of the species  $\text{FeOH}^{2+}$  and  $\text{Fe}(\text{OH})_2^+$ . Fig. 1 shows that both of these species are present in appreciable concentrations

decreasing with pH, which would account for the decrease in photo-activity as the pH is lowered from 2.94 to 2.20.

The curves have an isosbestic point (point in common) at 272 m $\mu$ , and it has been observed by a number of workers<sup>79, 83, 84</sup> that such a point also exists at 272 m $\mu$  for dilute ferric perchlorate solutions. Olson and Simonson<sup>79</sup> claim that this indicates that the iron is present in only two forms in this region, both of which absorb strongly. This suggests that in the present system both  $\text{FeOH}^{2+}$  and  $\text{Fe(OH)}_2^+$  contribute to the absorption band at 300 m $\mu$ .

It can be seen from Fig. 2 that at 300 m $\mu$  the optical density of the solution of pH 2.20 is half that of the solution of pH 2.94. Now if this were to be explained on the basis of a single absorbing species, the concentration of that species would be expected to decrease by 50% as the pH of the solution drops from 2.94 to 2.20. In actual fact, the concentration of the species  $\text{FeOH}^{2+}$  decreases by only 35% while that of the species  $\text{Fe(OH)}_2^+$  decreases by almost 90%. It will therefore be assumed that in the present system of  $1.3 \times 10^{-3}$  M ferric chloride solutions, both the species  $\text{FeOH}^{2+}$  and  $\text{Fe(OH)}_2^+$  contribute to the absorption in the region 300 to 400 m $\mu$ .

Since all irradiations in the present work were carried out with light of wavelength between 300 and 400 m $\mu$ , this

spectral region is of particular interest and it would therefore be desirable to have some idea of the absorption fractions of the two species. The lower limit of irradiation ( $300 \text{ m}\mu$ ) was achieved either by using 'Pyrex' apparatus which absorbs all light below  $300 \text{ m}\mu$  or by using a light source emitting only wavelengths above  $300 \text{ m}\mu$ . The upper limit of irradiation is  $400 \text{ m}\mu$  simply because the solutions show no absorption above this value.

The Absorption Fractions of the Species  $\text{FeOH}^{2+}$  and  $\text{Fe(OH)}_2^+$

in the Present System.

On the assumption that absorption in the region 300 to  $400 \text{ m}\mu$  is due only to the species  $\text{FeOH}^{2+}$  and  $\text{Fe(OH)}_2^+$ , their molar extinction coefficients at any wavelength can be calculated from the relation :

$$E = \epsilon_1 [\text{FeOH}^{2+}] + \epsilon_2 [\text{Fe(OH)}_2^+]$$

where  $\epsilon_1$  and  $\epsilon_2$  are the molar extinction coefficients of the species  $\text{FeOH}^{2+}$  and  $\text{Fe(OH)}_2^+$  respectively, and E is the optical density of the solution in a 1 cm. cell. Values of E at any particular wavelength can be obtained for the pH's 2.20 and 2.94 from Fig. 2 (remembering to double the values from Fig. 2 to convert to a path length of 1 cm.), while values for  $[\text{FeOH}^{2+}]$  and  $[\text{Fe(OH)}_2^+]$  are obtained from Table 7.

Molar extinction coefficients thus calculated at wavelengths 300 and 340  $\mu\text{m}$  are shown in Table 8.

TABLE 8

$\lambda \text{ mu.}$	Molar Extinction Coefficients	
	$\text{FeOH}^{2+}$	$\text{Fe(OH)}_2^+$
300	2556	1431
340	1446	522

Knowing the molar extinction coefficients, the respective light absorption fractions  $\alpha_1$  and  $\alpha_2$  of the species  $\text{FeOH}^{2+}$  and  $\text{Fe(OH)}_2^+$  may be evaluated from :

$$\alpha_1 = \frac{\epsilon_1 [\text{FeOH}^{2+}]}{\epsilon_1 [\text{FeOH}^{2+}] + \epsilon_2 [\text{Fe(OH)}_2^+]}$$

$$\text{i.e. } \alpha_1 = \frac{\epsilon_1 [\text{FeOH}^{2+}]}{E}$$

$$\text{and } \alpha_2 = 1 - \alpha_1$$

Values of  $\alpha_1$  and  $\alpha_2$  are given in Table 9.

TABLE 9

pH	$\lambda$ m $\mu$	Absorption Fractions	
		$\text{FeOH}^{2+}$	$\text{Fe(OH)}_2^+$
2.94	300	0.72	0.28
	340	0.80	0.20
2.20	300	0.94	0.06
	340	0.96	0.04

The light absorption fractions at either pH are seen to remain fairly constant in the range 300 - 340 m $\mu$ . At both wavelengths, the fraction of light absorbed by  $\text{FeOH}^{2+}$  increases while the fraction absorbed by  $\text{Fe(OH)}_2^+$  decreases with decrease in pH. This was to be expected since Fig. 1 shows that the concentration of  $\text{Fe(OH)}_2^+$  decreases with pH much more rapidly than that of  $\text{FeOH}^{2+}$ .

The mechanism for the absorption of light by these species will be discussed later.

---

PART 2

THE DETECTION AND QUANTITATIVE DETERMINATION OF PHOTO-  
CHEMICALLY PRODUCED OXYGEN.

## INTRODUCTION

Purdon<sup>75</sup> concluded that oxygen but no chlorine is produced in the course of irradiation of  $1.3 \times 10^{-3}$  M ferric chloride solutions. The detection of chlorine was attempted using a starch-iodide method. The oxygen was identified by its property of quenching the phosphorescence of uranin adsorbed on silica gel and quantitatively estimated by Dain and Kachan's<sup>54</sup> technique of degassing the solution by repeated freezing, evacuation, and thawing, before and after irradiation and measuring the evolved gas pressure on a McLeod gauge. Knowing the volume of the system, etc., the increase in pressure after exposure enabled the weight of photochemically produced oxygen to be calculated. By way of confirmation, the gas was sparked with hydrogen and subsequent combination in the volume ratio of 2 of hydrogen to 1 of gas verified that the latter was oxygen. He calculated that the amounts of oxygen and ferrous iron produced in each case were approximately equivalent and thus obtained strong evidence that oxygen is formed by photo-oxidation of the water by the ferric iron.

Irradiation of water was found to produce a small concentration of oxygen but it was concluded that this photo-decomposition of the water took place only to a negligible extent in iron solutions on account of their much higher

optical density. Purdon also observed that the degassing of photo-active iron solutions before irradiation did not seem so effective as with distilled water. For example, after three freezings the pressure of non-condensable gas above the water had dropped to about  $10^{-4}$  mm., whereas a  $1.3 \times 10^{-3}$  M ferric chloride solution at pH 3.05 showed a pressure of not less than  $4 \times 10^{-3}$  mm. and a further freezing made no difference. By varying the pH and age of the solution, it appeared that the difficulty of degassing a solution varied directly as its photoreducibility. The possibility of thermal oxidation of the water by ferric ion was ruled out since no ferrous ion could be detected, and no satisfactory explanation of the phenomenon was found.

Since the detection of oxygen is most important in establishing that water and not impurity in the water is oxidised by the ferric iron, some further evidence obtained by an entirely different method was considered desirable. This section of the thesis describes how oxygen was detected and estimated in irradiated aqueous solutions of ferric chloride by two entirely independent methods. The other product of photolysis, ferrous ion, was found to be produced in the same equivalent concentration as the oxygen.

The conventional methods of gas analysis based on such factors as chemical absorption, heat of combustion, thermal

conductivity, paramagnetism and so forth, all require cumbersome apparatus and are unreliable and even impracticable when the oxygen is present only in traces. Recently, however, Hersch<sup>99</sup> has described a highly specific and sensitive galvanic cell for determining molecular oxygen in the gas phase. The method is based on the cathodic reduction of oxygen and permits the accurate determination of oxygen in concentrations less than 1 vol. per million in, for example, hydrogen, nitrogen, argon, etc. By using pure nitrogen to scrub the oxygen out of the solutions, the Hersch cell was employed in the present study.

To confirm the results obtained from the gas phase determination, the oxygen was then estimated polarographically in the liquid phase using a Tinsley MK 19 pen-recording polarograph in conjunction with a dropping mercury electrode at which the oxygen was reduced. While eminently suitable for this investigation, the polarographic method is not as sensitive as the Hersch method and under certain conditions has the added disadvantage that reducible substances in the solution other than oxygen, can interfere.

SECTION A

ESTIMATION OF OXYGEN USING THE HERSCH  
GALVANIC CELL.

THEORY OF THE METHOD.

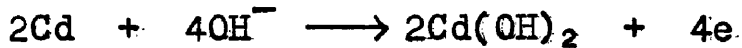
It is well known that gaseous oxygen can be produced by the electrolysis of a suitable electrolyte and that the rate of gas evolution is proportional to the current. The Hersch cell is based on the reverse reaction in which oxygen is absorbed on one of the electrodes to produce a current which is a function of the oxygen concentration in the gas, within certain concentration ranges.

The cell comprises an electrode which is not attacked by the electrolyte in either the presence or absence of oxygen and which is partly exposed to the gas, and a base-metal electrode readily attacked by the electrolyte in the presence of oxygen but not attacked in its absence. When the electrolyte is alkaline (e.g. potassium hydroxide solution) the unattackable electrode is preferably of silver and the base-metal electrode of lead, arsenic, antimony, antimony amalgam or cadmium; when the electrolyte is acid (e.g. sulphuric acid solution) the unattackable electrode is preferably of gold and the base-metal electrode of copper. The cell employed in this work had silver and cadmium electrodes with a 34% w/v. potassium hydroxide solution as electrolyte.

Oxygen is absorbed on the silver and reduced to hydroxyl ion :



The silver is therefore the positive electrode. The cadmium is oxidised to cadmium hydroxide :-



The cadmium is therefore the negative electrode.

It is believed that since the silver is partly exposed to the gas, oxygen molecules are adsorbed on to its surface directly from the gas phase without prior dissolution in the electrolyte. While adsorbed, the molecules travel swiftly towards the line of contact between the silver and the electrolyte where they are reduced to hydroxyl ions. If the silver were completely submerged, the oxygen molecules would have first to dissolve and then in the dissolved state diffuse towards the silver. This is a relatively slow process giving rise to small currents and accounts for the lower sensitivity of the polarographic method in which the oxygen in solution diffuses towards the dropping mercury electrode.

When the electrodes are connected by a suitable resistance such as 2000 ohms, the current flowing in the circuit is proportional to the concentration of oxygen in the atmosphere surrounding the silver, provided this concentration is below a certain limiting value which depends mainly on the dimensions of the particular electrode used. As the concentration rises above this value, proportionality ceases and the current rises less rapidly until it finally becomes

largely independent of oxygen concentration.

The explanation of this behaviour is that at sufficiently low oxygen concentrations, the silver is starved of oxygen which is reduced as soon as it arrives at the line of contact between the silver and electrolyte after adsorption and diffusion on the surface of the silver. Under these conditions, the current is proportional to the rate at which oxygen diffuses from the bulk of the gas towards the silver and this rate in its turn is proportional to the concentration of oxygen in the gas. At higher concentrations however, the current is limited by the rate at which the oxygen is reduced at the line of contact, so that the silver cannot adsorb all the oxygen at its disposal. Gases having an oxygen concentration above the limiting value can therefore be brought into the range of proportionality either by dilution or by lengthening the line of contact between the silver and the electrolyte.

The cadmium is slowly consumed in use and periodically must either be replaced or reconverted to its metallic state by applying a 'charging' current.

## EXPERIMENTAL

### Laboratory Lighting

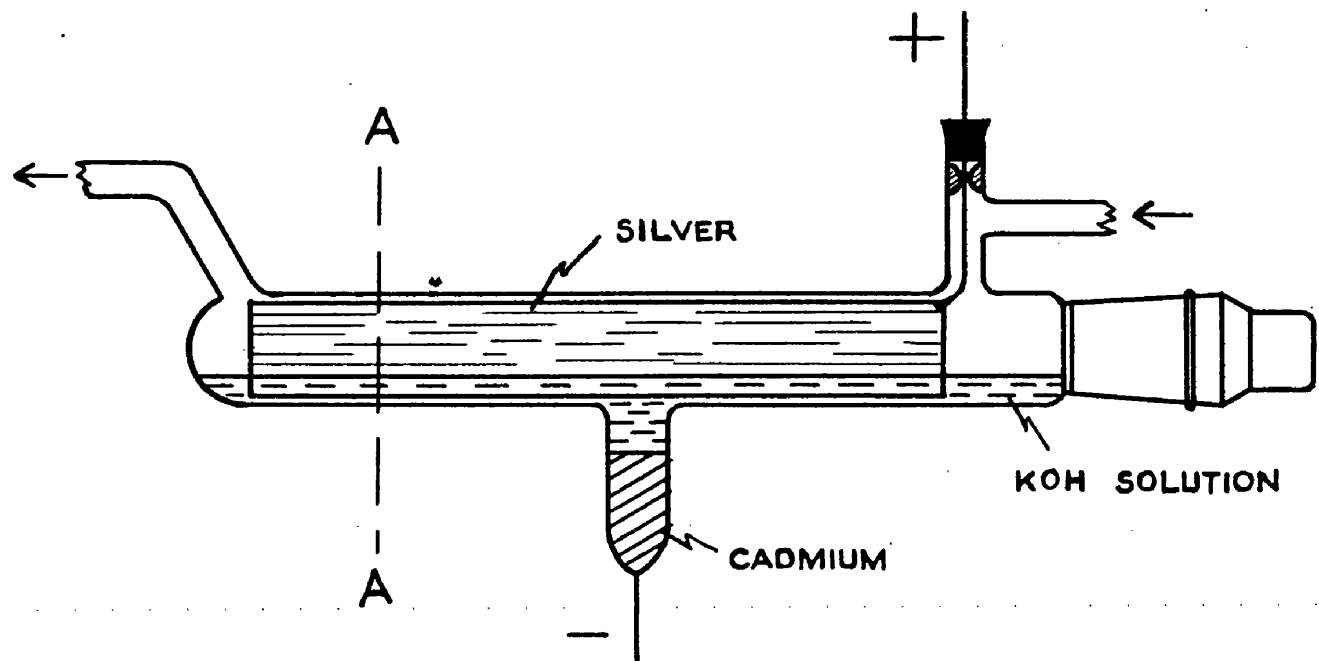
All work was carried out in a darkroom illuminated by Kodak O.B. Safelights (lime yellow).

### The Hersch Cell

In the initial stages of the work, experiments were carried out using a form of cell known as the Hersch dry cell<sup>100</sup>. It consisted of a cadmium rod  $3\frac{1}{2}$ " in length and 0.3" in diameter surrounded by a tube of porous polyethylene impregnated with the electrolyte (34% w/v KOH solution). The porous polyethylene was obtained under the name of "Vyon 3 filter tube" from Pritchett & Gold and E.P.S. Co., Ltd., Dagenham Dock, Essex. The positive electrode in the form of 30" of 22 S.W.G. silver wire, was wound evenly round the porous polyethylene from end to end, a total of about sixty turns. Electrical contact with the cadmium rod was made by fusing platinum wire into one end of the rod, a simple operation since the melting point of cadmium is comparatively low at  $321^{\circ}\text{C}$ . The silver wire was also fused to platinum for the convenience of making glass-platinum seals. The cell was suspended from a glass rod inside the apparatus and the platinum leads taken out through seals in the wall.

The cell, however, was found to be unsatisfactory since

**FIG. 3A**



**HERSCH CELL**

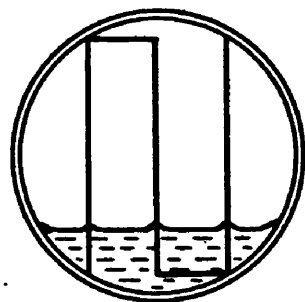
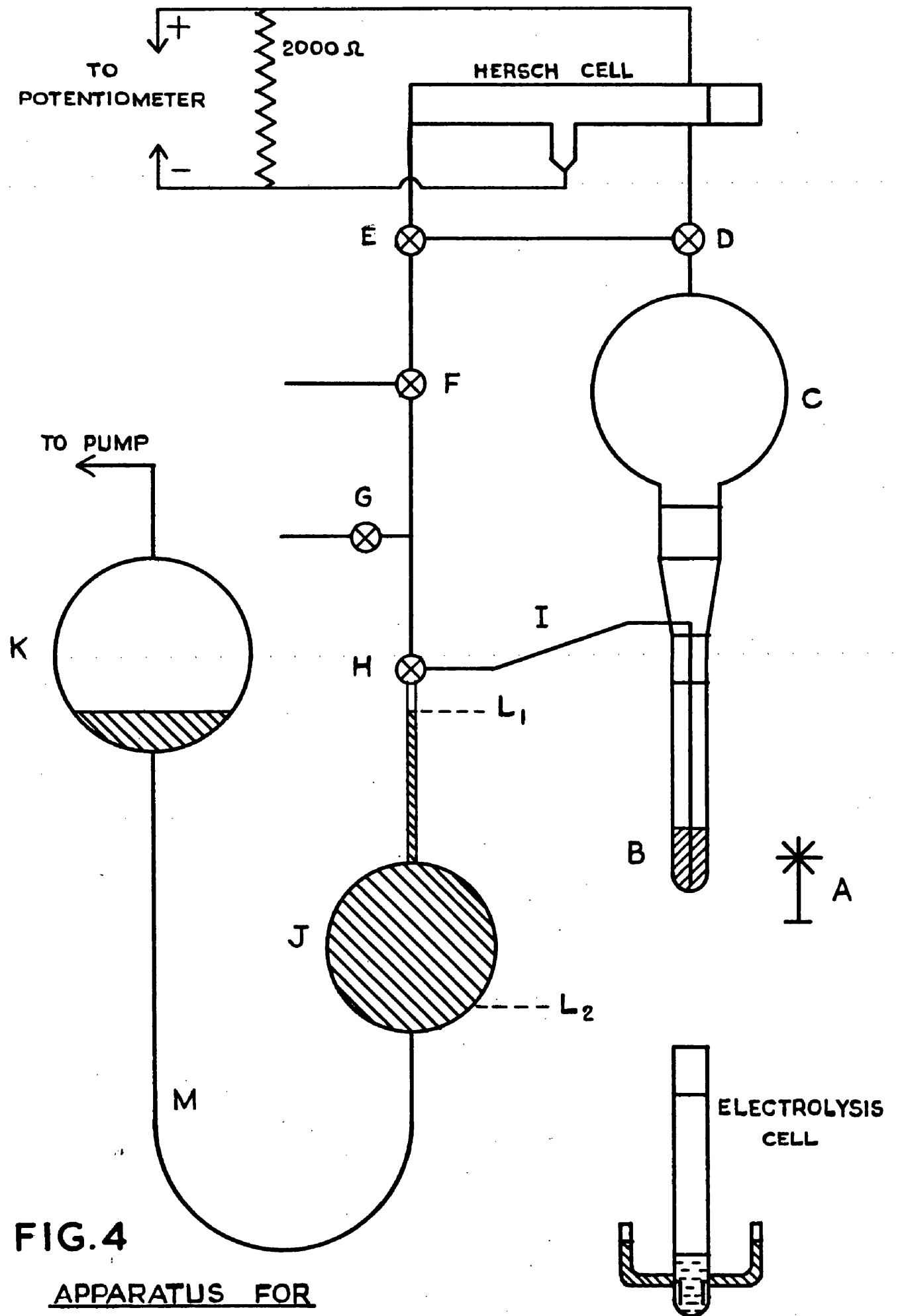


**FIG.3B**

on connecting a resistance across its terminals, a considerable "blank" current was obtained in the absence of oxygen, which made it insensitive to small variations in the oxygen concentration. The porous polyethylene was replaced by a 'Whatman' extraction thimble which fitted firmly over the cadmium rod, but the blank current remained high. No explanation, other than possible impurities in the materials, could be found and the cell was abandoned.

The form of cell finally adopted is shown in Fig. 3a, while Fig. 3b is an enlarged cross-section on the line A - A in Fig. 3a. It comprised a horizontal tube sealed at one end and with a stoppered B 19 socket at the other. The tube had a gas inlet and a gas outlet situated at opposite ends, while the pocket extending downwards in the middle contained a quantity of cadmium metal constituting the negative electrode with which electrical connection was made by a platinum wire sealed into the glass. The platinum-cadmium connection was achieved by first sealing the platinum in through the glass and then melting the cadmium into the pocket under an atmosphere of hydrogen to prevent atmospheric oxidation.

The tube contained the electrolyte (34% w/v KOH solution) which completely covered the cadmium. An N-shaped electrode of sheet silver was partly immersed in the electrolyte, about



three-quarters of its area being exposed. Connection was made to the silver sheet through a silver wire sealed by 'Araldite 101' resin into the gas inlet.

The leads were connected through a 2000 ohm resistance, and the concentration of oxygen in the gas inside the cell, being proportional to the resultant current, was also proportional to the potential drop across the resistance. It was found that 1 part of oxygen per million was indicated by a potential drop of the order of 3 millivolts measured by a potentiometer which in conjunction with a d'Arsonval galvanometer, was sensitive to  $\pm 0.05$  millivolt.

### Apparatus.

A diagrammatic representation of the apparatus is shown in Fig. 4. The light source was a G.E.C. 250 watt MED compact source mercury vapour lamp A, situated about 7 inches from the tube B which contained up to 10 ml. of the solution to be irradiated. The apparatus was designed to remove any oxygen from the solution by circulating nitrogen round the enclosed system BCDEFGHI.

The flasks J and K were connected by PVC tubing M and contained sufficient mercury to bring the level L<sub>1</sub> just short of the stopcock H. K was also connected to a 'Speedivac' high vacuum pump, enabling mercury to be drawn from J into K. By setting the 3-way stopcock H, so as to shut off I from GHJ

and drawing mercury into K until the level in J falls to about L<sub>2</sub>, the nitrogen in the flask C was expanded into J. The vacuum in K was then released and H adjusted so that the mercury flowing back into J forced the nitrogen via I, through the solution, back into C. By repeating this process for about 15 minutes, practically all the oxygen originally in the solution was transferred to the nitrogen. The stop-cocks D and E were then turned and the gas circulated a few times through the Hersch cell (previously filled with pure nitrogen) to ensure that the latter became filled with gas representative of that in the rest of the system, after which, the potential drop across the 2000 ohm resistance was noted.

The system had a gas inlet and outlet at G and F. The apparatus was of 'Pyrex' glass and all stopcocks were greased with Edwards' silicone high vacuum grease and all quickfit joints with 'Apiezon N' grease. To facilitate turning stopcock H while releasing the vacuum in K, a simple foot-operated device was constructed by which the vacuum could be released. The section BCD of the apparatus was mounted over a thermostat tank from which water was pumped by a small centrifugal pump and sprayed over the tube B keeping its temperature at  $20^\circ \pm 0.1^\circ\text{C}$ .

The apparatus was calibrated by generating electrolytically a known amount of oxygen in a special cell which

replaced tube B. The cell is shown in Fig. 4 and consisted of a tube identical in size to B but with two small side arms into which platinum electrodes were sealed inside the tube. The arms were filled with mercury to make electrical contact with the electrodes; the electrolyte was 10 ml. of a 10% w/v potassium hydroxide solution.

After replacing the tube B by the cell, the leads from a battery-galvanometer-variable resistance circuit were dipped into the mercury in the side arms and a steady current (0.5 mA.) passed for an appropriate time. Knowing the current and the time, the amount of oxygen generated could easily be calculated from Faraday's Law. The oxygen was removed from the solution by circulating nitrogen as explained above and the corresponding potential drop across the 2000 ohm resistance noted. Further quantities of oxygen were then generated and a calibration curve drawn relating mV. potential drop to the total amount of oxygen in the system.

Except with the most elaborate apparatus, it is impossible to remove from cylinder nitrogen the last traces of oxygen to which the Hersch cell is sensitive. Therefore, before any oxygen was generated in the solution either photochemically or <sup>e</sup><sub>c</sub>lectrolytically, a blank determination had to be made of the potential drop corresponding to the oxygen initially in the nitrogen and this value subtracted from all

subsequent readings.

Preparation of Ferric Chloride Solutions.

Throughout the entire work,  $1.3 \times 10^{-3}$  M ferric chloride solutions were used and were prepared by the method evolved by Purdon<sup>75</sup>. A.R. ferric chloride  $\text{FeCl}_3 \cdot 6\text{H}_2\text{O}$  was melted in a small tube fitted with a ground glass cap and maintained at  $45^\circ\text{C}$  for about 30 minutes after which it was allowed to come to room temperature in a supercooled state. The melt was then stirred with a glass stirrer and 0.1 ml. delivered dropwise from an "Agla" micrometer syringe (supplied by Burroughs Wellcome & Co.) into 500 ml. of stirred water. Prepared thus, a  $1.3 \times 10^{-3}$  M ferric chloride solution at  $20^\circ\text{C}$  had a pH of 2.94. When not in use, the melt was allowed to resolidify.

The concentration of the ferric chloride solution was checked from time to time by titration with titanous chloride, but was found to be constant at  $1.3 \times 10^{-3}$  M. All pH measurements were carried out with a dip-type glass/calomel electrode system in conjunction with a 'Cambridge' pH meter accurate to  $\pm 0.01$  pH unit. The instrument was standardised with 0.05 M potassium hydrogen phthalate buffer solution, pH 4.00 at  $20^\circ\text{C}$ .

Analysis of Ferrous Ion.

The irradiated ferric chloride solutions were generally of the order of  $10^{-4}$  M in ferrous ion.

For the colorimetric analysis of small concentrations of ferrous ion, the best and most convenient reagents are probably o-phenanthroline and 2-2'dipyridyl used in solutions buffered to a pH in the region of 4. These reagents can be employed with  $1.3 \times 10^{-3}$  M ferric chloride solutions only if some suitable ion is added to complex the ferric ion and prevent its hydrolysis which at pH 4 is considerable and interferes with the analysis. Fluoride ion, complexing the ferric iron as  $[FeF_6]^{3-}$  is ideal for the purpose and was found not to interfere with the red colour of the ferrous-2-2'dipyridyl complex. 2-2'dipyridyl was therefore used in the following procedure.

Up to 10 ml. of photolysed solution were transferred to a 20 ml. graduated flask containing 2 ml. of 0.08% 2-2'dipyridyl solution, 5 ml. of buffer solution and 2 ml. of 0.25 M ammonium fluoride solution. The resulting solution was diluted to 20 ml. with distilled water, thoroughly shaken, and allowed to stand overnight in the dark to allow full colour development. The extinction was measured at 520 m $\mu$  in a 'Unicam' SP 600 spectrophotometer and the ferrous ion concentration calculated by reference to the linear calibration

curve previously obtained using ferrous ammonium sulphate solutions of known concentrations. The appropriate blank correction was applied in each case.

Depending upon the ferrous ion concentration, 1 cm. or 2 cm. cells were used in the spectrophotometer giving an average blank extinction in the region of 0.01. An extinction of 0.857 in a 2 cm. cell was produced by a concentration of  $5 \times 10^{-5}$  M ferrous ion, corresponding to a molar extinction coefficient of 8570 for the complex.

Details of the solutions used in the analysis are:-

0.08% 2-2'dipyridyl solution 0.8 gm. of 2-2'dipyridyl dissolved in 1 litre of 0.05 N hydrochloric acid.

Buffer solution 80 gm. of ammonium acetate together with 20 ml. of concentrated sulphuric acid dissolved in water and the mixture diluted to 1 litre. This was found to give the final solution as prepared for colorimetric analysis, a pH of 4.24.

0.25 M ammonium fluoride solution 9.26 gm. of ammonium fluoride dissolved in 1 litre of water.

#### Reaction Technique.

Distilled water was degassed by boiling for 5 minutes and then cooled to 15°C under an atmosphere of nitrogen, after which the requisite quantity of ferric chloride melt was added

to give a  $1.3 \times 10^{-3}$  M solution. 10 ml. of the solution was pipetted into the tube B (Fig. 4) which was fitted into position and surrounded by a beaker of ice-water to lower the temperature of the solution quickly to 0°C and prevent the ferric ion hydrolysing while oxygen was flushed out of the apparatus. This was accomplished by passing in purified nitrogen at G, down via H and I, through the solution and round the circuit leaving at F. 30 minutes was found to be long enough to ensure that all oxygen was removed, and for the last 5 minutes, after removing the beaker of ice-water, water from the thermostat tank was sprayed over B to raise the temperature of the solution to 20°C. The nitrogen was then shut off and the inlet and outlet at G and F closed.

The blank determination corresponding to the oxygen in the nitrogen was next made as follows. The gas in the apparatus was circulated for 15 minutes as previously described after which D and E were turned to include the Hersch cell in the circuit. The gas was recirculated a further three times and then the potential drop across the 2000 ohm resistance immediately recorded. The blank value varied from day to day between 7 and 9 mV. The leads from the Hersch cell were always connected through the 2000 ohm resistance about three minutes before the cell was included in the circuit and disconnected as soon as the reading was

taken.

The solution was irradiated for the desired period after which the gas was recirculated and a second value for the potential drop recorded. After subtracting the initial blank from this reading, the amount of oxygen produced photo-chemically was read from the calibration graph. The tube B was then removed from the apparatus and samples taken for ferrous analysis. The apparatus was calibrated at the end of each set of estimations by means of the electrolysis cell previously described. After use, the Hersch cell was always flushed out with nitrogen and the leads short-circuited overnight so that traces of oxygen remaining in the cell would be absorbed.

A procedure identical to that outlined above, was adopted in every estimation.

#### Materials.

Nitrogen 'White Spot' cylinder nitrogen of oxygen content less than 0.0001% was used (supplied by the British Oxygen Co.) The gas was further freed from oxygen by passage over reduced copper oxide heated electrically to 400 to 450°C and scrubbed with water before entering the apparatus. All connecting tubing was of PVC.

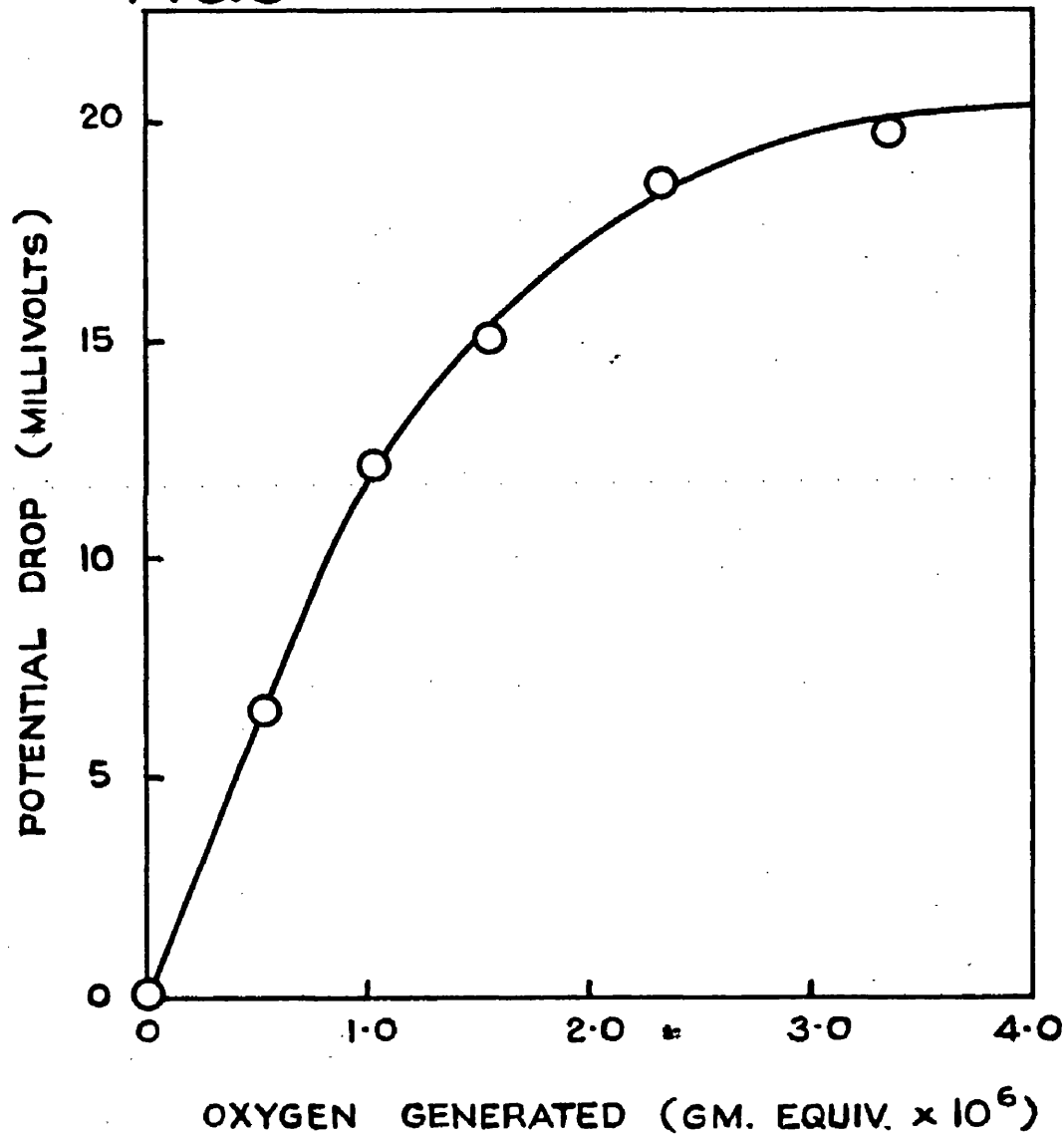
Cadmium The cadmium metal was supplied in the form of sticks

by British Drug Houses, Ltd. It was sawn into pellets and cleaned with dilute nitric acid before use.

Silver The silver wire and sheet were supplied by Johnson, Matthey & Co., Ltd.

Mercury The mercury was cleaned by passing it in a fine spray down a long column of dilute (1:19) nitric acid. For the various other solutions, 'Analar' materials were always used if obtainable.

**FIG. 5** CALIBRATION CURVE



RESULTS.

(A) Calibration of the Hersch Cell.

A typical calibration curve is shown in Fig. 5. The first reading at 6.5 mV. was obtained after passing a current of 0.5 mA. for 100 seconds through the electrolysis cell. The oxygen generated may be calculated as follows:-

From Faraday's Law, 96494 coulombs liberate 1 gm.equiv.  
 $\therefore$  1 coulomb liberates  $1.036 \times 10^{-5}$  gm.equiv.

$$\begin{aligned}0.5 \text{ mA for 100 seconds} &= 5 \times 10^{-4} \times 100 \\&= \underline{\underline{5 \times 10^{-2} \text{ coulombs}}}\end{aligned}$$

$$\begin{aligned}\therefore \text{Amount of oxygen generated} &= 1.036 \times 10^{-5} \times 5 \times 10^{-2} \\&= \underline{\underline{0.518 \times 10^{-6} \text{ gm.equiv.}}}\end{aligned}$$

It is of interest to calculate the sensitivity of the Hersch cell from this result.

32 gm. of oxygen occupy 22400 ml. at s.t.p.

Since the gm. equiv. wt. is 8,

1 gm.equiv. occupies  $22400 \times 8/32 = 5600$  ml.

$$\begin{aligned}\therefore 0.518 \times 10^{-6} \text{ gm.equiv.} &\text{ occupies } 0.518 \times 10^{-6} \times 5600 \\&= \underline{\underline{2.9 \times 10^{-3} \text{ ml.}}}\end{aligned}$$

The volume of the apparatus was approximately 1100 ml.

$$\begin{aligned}\therefore \text{The concentration of oxygen is } 2.9 \times 10^{-3} \text{ parts per 1100} \\&= \underline{\underline{2.6 \text{ parts per million.}}}\end{aligned}$$

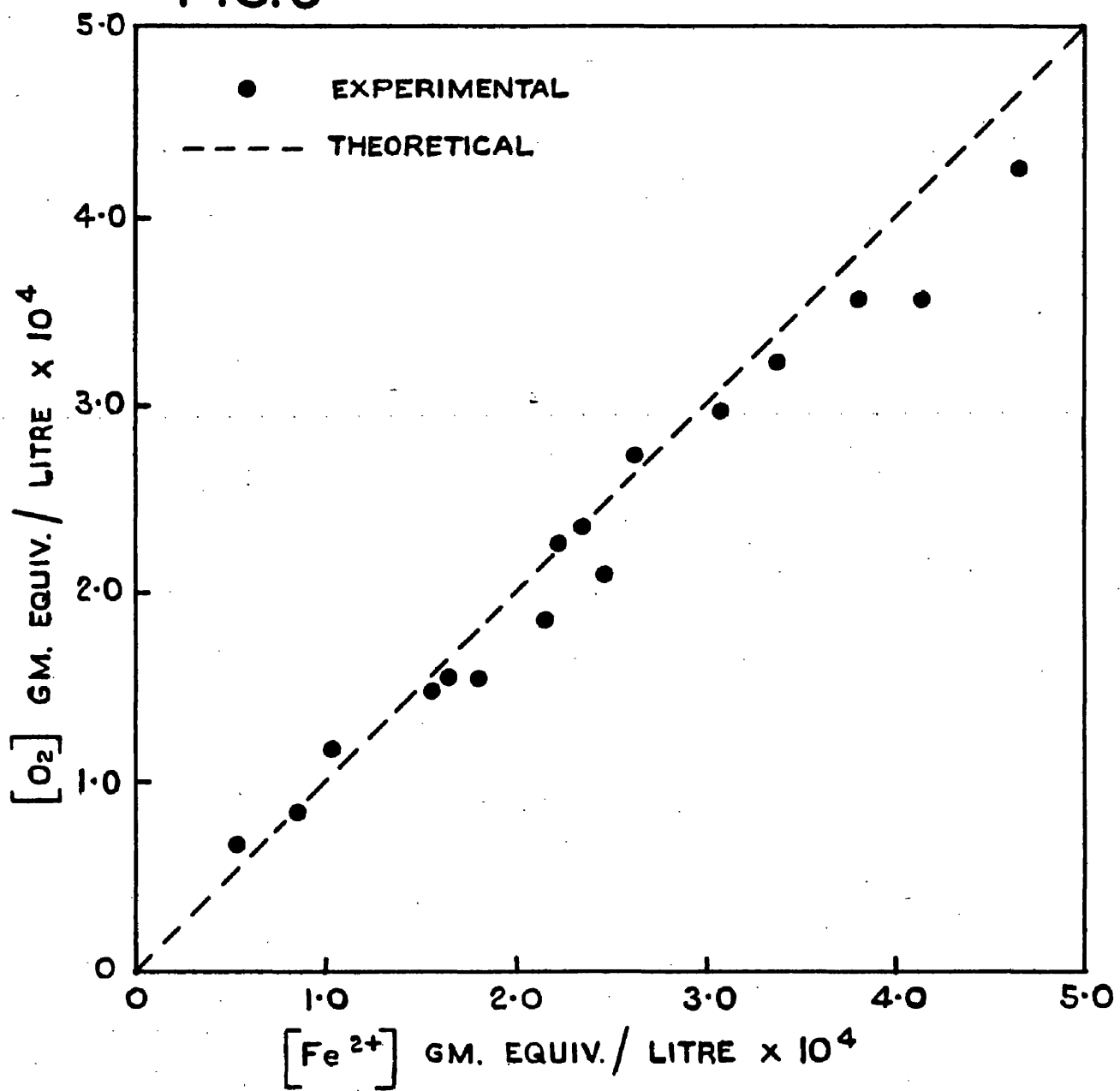
i.e. 2.6 p.p.m. is indicated by a potential drop of 6.5 mV.  
∴ 1 part per million is indicated by a potential drop of  
2.5 mV across 2000 ohms.

Although the limit of proportionality between potential drop and oxygen concentration is reached at  $1.0 \times 10^{-6}$  gm. equiv. of oxygen (5 p.p.m.), it was found that by reference to the calibration curve, amounts of oxygen up to  $2.0 \times 10^{-6}$  gm.equiv. could be accurately estimated.  $2.0 \times 10^{-6}$  gm. equiv. of oxygen generated, for example, photochemically in 10 ml. of solution is equivalent to an oxygen concentration in solution of  $2.0 \times 10^{-4}$  gm.equiv./litre. Previous work showed that the maximum concentration of oxygen to be expected in the present investigation was in the region of  $4 \times 10^{-4}$  gm.equiv./litre and this was brought into the range of the apparatus by reducing the volume of solution irradiated to 5 ml.

(B) The Irradiation of  $1.3 \times 10^{-3}$  M Ferric Chloride Solutions.

Each of the solutions was at 20°C and initially at pH 2.94 although the pH slowly decreased as the solution hydrolysed during irradiation. The u.v. lamp was situated about 7 inches from the irradiation vessel and solutions were irradiated for various periods of time up to 2½ hours to cover the full range of oxygen-ferrous ion production.

FIG. 6



The concentrations of oxygen and ferrous ion produced photochemically by the irradiation of  $1.3 \times 10^{-3}$  M ferric chloride solutions are shown in Table 10.

TABLE 10

Concentrations Gm.Equiv./Litre x $10^4$			
Oxygen	Ferrous Ion	Oxygen	Ferrous Ion
0.67	0.52	2.35	2.35
0.83	0.85	2.10	2.47
1.17	1.03	2.73	2.62
1.48	1.56	2.98	3.08
1.55	1.64	3.23	3.38
1.54	1.80	3.56	3.80
1.86	2.15	3.56	4.14
2.27	2.22	4.26	4.65

The oxygen and ferrous ion concentrations are plotted against each other in Fig. 6; the dotted line is for the theoretical relation  $[Fe^{2+}] = [O_2]$ . The excellent agreement of the experimental results with the theoretical, shows that oxygen and ferrous ion are produced photochemically in equal (gm. equiv.) concentrations.

Oxygen estimations on irradiated water showed that a very slight photodecomposition occurred. However, in the

presence of ferric iron, the photodecomposition of water will be negligible since the extinction coefficient of ferric iron is so much higher than that of water.

The results are discussed on page 95 along with those of the next section.

---

SECTION B.

THE POLAROGRAPHIC ESTIMATION OF PHOTOCHEMICALLY  
PRODUCED OXYGEN.

THEORY OF THE METHOD.

The polarographic method of analysis is the result of research carried out at the University of Prague by Professor Heyrovsky in 1922 and is based on the current-voltage relationships obtained when solutions of electro-oxidisable or electro-reducible substances are electrolysed in a cell in which one electrode consists of mercury falling dropwise from a fine bore capillary tube. From the characteristics of the current-voltage curve it is possible not only to identify but also to determine the concentration of the oxidisable or reducible substance, and as many as five or six substances can be estimated in the one solution if their curves are sufficiently separated.

An outline of the basic apparatus for polarographic analysis is shown in Fig. 7a. It consists essentially of a capillary glass tube supplied with mercury from a reservoir and dipping into the solution to be analysed, contained in the cell. The capillary diameter (approx. 0.05 mm.) and the height of the reservoir are adjusted so that the mercury falls into the solution at the rate of about one drop every 3 seconds. In the diagram, the mercury electrode is shown as the cathode, the anode being a large pool of mercury at the bottom of the cell. The voltage applied across the cell can be varied from zero up to the maximum e.m.f. of the

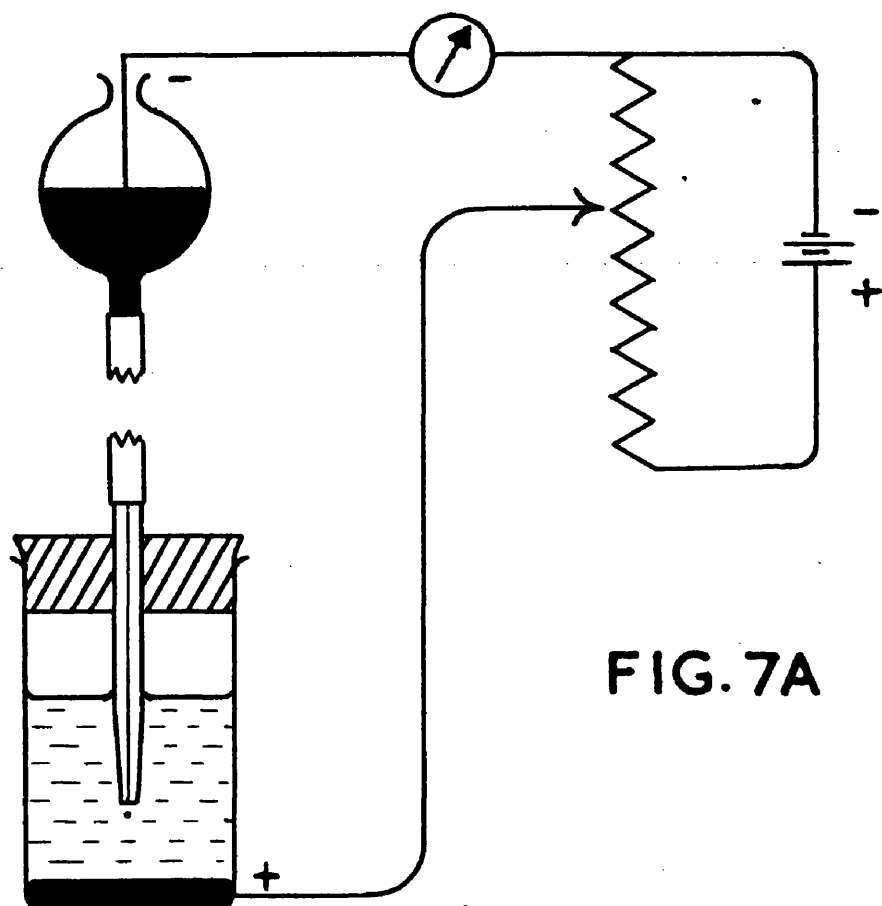
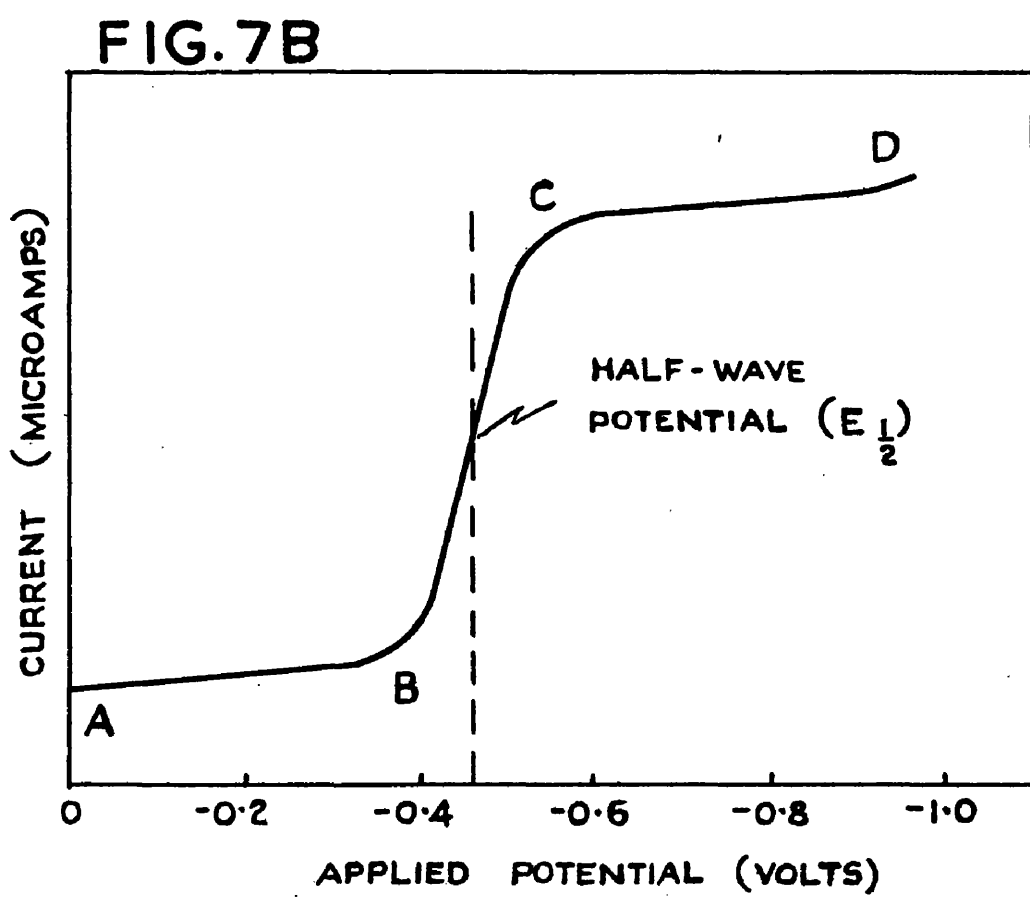


**FIG. 7A**



battery by means of the rheostat, while the current is recorded on the galvanometer.

On account of the small surface area of mercury exposed to the solution at the end of the capillary, the electrode is capable of becoming polarised i.e. of adopting an externally applied potential with little or no change in the current. The anode mercury pool, on the other hand, being of relatively large surface area remains unpolarised. The galvanometer readings oscillate between maximum and minimum values owing to the periodic change in area as each drop grows and falls.

Electro-active material reaches the electrode surface by the two processes of migration of charged particles in the electrical potential gradient in the vicinity of the electrode and the diffusion of particles in the concentration gradient at the electrode surface. The total current passing through the electrolytic cell can be regarded as the sum of these two factors.

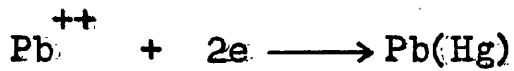
In polarographic analysis the migration current must be suppressed since only the diffusion current is desired, being proportional to the concentration of the electro-active material. This is readily achieved by the addition to the sample solution of an indifferent electrolyte in a concentration of at least 100-fold that of the electro-active

material, so that the transference number of the latter becomes negligible and practically all the current is carried by the ions of the 'base electrolyte' or 'supporting electrolyte' as it is called. Under these conditions the electro-active material can reach the electrode surface only by diffusion and the currents obtained at the dropping mercury electrode are limited by this process. It should be noted that the supporting electrolyte must be composed of ions which are discharged at potentials which will not interfere nor interact chemically with the ions under investigation.

Fig. 7b shows a cathodic current-voltage curve or polarogram for lead ions in a solution of potassium chloride as supporting electrolyte. Most metal ions give polarograms of similar shape and lead is chosen quite arbitrarily as a typical example. It is seen that the curve falls into three distinct sections. In the section AB, from zero applied potential to the decomposition potential of the lead ions B, only a very small current called the residual current passes through the solution. This residual current is the sum of two factors; a condenser or charging current arising from the continual charging of new mercury drops to the applied potential and a slight current due to the reduction of traces of reducible impurities in the solution.

Increase in the applied potential beyond B causes the

reduction of lead ions at the dropping mercury electrode according to the equation



When the mercury drop falls away from the electrode the lead is removed as a weak amalgam. As the lead ions are discharged their concentration at the mercury surface is reduced and this loss is compensated by the diffusion of lead ions from the bulk of the solution, at a rate governed by the difference between the concentration at the mercury surface and the rest of the solution. As the applied potential is further increased, more lead ions are discharged, the rate of diffusion increases and the current increases rapidly giving section BC of the polarogram.

On increasing the applied potential beyond C, a condition is reached when the lead ions are discharged so rapidly that the concentration of the latter at the mercury surface is virtually zero. The electrode is then in a state of complete concentration polarisation and the current can no longer increase because it is determined by the rate of diffusion of lead ions from the bulk of the solution to the mercury surface. The steady current represented by CD is therefore called the diffusion or limiting current. Since the rate of diffusion is proportional to the difference in concentration in the two regions between which diffusion

occurs, the diffusion current is proportional to the concentration of lead ions in the bulk of the solution. This proportionality is the basis of quantitative determinations from current-voltage curves.

The potential at the point in the current-voltage curve where the current is equal to one half its limiting value is known as the half-wave potential, denoted by  $E_{\frac{1}{2}}$ . This potential is characteristic of the reacting substance in the solution but is independent of its concentration, the dimensions of the electrode, etc. Polarography can therefore be applied in certain cases to qualitative analysis problems. Half-wave potentials, like ordinary standard potentials, are functions of the molecular state of the electro-active substance and can thus be altered by complexing, pH changes, etc., a fact which is often used to advantage to separate overlapping waves.

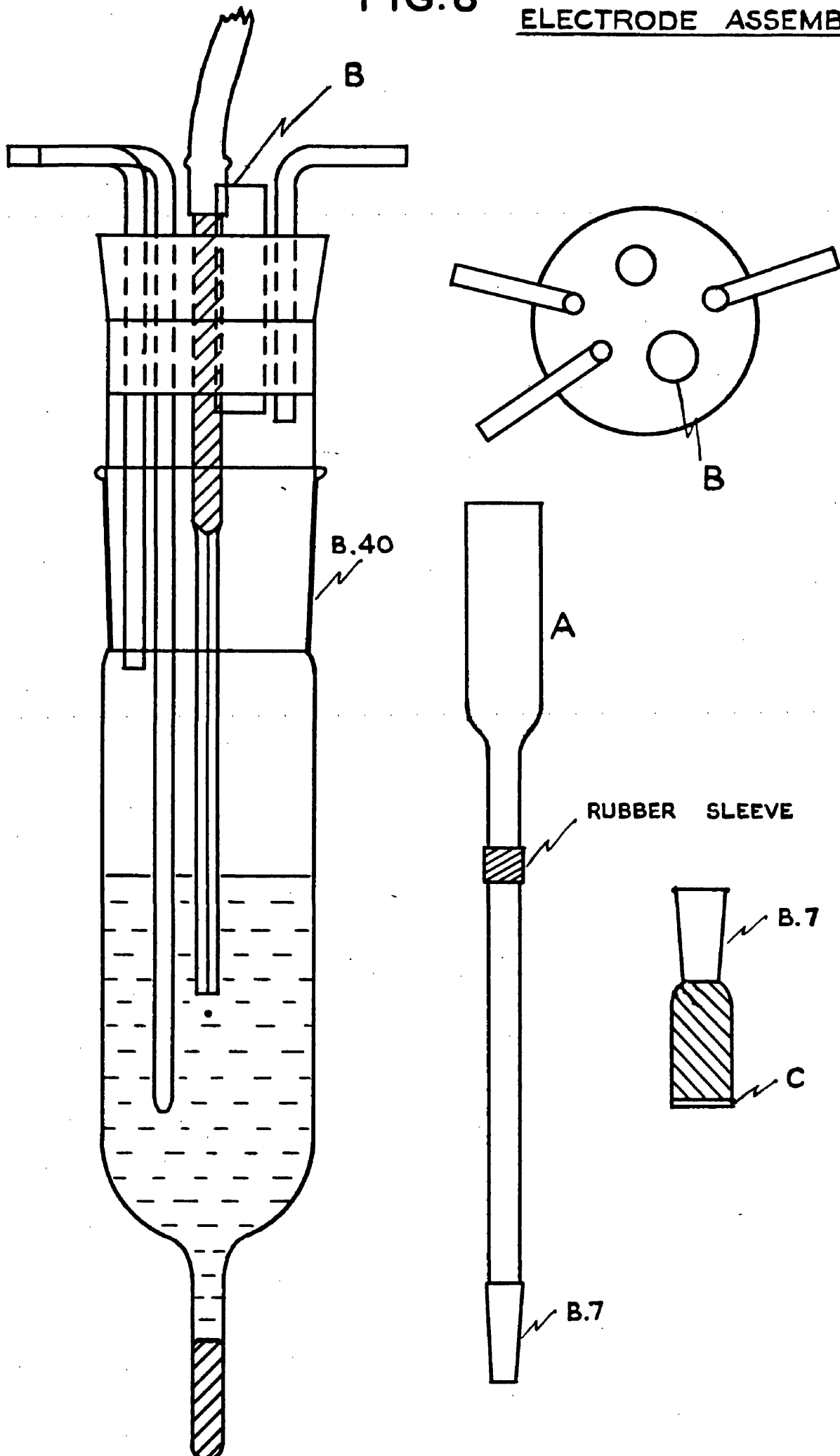
In determinations with the dropping mercury electrode, the diffusion current sometimes rises to a very high peak subsequently falling to the normal diffusion current plateau as the applied voltage is increased. These peaks, known as 'maxima', are believed to be due to preferential adsorption of ions on the individual mercury drops and must be suppressed before an accurate measurement of the diffusion current can be made. This is easily accomplished by the addition of

small quantities of surface active agents such as colloids or dye ions e.g. gelatin, methyl red, tylose, etc.

In early work with the dropping mercury electrode, the mercury pool covering the bottom of the electrolytic cell served as the non-polarisable reference electrode. Unfortunately the potential of the mercury pool is variable, depending upon the composition and nature of the electrolyte in contact with it and must be determined after each polarogram has been obtained, by balancing against some standard reference electrode. The mercury pool is now often replaced by electrodes such as the saturated calomel electrode (S.C.E.) whose potential is constant and not appreciably altered by the small currents passing through the cell. In this way, the potential of the dropping mercury electrode is immediately referred to a standard electrode. In the present work, whether stated or not, all potentials should be taken as being relative to the saturated calomel electrode.

FIG. 8

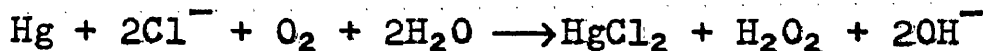
DROPPING MERCURY  
ELECTRODE ASSEMBLY



EXPERIMENTAL.

Dropping Mercury Electrode Assembly.

The electrode assembly is shown in Fig. 8. The cell containing the liquid to be analysed was made from a B.40 pyrex 'quickfit' socket and the rubber stopper carrying the mercury capillary, gas inlets, etc., was inserted in the cell by means of a B.40 cone as adaptor to avoid contamination of the solution by the stopper. A short tube was sealed to the bottom of the cell to collect the mercury drops after they fell through the solution in order to minimise the removal of dissolved oxygen according to the reaction :



which may take place in solutions of large chloride ion concentration, e.g. where potassium chloride is used as the supporting electrolyte, as in the present work.

Connection of the solution to the calomel electrode was made by means of tube A which was inserted through the tube B in the stopper and held firm by the rubber sleeve. C is a small sintered glass disc sealed to a B.7 socket which was filled with agar gel and joined to the B.7 cone at the end of A. The latter was then filled with saturated potassium chloride solution which was prevented by the agar gel and glass sinter from running into the solution to be polarographed

This provided a convenient method of electrical connection to the calomel electrode, the arm of which dipped into the solution at the upper end of A, while maintaining the gas-tightness of the cell and preventing contamination of either the solution being analysed or the calomel electrode by the other.

The mercury reservoir was similar to that shown in Fig. 7b and was connected to the capillary by vinyl tubing which was cleaned before use by steaming for 30 minutes and drying with a stream of filtered air. Contact between the mercury and the electrical circuit was made by a platinum wire sealed into the end of a glass tube and supported in position in the reservoir by a rubber stopper so that it dipped below the mercury surface. The glass tube contained a small amount of mercury with a length of copper wire making contact with it. This arrangement avoided any contamination of the mercury in the dropping mercury electrode. The capillary was supplied by Tinsley (Industrial Instruments) Ltd., London, and gave a drop time of 2.8 seconds with a 55 cm. head of mercury.

The whole assembly was mounted on a retort stand so that the cell could be partially immersed in a thermostat maintaining the temperature of the solution at  $20^\circ \pm 0.1^\circ\text{C}$ . After

use, the capillary was washed with distilled water and dried with filter paper and then the mercury reservoir lowered until the mercury ceased to flow. Any mercury dropping from the electrode and not collected in the cell fell into the thermostat tank from which it was recovered when convenient.

Calomel Electrode.

The calomel electrode was of the bottle and side arm variety. To set up the electrode, pure calomel to which a little mercury had been added was shaken in a flask with saturated potassium chloride solution to remove traces of mercuric compounds, after which the solution was decanted and rejected. This procedure was repeated twice except that after the second time the solution of potassium chloride was retained after decantation for the final filling of the cell. Pure mercury was then placed in the bottle (200 ml. capacity) to give a layer of about 1 cm. deep and the pasty calomel carefully poured on top followed by a few grams of potassium chloride. The rubber stopper carrying the side arm etc. was then firmly set in position and the electrode completed by drawing into it through the side arm by suction at a small tube, a quantity of the potassium chloride solution reserved from the third washing. Electrical connection with the

electrode was made by a platinum wire sealed into the end of a glass tube and supported in position by the stopper so that it dipped below the mercury surface. The glass tube contained a small amount of mercury with a length of copper wire making contact with it.

Polarograph.

A Tinsley pen-recording polarograph (Model MK 19) was employed, a simplified schematic diagram of which is shown in Fig. 9a. The instrument incorporates a polarising unit, an amplifier and a pen recorder. The various controls detailed below are mounted on the operating panel.

(a) Auto-potentiometer. The auto-potentiometer has a circular scale 6 in. in diameter which is calibrated from +0.5 to -3.0 volts in 20 millivolt steps. It is driven by a synchronous motor through a friction clutch at the rate of 0.3 or 0.15 volt/min. while the chart moves at the rate of 2 in. of chart/volt, the speed change being by a knob on the panel. The potentiometer scale and recorder chart can also be set by hand to any desired position.

The potentiometer applies the polarising potential across the polarographic cell and the resulting current is amplified by the mirror galvanometer D.C. amplifier, the output of which operates the recorder. The latter is a moving-coil

# FIG. 9A

POLARIZING POTENTIAL  
SUPPLY UNIT

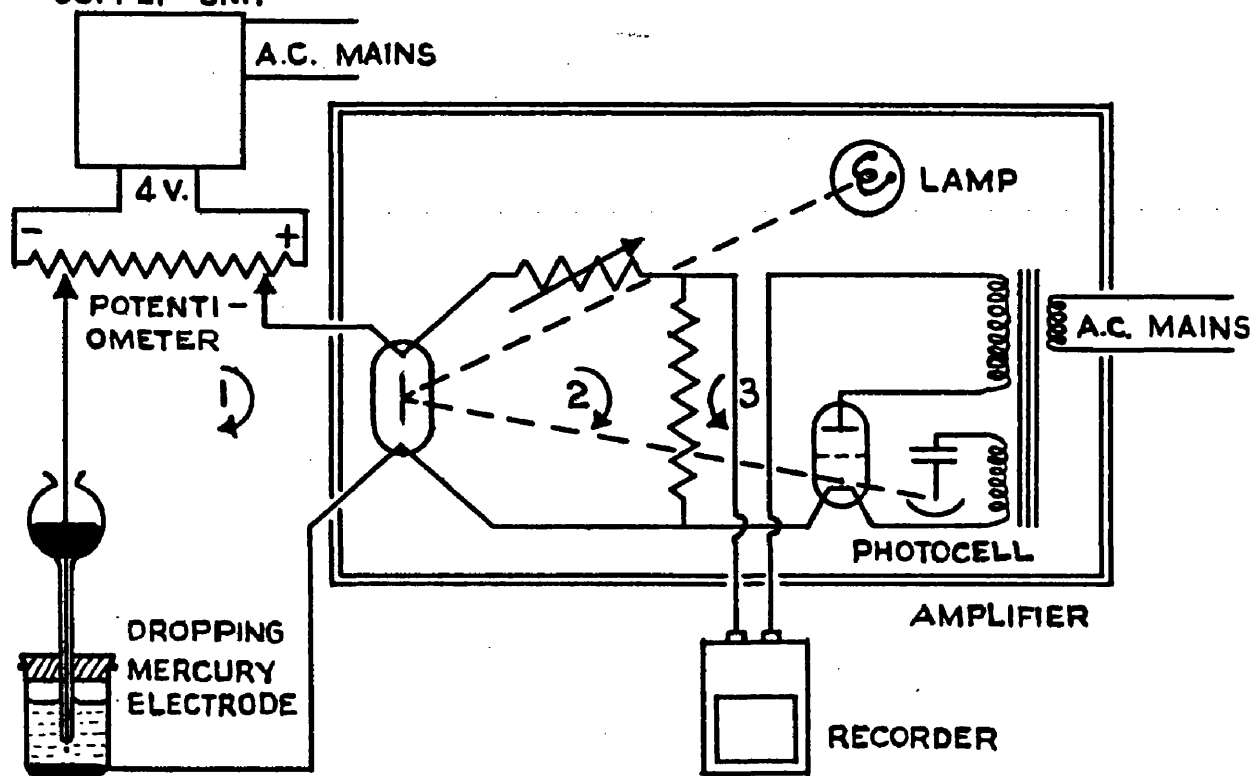
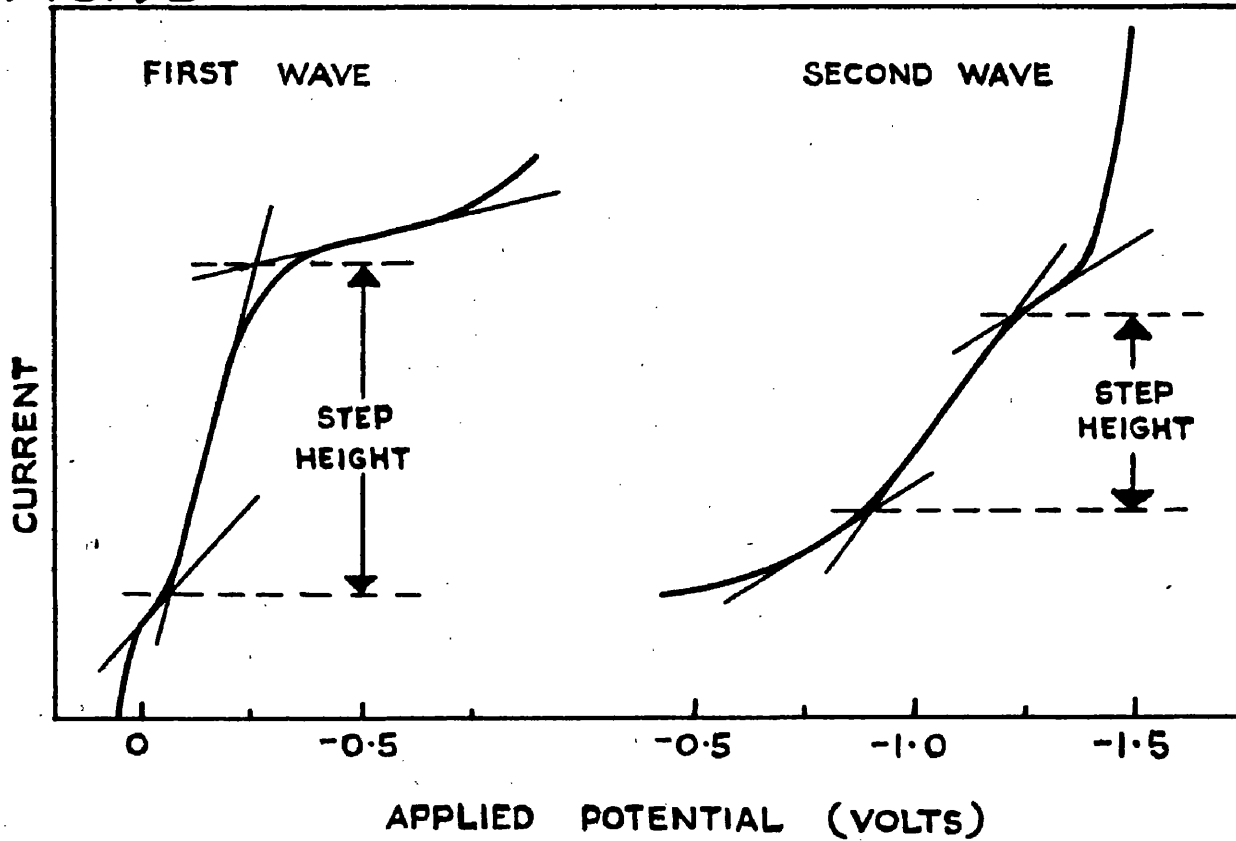


# FIG. 9B MEASUREMENT OF STEP HEIGHT



pen-type milliammeter and has a continuous roll chart 3.5 in. wide calibrated in 100 units, and divided into 50 parts on the current axis and in 0.1 volt along the potential axis. The polarising voltage is standardised directly by a rheostat against a standard cell. There are three switches, one to operate the recorder, one for the potentiometer motor, and the third for the direction of rotation of the potentiometer, i.e. either to increase or decrease the polarising potential.

(b) Zero Setting. Electrical zero controls (coarse and fine) are provided for centralising the chart record and also to facilitate the measurement of a small diffusion step in the presence of a larger one.

(c) Sensitivity. The polarograph is calibrated in 12 ranges from 100 to 0.1 microamps. which represents the current passing through the polarographic cell for full-scale deflection on the chart. The range used depends upon the concentration of the substances in the solution.

(d) Range Multiplier. The factors  $x_1$ ,  $x_1.2$  and  $x_1.5$  are to increase the sensitivity ranges from 12 to 34, enabling more accurate work to be carried out by utilising the chart width to the best advantage. Also incorporated in the range multiplier is the direct/derivative switch. The direct polarograms are the conventional current-voltage stepped curves where half-wave potentials indicate the species, and

the step height the concentration. The derivative polarograms are the first derivative of the direct waves, and give a peaked curve where the potentials at the peaks indicate the species and the height the concentration.

(e) Counter-current. This control which can only be used when taking direct polarograms, gives a regularly increasing negative bias to counteract the residual cell current and is calibrated in ten equal steps.

(f) Damping. The damping control introduces electrolytic condensers across the recorder to provide variable damping of the pen excursions caused by the mercury drops.

#### The Interpretation of Polarographic Steps.

##### (a) Measurement of Step Height.

There are numerous procedures for measuring the step heights of current-voltage curves and while the final choice is quite arbitrary, it depends to some extent on the shape of the curves. Many of these procedures do not give true measures of the magnitudes of the diffusion currents, but where a comparative method is employed for calibration this is unimportant. Fig. 9b illustrates the procedures adopted in the present work for determining the step height of each of the oxygen waves.

For the first wave, where the step is fairly well defined

tangents were drawn to the flattest portions at the top and bottom of the step and a further tangent at the point of greatest slope. The vertical height between the two points of intersection gave the step height. Since the second wave was not so well defined, especially at the beginning, the procedure differed in that the tangent to the bottom part was drawn parallel to that to the top part of the step.

A step height so measured was obtained in terms of the units into which the chart was divided. To convert to the diffusion current in microamps, the above figure was divided by 100 and multiplied by the sensitivity expressed in microamp./full scale deflection at which the polarogram was recorded. It sometimes happened that the mercury drops falling from the electrode caused large pen oscillations making the wave trace rather broad. In this case it is the convention to draw the tangents to the upper edge of the trace, i.e. at the points immediately before the drops fall off.

(b) Determination of Concentration from Diffusion Currents.

The method adopted was that of standard addition, being most suited to the determination of oxygen. The polarogram of the unknown oxygen solution was first recorded after which, the solution was saturated with air and a second polarogram taken. From the heights of the two waves the concentration

of oxygen in the unknown solution could readily be calculated by direct proportion, the oxygen concentration in an air saturated solution being taken as  $1.142 \times 10^{-3}$  gm.equiv./litre,  $(0.286 \times 10^{-3} M)^{101}$ . While this figure is actually given for air in water, the reduction in oxygen solubility caused by the small amount of supporting electrolyte in the solution was considered to be negligible. The assumption that the wave height is a linear function of the oxygen concentration, was examined and found to hold good, (see page 87).

#### Irradiation Apparatus.

The solutions were irradiated in the cell which was described on page 71 as part of the dropping mercury electrode assembly. The cell was clamped over a thermostat tank from which water was pumped by a small centrifugal pump and sprayed over the cell maintaining its temperature at  $20^\circ \pm 0.1^\circ\text{C}$ . The rate of flow of the water was regulated by varying the voltage supplied to the pump motor by means of a 'Variac' transformer. The water drained back into the tank, splashing being prevented by allowing the small tube at the lower end of the cell to dip into the tank water. The tank was equipped with cooling coils since the heat from the u.v. lamp caused the water temperature to rise above  $20^\circ\text{C}$ . A Hanovia UVS 500 lamp was used, situated about 7 cm. from the cell.

Provision was made for the exclusion of air from the cell during irradiation, either by passing nitrogen over the surface of the solution or by completely filling the cell with solution and stoppering to exclude gas space.

Reaction Technique.

Distilled water was degassed by boiling for 5 minutes and poured hot into the cell which was then placed in the thermostat where the water was allowed to cool to 20°C under an atmosphere of nitrogen. If the solution was to be irradiated under an atmosphere of nitrogen, 100 ml. of hot water were placed in the cell, whereas if the cell was to be stoppered, it was completely filled (182 ml.). The requisite quantity of ferric chloride melt was then added to give the  $1.3 \times 10^{-3}$  M solution which was irradiated.

After irradiation, a sample was taken for ferrous analysis and, if the cell had been completely filled, sufficient solution was removed to reduce the volume to about 100 ml. Small volumes of concentrated supporting electrolyte solution, previously freed from oxygen by nitrogen, and maximum suppressor were added and the oxygen polarogram recorded. Air was then drawn through the solution for one hour and a second polarogram taken. From the respective wave heights the concentration of oxygen in the irradiated solution was

calculated. The ferrous ion was determined colorimetrically by complexing with 2-2'dipyridyl as described in Section A.

Materials.

Mercury. The mercury was initially distilled under vacuum to remove any dissolved metal impurities and then passed in a fine spray down a long column of dilute (1:19) nitric acid and finally stored in a Pyrex flask. Prior to use in the dropping mercury electrode it was filtered through a filter paper cone with a pin-hole in the tip, to remove surface oxides or dust.

Nitrogen and Air. 'White Spot' cylinder nitrogen of oxygen content less than 0.0001% was used (supplied by the British Oxygen Co.). The gases were scrubbed with water before use to saturate them with water vapour and prevent change in the concentration of the solution in the cell.

Agar Gel. The agar gel was prepared by adding 100 ml. of cold water to 3 to 3.5 gm. of agar powder and heating the mixture on a steam bath until a homogeneous solution was obtained. 25 gm. of solid potassium chloride were then added and the solution stirred until the salt dissolved. The solution was pipetted hot into the small sintered glass vessel C (see page 71) where it cooled to a gel. When not in use, the vessel C was kept immersed in saturated potassium

chloride solution.

1% Gelatin Solution. 1 gm. of powdered gelatin was dissolved in 50 ml. of water heated on a steam bath and the solution cooled and diluted to 100 ml. with water.

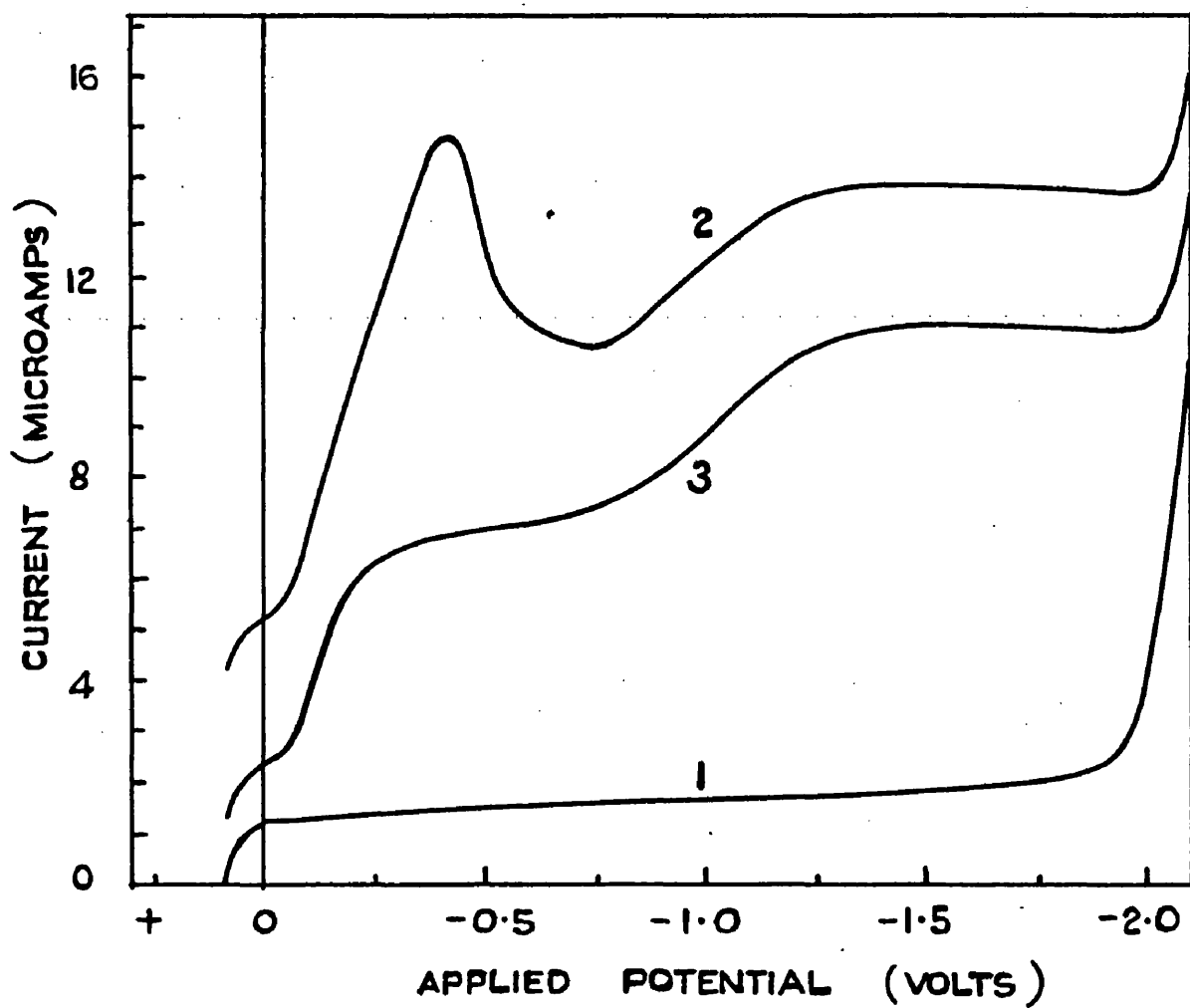
For the various other solutions, 'Analar' materials were always used if they were obtainable.

FIG. 10

SOLN. 1 :- 0.08 M KCl

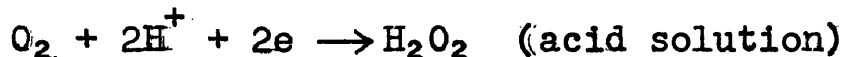
SOLN. 2 :- AS ABOVE, BUT AIR SATURATED

SOLN. 3 :- AS ABOVE + 0.01 % GELATIN

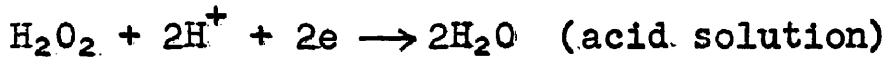


RESULTS.

Fig. 10 shows typical polarograms of 0.286 millimolar oxygen obtained with air-saturated 0.08 M potassium chloride solution. The first wave results from the reduction of oxygen to hydrogen peroxide at  $E_{\frac{1}{2}} = -0.13$  V vs. S.C.E.

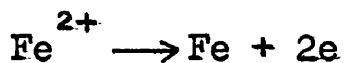
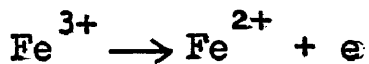


and the second wave corresponds to the reduction of the hydrogen peroxide either to water or hydroxyl ions at  $E_{\frac{1}{2}} = -1.05$  V vs. S.C.E.



The first oxygen wave shows a very pronounced maximum which, fortunately, is readily suppressed by surface active agents such as colloids or dye ions. The suppressive effect of 0.01% gelatin is shown in Fig. 10.

Ferric iron can also give two waves, depending upon the supporting electrolyte, pH, etc., corresponding to :-



which considerably complicates the oxygen determination.

The following factors had therefore to be taken into consideration when choosing a suitable supporting electrolyte

and maximum suppressor for the determination of oxygen in the presence of ferric iron and photoproduced ferrous iron.

(1) It is easier to make step height measurements on the narrower first oxygen wave, especially since the hydrolysis of the ferric iron causes many solutions to have a pH sufficiently low to give a hydrogen wave which cuts short the second oxygen wave.

(2) The iron must not give waves or form complexes with the supporting electrolyte or maximum suppressor, which give waves interfering with the oxygen wave.

(3) The supporting electrolyte or maximum suppressor must not form complexes with the ferrous iron which are readily oxidised by oxygen.

(4) The required weights of supporting electrolyte and maximum suppressor should be easily added, preferably as small volumes of concentrated solution so that the volume of the solution to be analysed will not be appreciably altered.

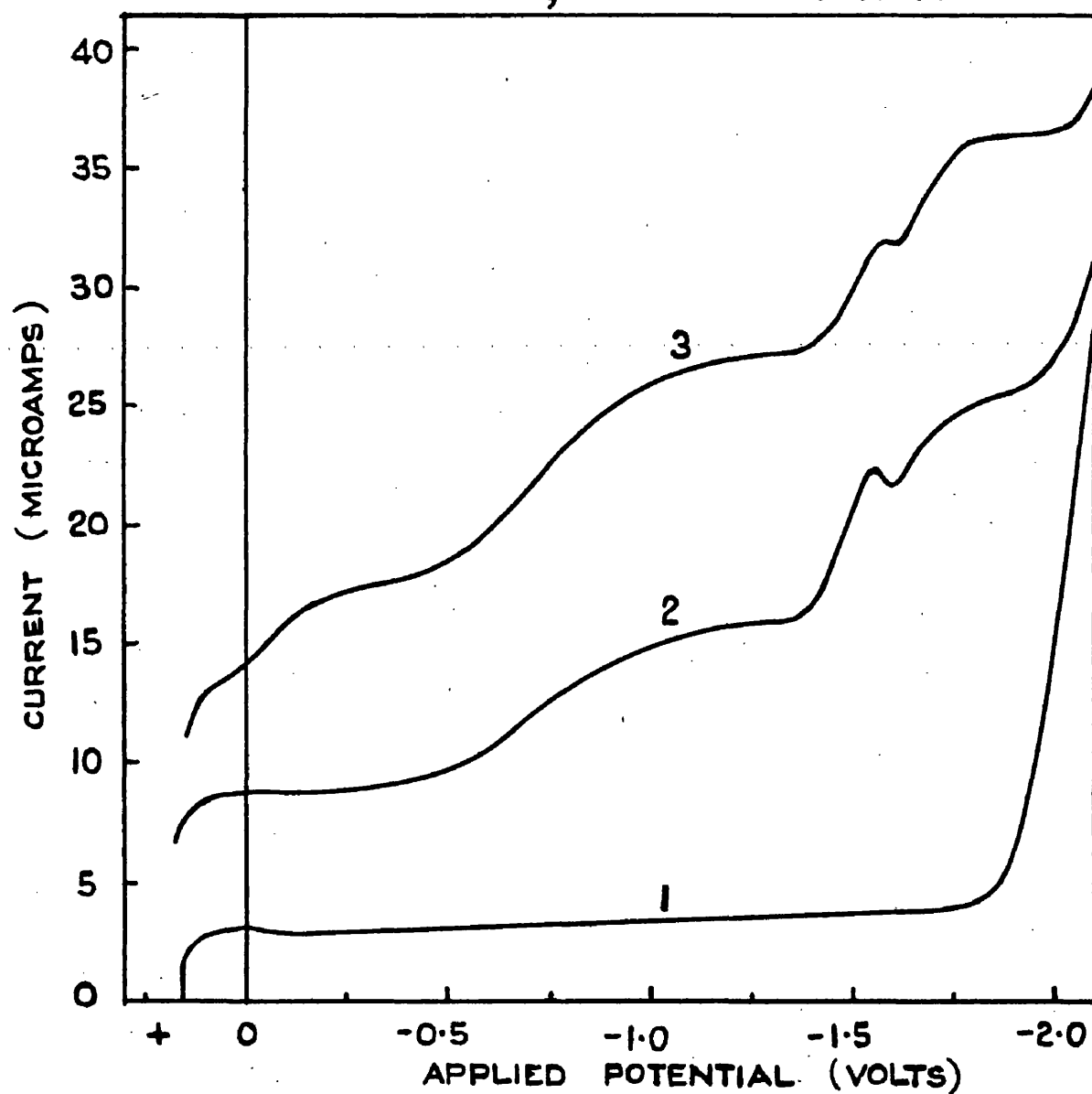
The first electrolyte to be tried was ammonium fluoride, since there was the possibility that by complexing the iron as  $[FeF_6]^{3-}$  it might not be reduced at the dropping mercury electrode. Reports in the literature are rather contradictory on the polarography of iron in fluoride media. Von Stackelberg and von Freyhold<sup>102</sup> report that ferric iron

FIG. II

SOLN. 1. :- 0.25 M.  $\text{NH}_4\text{F}$  + 0.0002% METHYL RED

SOLN. 2. :- AS ABOVE +  $1.3 \times 10^{-3}$  M  $\text{FeCl}_3$

SOLN. 3. :- AS ABOVE, BUT AIR SATURATED



produces a reduction wave in fluoride medium (pH not specified), and that the half-wave potential is constant at -1.36 V vs. S.C.E. when the concentration of potassium fluoride is increased from 0.04 to 0.8 M. Heyrovsky<sup>103</sup> also shows a polarogram of the ferric-fluoride complex in 0.1 M KHF<sub>2</sub> as supporting electrolyte. On the contrary, West and Dean<sup>104</sup> using a 0.5 M sodium fluoride supporting electrolyte of pH about 5 containing 0.004% gelatin, claim that no reduction wave for the ferric-fluoride complex is observable below the discharge potential of the sodium ion.

Polarograms obtained with  $1.3 \times 10^{-3}$  M ferric chloride in 0.25 M ammonium fluoride and 0.0002% methyl red solution, in the absence and presence of oxygen, are shown in Fig. III. The pH of these solutions was 6.5. Polarogram 2 shows the ferric and ferrous waves quite clearly at  $E_{\frac{1}{2}}$ 's -0.74 and -1.55 respectively (the latter figure is approximate due to the irregularity in the wave); while Polarogram 3 shows that the first iron wave does not interfere with the first oxygen wave at  $E_{\frac{1}{2}}$  -0.13. The second wave ( $E_{\frac{1}{2}} \sim -0.73$ ) in Polarogram 3 is the combined effect of the first iron wave and the second oxygen wave.

Since photochemically produced ferrous iron would be present in the irradiated solution, it was decided to investigate its effect on the above polarograms. Ferrous

chloride solutions were prepared from the ferrous chloride - hydrochloric acid stock solution described on page 126. The polarogram of  $1.3 \times 10^{-3}$  M ferrous chloride in 0.25 M ammonium fluoride and 0.0002% methyl red solution was similar to that for  $1.3 \times 10^{-3}$  M ferric chloride except that the first wave ( $\text{Fe}^{3+} \rightarrow \text{Fe}^{2+}$ ) was missing. After saturating the solution with air, however, a polarogram identical to No. 3 in Fig. 11 was obtained, showing that all the ferrous iron had been oxidised to ferric by the oxygen in the air. This was confirmed by subsequently removing the oxygen from the solution with nitrogen, when a polarogram identical to No. 2 was obtained.

The addition of 2-2'dipyridyl to complex the ferrous iron and prevent its oxidation by the oxygen was investigated, since any oxidation of the ferrous iron by photoproduced oxygen on the addition of the supporting electrolyte to the irradiated solution, would lead to low and unreliable results. The ferrous-dipyridyl complex was found to be stable in air saturated solutions of  $1.3 \times 10^{-3}$  M ferrous chloride in 0.25 M ammonium fluoride and  $10^{-2}$  M dipyridyl and gave no wave between 0 and -1.0 V vs. S.C.E. where the dipyridyl wave begins. Unfortunately, however, the ferric-dipyridyl complex in the corresponding  $1.3 \times 10^{-3}$  M ferric chloride solution produced a wave between 0 and -0.6 V vs. S.C.E. which interfered with

# FIG.12

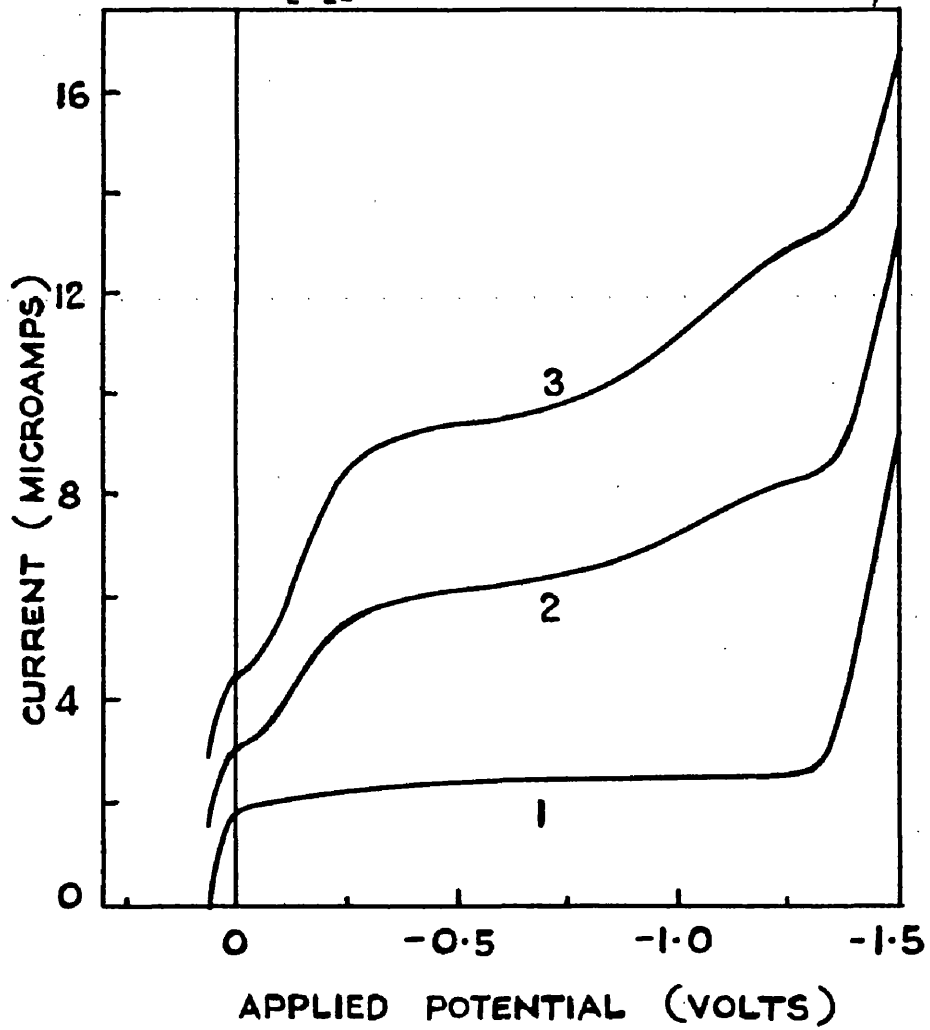
$1 \cdot 3 \times 10^{-3}$  M  $\text{FeCl}_3$  0.08 M KCl

0.01 % GELATIN

SOLN.1 :-  $[\text{O}_2] = 0$

SOLN.2 :-  $[\text{O}_2] = 0 \cdot 571 \times 10^{-3}$  GM. EQUIV./L

SOLN.3 :-  $[\text{O}_2] = 1 \cdot 142 \times 10^{-3}$  GM. EQUIV./L



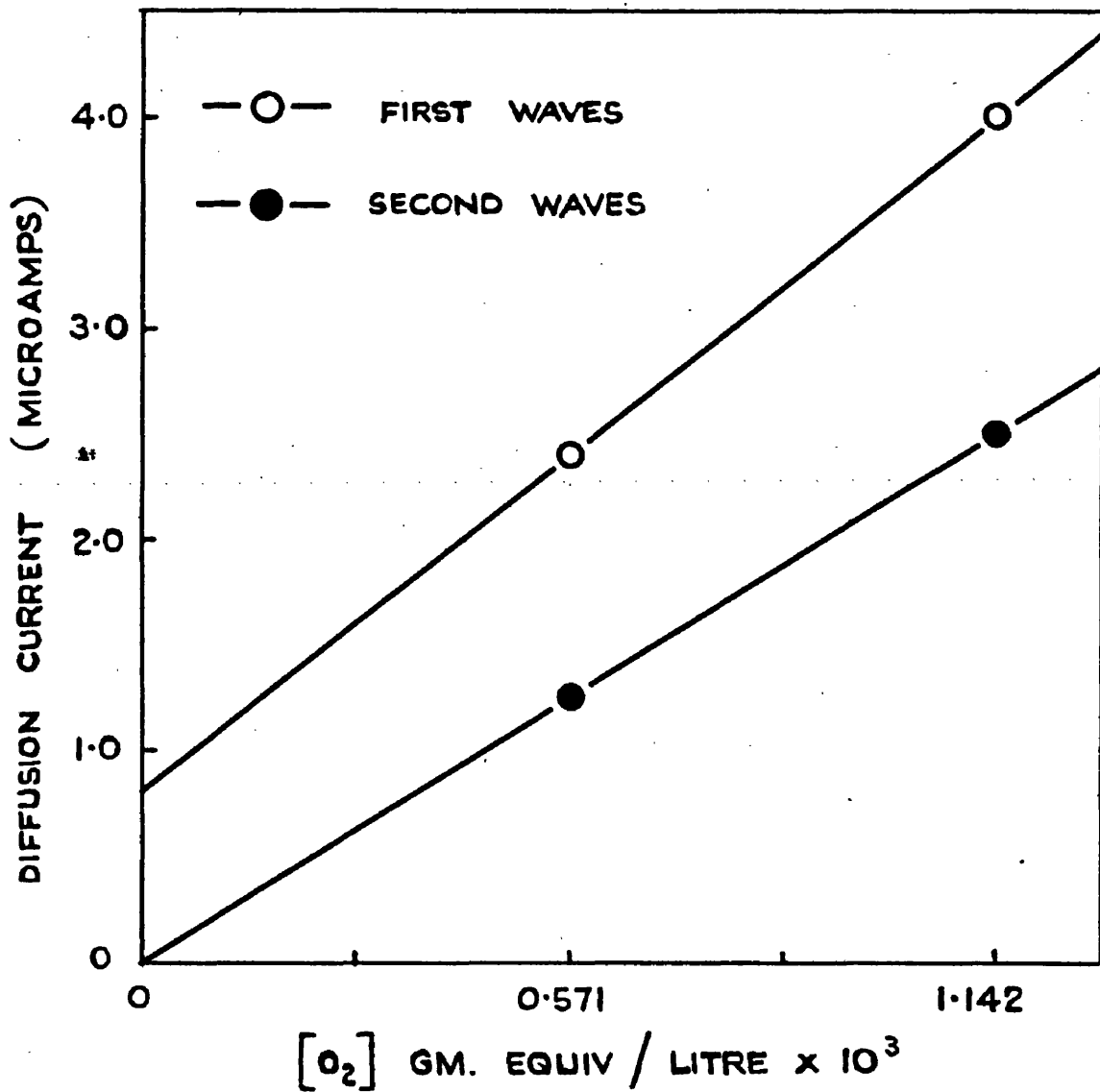
the first oxygen wave. The use of ammonium fluoride as a supporting electrolyte was therefore discontinued.

Hydrochloric and perchloric acids were then tried but were found to be unsuitable since the iron gave waves interfering with the oxygen wave.

Up to this point work was mainly directed towards finding a supporting electrolyte which would enable the oxygen to be estimated by the narrower first wave. It now appeared, however, that there was no alternative but to employ the second wave, for which potassium chloride was found to be a suitable supporting electrolyte. The 100 ml. of solution to be analysed was made 0.08 M in potassium chloride by adding to it 2 ml. of an oxygen free saturated potassium chloride solution at 20°C which is exactly 4.00 M. The maximum suppressor was 0.01% gelatin added as 1 ml. of a 1% solution.

Polarograms obtained with solutions of  $1.3 \times 10^{-3}$  M ferric chloride in 0.08 M potassium chloride and 0.01% gelatin are shown in Fig. 12 which also serves to illustrate the proportionality of step height to oxygen concentration. The solution corresponding to Polarogram 1 contained no oxygen, while that corresponding to Polarogram 2 contained  $0.571 \times 10^{-3}$  gm. equiv. of oxygen/litre. This solution was prepared by adding 50 ml. of air saturated water to 50 ml. of

**FIG.13**



oxygen free  $2.6 \times 10^{-3}$  M ferric chloride solution to give 100 ml. of  $1.3 \times 10^{-3}$  M ferric chloride solution to which the supporting electrolyte and maximum suppressor were added in the usual manner. Polarogram 3 was taken after saturating the latter solution with air to give an oxygen concentration of  $1.142 \times 10^{-3}$  gm. equiv./litre. The half-wave potentials of the two waves are -0.16 V vs. S.C.E. (1st. wave) and -1.05 V vs. S.C.E. (2nd. wave). The diffusion currents (step heights) and corresponding oxygen concentrations are given in the Table below. In order to get accurate values for the diffusion currents, a polarogram was recorded for each wave separately at a higher sensitivity than that used for the polarograms in Fig. 12.

TABLE 11

Oxygen x $10^3$ Gm. Equiv./Litre	Diffusion Current - Microamps. First Wave.	Second Wave.
0.571	2.40	1.25
1.142	4.00	2.50

These results are plotted in Fig. 13 from which it can be seen that the line joining the two points obtained from the second waves of Polarograms 2 and 3 (Fig. 12) passes through the origin, showing direct proportionality between

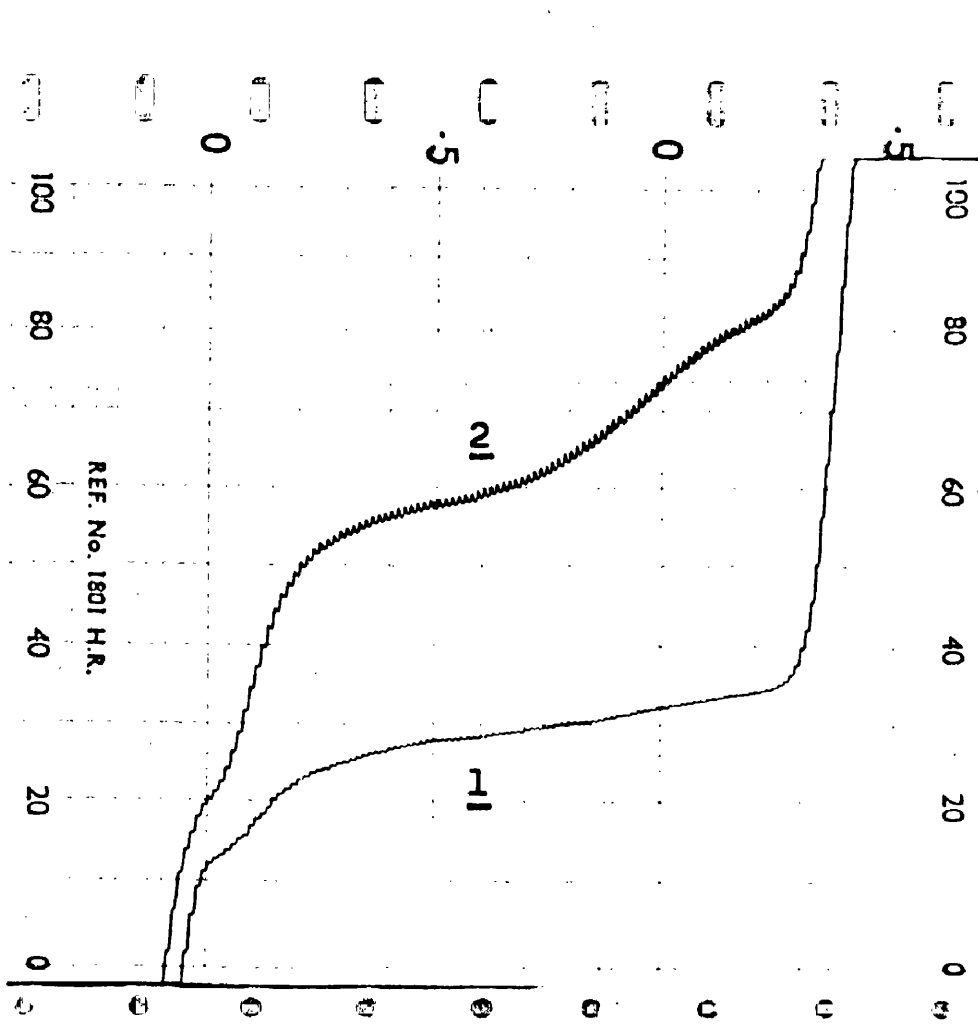
oxygen concentration and diffusion current. The second wave is therefore ideal for the quantitative estimation of dissolved oxygen.

The corresponding line for the first waves, on the other hand, cuts the vertical axis well above the origin at  $0.8 \mu\text{A}$  indicating that there must be a significant rise in the residual current for the oxygen free solution. This rise in the residual current between 0 and -0.5 V vs. S.C.E. is shown in Polarogram 1, Fig. 12 and is the upper end of the ferric iron wave which is shifted to the positive side of zero applied potential by complexing with the chloride ions of the supporting electrolyte, (the ferrous iron wave does not appear).

If the ferric iron concentration had been identical in every estimation, the first wave could have been used by subtracting the blank value of  $0.8 \mu\text{A}$  from every measurement of the diffusion current which would then have been directly proportional to the oxygen concentration. In actual fact, however, the ferric iron concentration varies as a result of photoreduction and this in turn leads to variations in the residual current and therefore in the blank value of the diffusion current. The first wave was therefore considered unreliable for oxygen determination and the second wave was employed.

## FIG. 14

Polarograms of the Oxygen in (1) Non-irradiated  
and (2) Irradiated  $1.3 \times 10^{-3}$  M Ferric Chloride  
Solution.



For any given oxygen concentration, the heights of the two waves in the polarogram should be approximately equal and the discrepancies in the values shown in Table II are due partly to the first wave not being produced entirely by oxygen and partly to the second wave being cut short by the appearance of the hydrogen wave at -1.35 V vs. S.C.E., making the diffusion current as measured, smaller than it would otherwise have been. This is unimportant where a comparative method of calibration is employed as in the present work.

#### The Detection of Photochemically Produced Oxygen.

The polarographic technique is convenient in that the characteristic double wave polarogram of oxygen serves for its qualitative detection.

A  $1.3 \times 10^{-3}$  M ferric chloride solution was irradiated for 5 hours (irradiation vessel completely filled) and the polarogram recorded; the procedure was then repeated under exactly the same conditions except that the solution was not irradiated but kept in the dark. A photograph of the polarograms actually recorded is shown in Fig. 14. Polarogram 2 is for the irradiated solution and Polarogram 1 for the dark solution, both being recorded at the same sensitivity 4.8  $\mu$ A per full scale deflection.

There is no indication of a second wave at  $E_{\frac{1}{2}} -1.05$  V vs. S.C.E. in Polarogram 1, showing that there was no oxygen in the non-irradiated ferric chloride solution. This is also shown by the fact that the value of the diffusion current for the first wave is approximately  $0.8 \mu A$  which, from the calibration curve in Fig. 13, is the value to be expected for a solution containing no oxygen. The half-wave potentials of the two waves in Polarogram 2 correspond exactly with those of the two waves in Polarogram 3, Fig. 12 in which an oxygen-free  $1.3 \times 10^{-3}$  M ferric chloride solution was saturated with air. It is evident, therefore, that the second wave in Polarogram 2, Fig. 14 and the considerable increase in the height of the first wave compared to that in Polarogram 1, must be due to oxygen having been produced photochemically in the irradiated solution.

In support of this conclusion, it was easily shown that Polarogram 2 (Fig. 14) is that of a dissolved gas. After Polarogram 2 had been recorded, nitrogen was bubbled through the solution to remove any other dissolved gases (i.e. other than nitrogen). A second polarogram was then recorded which was found to be identical to Polarogram 1 (Fig. 14), i.e. the nitrogen must have removed the dissolved gas which produced the waves in Polarogram 2.

That oxygen was not produced by the photodecomposition

of water, was shown by the identical polarograms recorded for irradiated and non-irradiated water. This is in accordance with the findings of other workers<sup>105</sup> who have shown that photodecomposition of water does not become appreciable until wavelengths below 190 m $\mu$  are employed, whereas in the present work, the pyrex glass of the irradiation vessel transmits only wavelengths above 300 m $\mu$ .

It therefore appears beyond doubt, that at the wavelengths employed, photochemical oxidation of water in irradiated  $1.3 \times 10^{-3}$  M ferric chloride solutions does take place.

The Relation between the Concentration of Oxygen and Ferrous Iron Produced Photochemically by the Irradiation of  $1.3 \times 10^{-3}$  M Ferric Chloride Solutions

(A) Solutions Irradiated Under an Atmosphere of Nitrogen.

In this series of experiments, a very slow stream of nitrogen was passed over the surface of the 100 ml. of irradiated solution. When irradiation was complete, duplicate 2 ml. samples of the solution were withdrawn for ferrous analysis after which, the 2 ml. of oxygen-free saturated potassium chloride solution and 1 ml. of 1% gelatin solution were added and the polarogram recorded. The solution was then saturated with air for 1 hour and a second

polarogram taken, enabling the oxygen concentration in the irradiated solution to be calculated. Solutions were irradiated for periods up to 6 hours at  $\frac{1}{2}$  hour intervals.

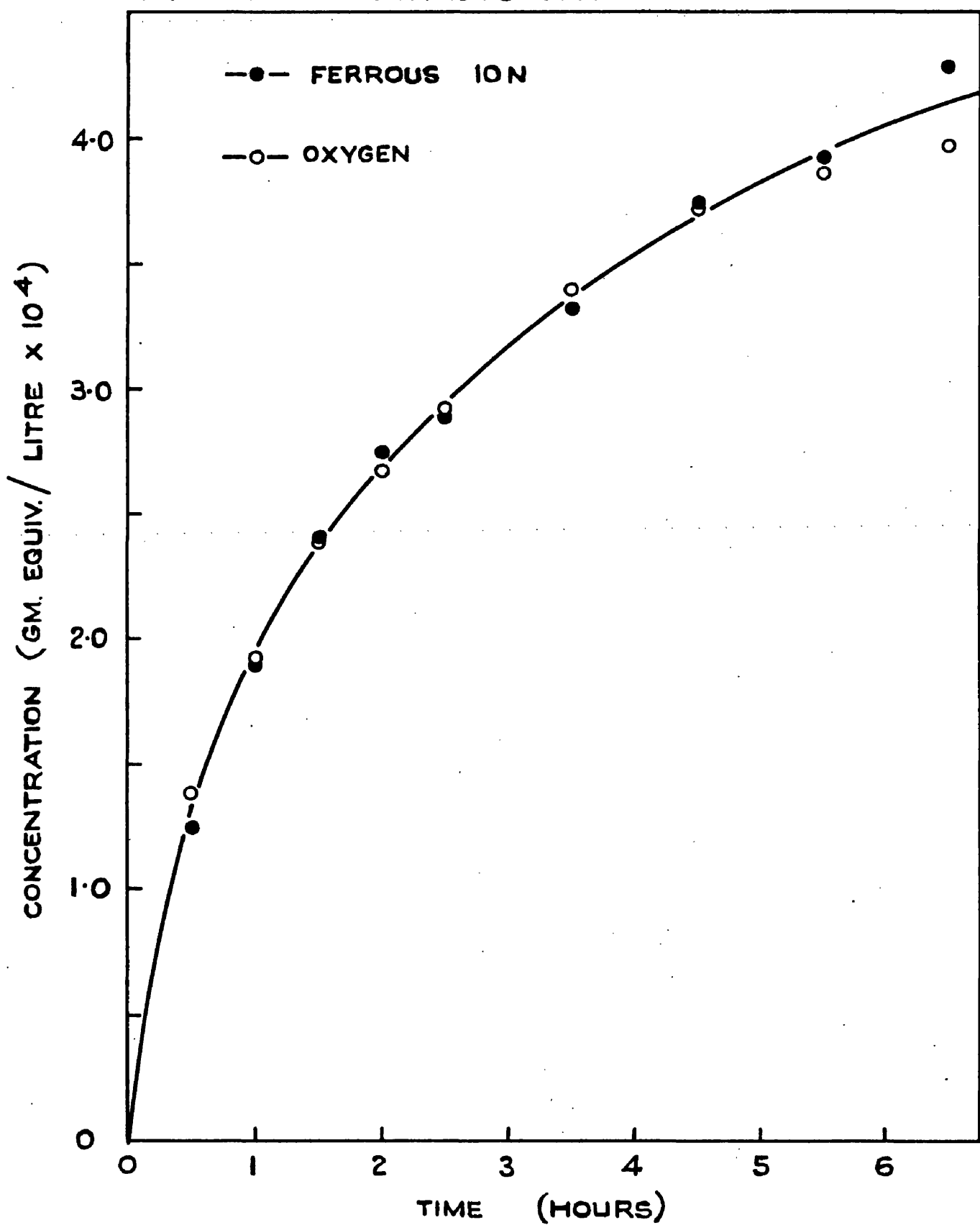
The oxygen concentrations were found to be considerably lower than the corresponding ferrous ion concentrations, the discrepancy becoming greater with increasing periods of irradiation. This was attributed to the loss of oxygen from solution during irradiation, a process which would certainly be encouraged by the slow stream of nitrogen passing over the surface. It was clearly necessary to eliminate this source of error and this was achieved by completely filling the irradiation vessel and stoppering so as to leave no gas space above the solution. This procedure would almost certainly keep the relatively small amount of photoproduced oxygen in solution, but if any gas did come out of solution it would be easily seen.

(B) Solutions Irradiated with the Vessel Completely Filled

and Stoppered.

The procedure in this series of experiments was similar to that above except that after the samples for ferrous analysis were taken, sufficient solution was withdrawn from the cell and discarded in order to reduce the volume remaining in the cell to approximately 100 ml. This was done merely

**FIG. 15**  
**THE PHOTOCHEMICAL PRODUCTION OF**  
**OXYGEN AND FERROUS ION**



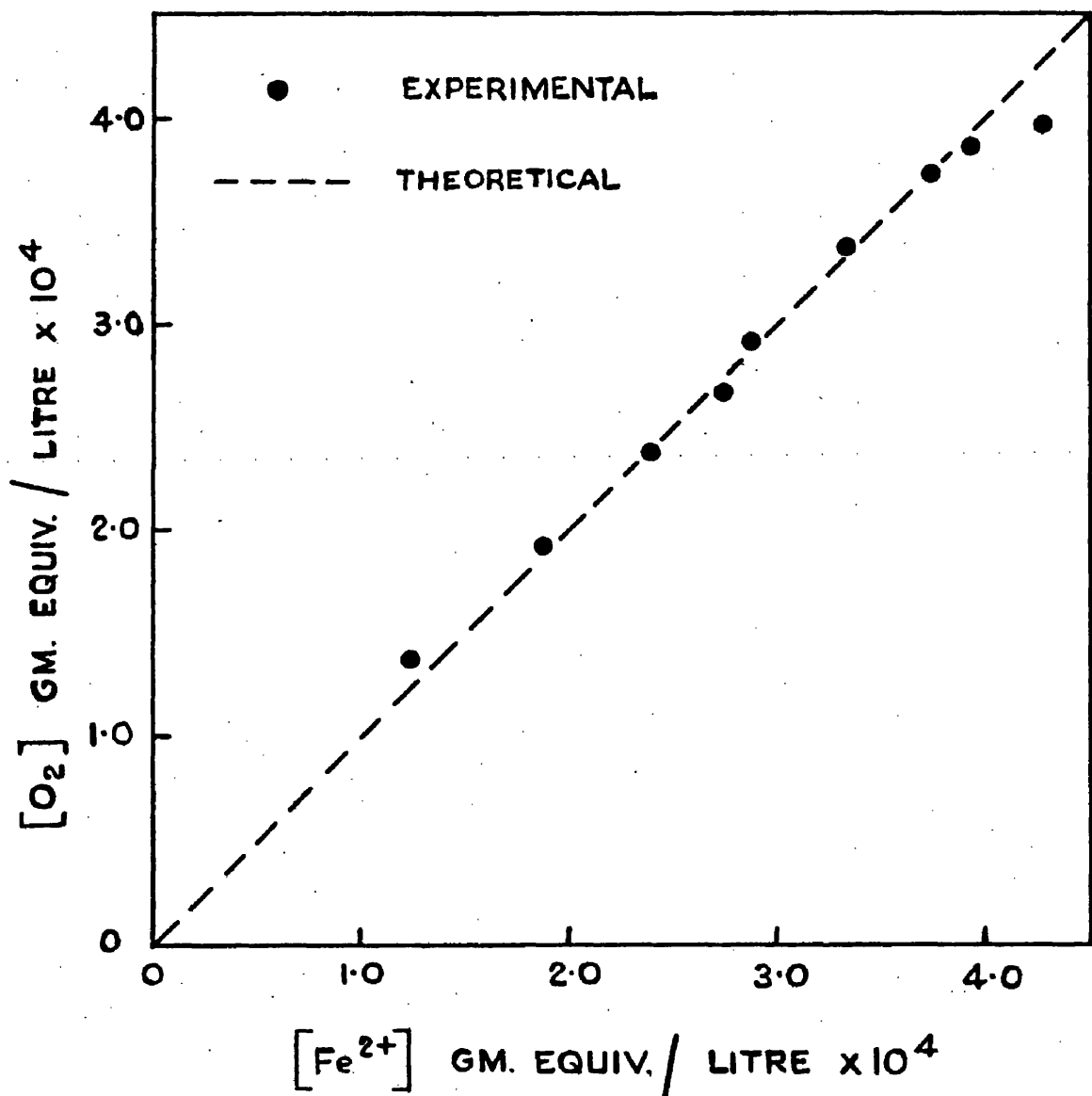
to suit the polarographic assembly which was designed for 100 ml. of solution in the cell.

The results are listed in Table 12, while the oxygen and ferrous ion concentrations are plotted against time in Fig. 15. It can be observed that the oxygen and ferrous ion are formed in equal (equivalent) concentrations and the curves coincide. The shape of the curve is in good agreement with that obtained by Purdon<sup>75</sup> from work on the photo-production of ferrous ion.

TABLE 12

Time Hours.	Concentration.	
	Gm. Equiv./Litre $\times 10^4$	$\text{Fe}^{2+}$
0	0	0
$\frac{1}{2}$	1.38	1.24
1	1.92	1.89
$1\frac{1}{2}$	2.38	2.40
2	2.67	2.74
$2\frac{1}{2}$	2.92	2.88
$3\frac{1}{2}$	3.39	3.32
$4\frac{1}{2}$	3.72	3.74
$5\frac{1}{2}$	3.86	3.92
$6\frac{1}{2}$	3.97	4.28

FIG. 16



In Fig. 16, the oxygen and ferrous ion concentrations are plotted against each other, and the experimental results are seen to be in excellent agreement with the theoretical relation  $[Fe^{2+}] = [O_2]$  indicated by the dotted line.

While the results plotted in Fig. 16 show that the oxygen and ferrous ion are produced in equivalent amounts, that does not prove that they are in fact the true values since it is possible that some back oxidation of the ferrous ion by an equivalent amount of oxygen may have occurred when the supporting electrolyte was added, making all the values somewhat low. However, it was easily shown as follows, that no back oxidation took place.

A  $1.3 \times 10^{-3}$  M ferric chloride solution was irradiated in the normal manner for  $6\frac{1}{2}$  hours after which samples for ferrous analysis were withdrawn. The potassium chloride and gelatin solutions were then added and further samples taken for ferrous analysis at 5 minute intervals for 1 hour. In this way it was found that the total amount of ferrous ion in the solution remained unaltered by the addition of the potassium chloride and gelatin solutions. It can therefore be concluded that no back oxidation of the ferrous ion took place between stopping the irradiation and recording the polarogram, and the values given may be taken as representing the concentrations of oxygen and ferrous ion at the end of the irradiation period.

DISCUSSION.

Of the two methods adopted for the determination of oxygen, the greater sensitivity of the Hersch method is indicated by its ability to detect oxygen (a) in purified 'white spot' nitrogen, (b) from the photodecomposition of water. From a practical point of view, however, the polarographic estimation is probably the simpler to carry out.

It has been shown by these two completely independent methods of oxygen estimation, that oxygen and ferrous ion are produced in equal (equivalent) concentrations in irradiated  $1.3 \times 10^{-3}$  M ferric chloride solutions. Therefore, since the only constituents of the solutions were ferric chloride and water, and since no significant photodecomposition of the water was detected, the oxygen must be formed by the photo-oxidation of water by ferric iron which is thereby reduced to ferrous iron in accordance with the stoichiometry of the equation



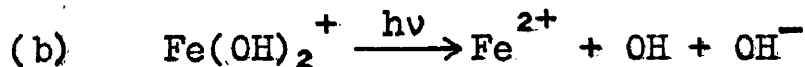
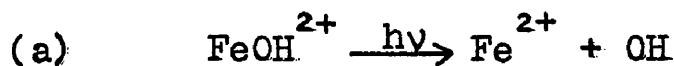
There can be no doubt that the gas was, in fact, oxygen since (a) the Hersch cell is highly specific for oxygen and (b) the double wave polarograms which were recorded were shown to be characteristic of oxygen.

The photo-oxidation of water by ferric iron is thus established.

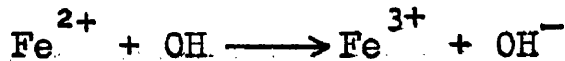
### The Mechanism of the Reaction.

It has been shown in Part 1 that under the conditions of the present investigation, the absorbing species in the solutions are  $\text{FeOH}^{2+}$  ( $\sim 80\%$ ) and  $\text{Fe(OH)}_2^+$  ( $\sim 20\%$ ). The following mechanism is therefore proposed to account for the experimental results:

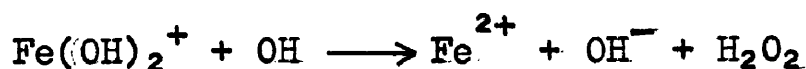
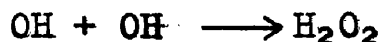
Primary reactions -



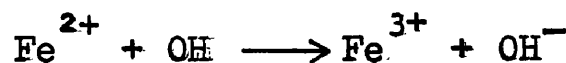
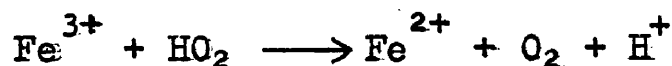
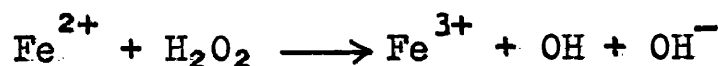
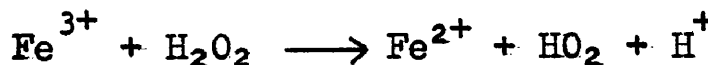
followed by the back reaction-



Formation of hydrogen peroxide by one or more of the following steps -

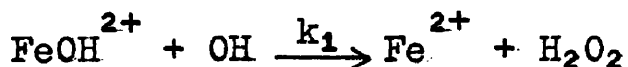
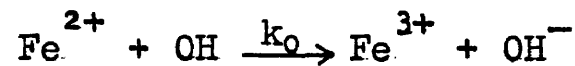


Decomposition of the hydrogen peroxide by iron catalysis -





Uri<sup>4</sup> considers that in the photo-oxidation of water by ferric ion, the two competing reactions would be :-



and concludes that in view of the low ionization potential of ferrous ion in aqueous solution,  $k_0/k_1$  will be very large (compared to the ceric - cerous system) and that extremely high light intensities and large  $\text{FeOH}^{2+}$  concentrations would be required to obtain measurable oxygen yields. It should be noted, however, that in the work described in this section of the thesis, the conditions specified by Uri were, in fact, satisfied. The solutions were irradiated by unfiltered high intensity lamps (e.g. a Hanovia UVS 500) at distances between 3 and 7 inches, and it can easily be shown from Table 7 (page 36) that the solutions had an  $\text{FeOH}^{2+}$  molar concentration of 48%.

Although many modifications of the above reactions are thermodynamically possible in this system, the proposed scheme enables many of the phenomena associated with the photo-oxidation of water by ferric ion, to be qualitatively discussed

The effect of variations in pH and light intensity on the initial reaction rate are described in Part 3.

PART 3

THE VARIATION WITH LIGHT INTENSITY AND pH, OF THE INITIAL  
RATE OF PHOTOCHEMICAL REDUCTION OF FERRIC CHLORIDE SOLUTIONS.

THE QUANTUM YIELD OF THE REACTION.

## INTRODUCTION

The aim of this investigation was to determine the rate of photoreduction of  $1.3 \times 10^{-3}$  M ferric chloride solutions during the first minute of irradiation when the reaction rate is at its highest and the system is uncomplicated by the products of secondary hydrolysis, i.e. the gradual formation of colloidal ferric hydroxide.

Initial experiments were carried out with homogeneous light of wavelength  $365/6 \text{ m}\mu$ , obtained by filtering the light emitted by a 250 watt MED compact source mercury vapour lamp. It was found, however, that there was not sufficient ferrous iron formed to permit of an accurate analysis, and therefore in subsequent work the unfiltered radiation was used consisting of the principal mercury lines between 300 and  $600 \text{ m}\mu$ .

The light energy entering the reaction cell was measured by Parker's <sup>107</sup> actinometric method based on the colorimetric estimation of the ferrous ion formed as a result of the photoreduction of potassium ferrioxalate solution. The light intensity was reduced by the insertion in the beam of an 80 mesh nickel screen, the transmission value of which was found, by separate experiment, to be 0.37. All measurements were carried out on  $1.3 \times 10^{-3}$  M ferric chloride solutions, the pH (2.94) being reduced or increased by the addition of hydrochloric acid or sodium hydroxide respectively.

The variation with light intensity and pH, of the initial rate of reduction was investigated. The reaction rate was observed to increase with increasing light intensity for all pH's within the range studied, viz. 2.1 to 3.7. At a constant light intensity, on the other hand, the reaction rate reached a sharp maximum in the region of pH 2.94 i.e. the 'natural' pH of the solution without the addition of either acid or alkali.

Quantum yields for the ferrous ion production were also calculated. The quantum yield was found to increase (a) as the light intensity decreased, (b) as the pH increased within the range 2.1 to 2.94. The maximum value of the quantum yield obtained at pH 2.94 was  $\sim 0.05$ .

THEORY

The quantum yield  $\phi$  of a photochemical reaction may be expressed in the form

$$\phi = \frac{\text{Chemical change / unit of time}}{\text{Light energy absorbed / unit of time}}$$

When the chemical change is expressed in gm. mol., the light energy is expressed in Einsteins (E) or  $N\hbar\nu$  units, where

$N$  = Avogadro's Constant       $h$  = Planck's Constant

$\nu$  = Frequency of the absorbed radiation.

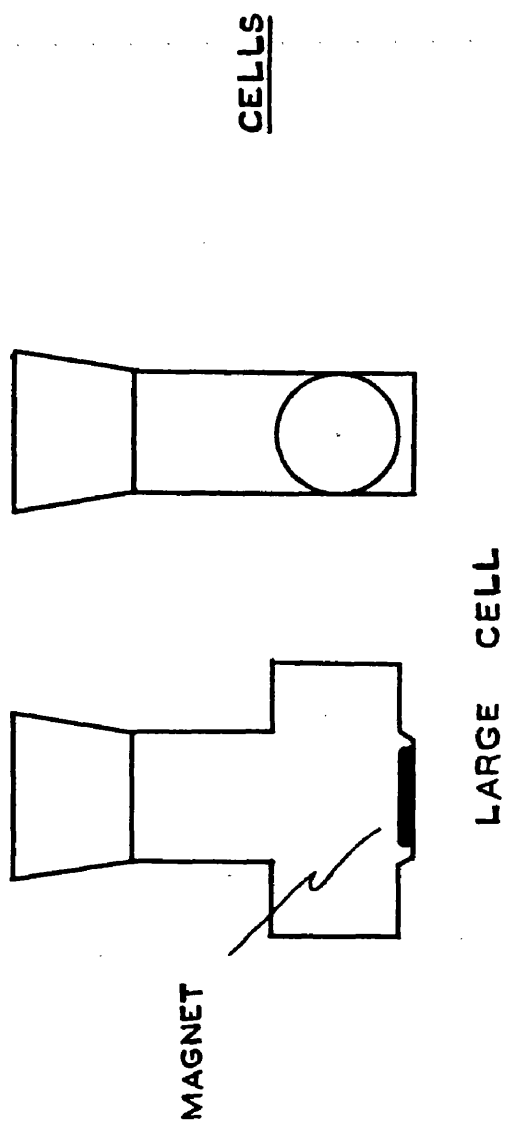
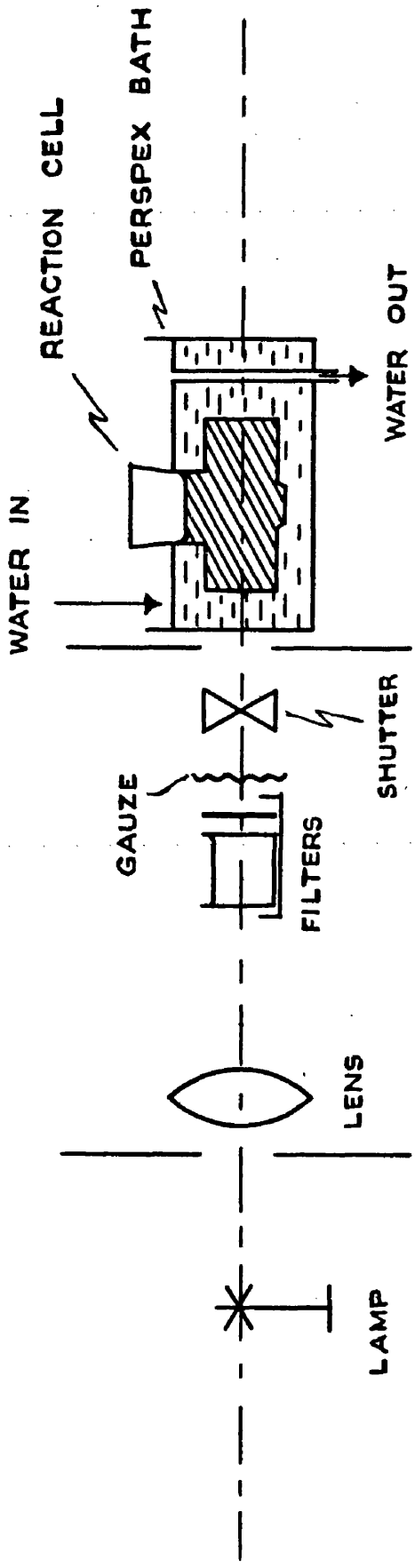
Hence       $\phi = \frac{\frac{dFe}{dt}^{2+}}{kI}$

where,  $k$  = Light absorption fraction

$I$  = Incident Energy in E/unit time.

FIG.17 PHOTOCHEMICAL APPARATUS

OPTICAL ARRANGEMENT



EXPERIMENTAL

Optical Arrangement.

The apparatus is shown in Fig. 17. The light source was a G.E.C. 250 watt MED compact source mercury vapour lamp operated from the mains through a power factor control unit (choke and condenser). The emergent light was brought to a parallel beam by means of a quartz condenser lens of 6.5 cm. focal length.

For the isolation of the 365/6  $\mu$  group of lines, the parallel beam was passed through 2 cm. of 10% copper sulphate solution in conjunction with 2 mm. of Chance Glass OX.I. After the filters, the beam passed through two circular stops to reduce stray light and then through a 'Prontor' camera shutter operated by a cable release. The light then passed through the quartz window of the perspex box (15 cm. x 12 cm. x 11 cm.) through which circulated distilled water at 20°C, and into the irradiation cell clamped in position inside the box. When using polychromatic light, the filters were removed; the nickel screen, when desired, was inserted before the stops.

The lamp and filter section were enclosed in blackened aluminium shields. The whole apparatus was mounted on an optical bench supported over a thermostat tank from which water was pumped into the perspex box which was fitted with

a constant level device. Since the rate at which the ferric chloride solutions hydrolyse varies with temperature, the maintaining of the irradiated solution at constant temperature was very important.

Reaction Cells.

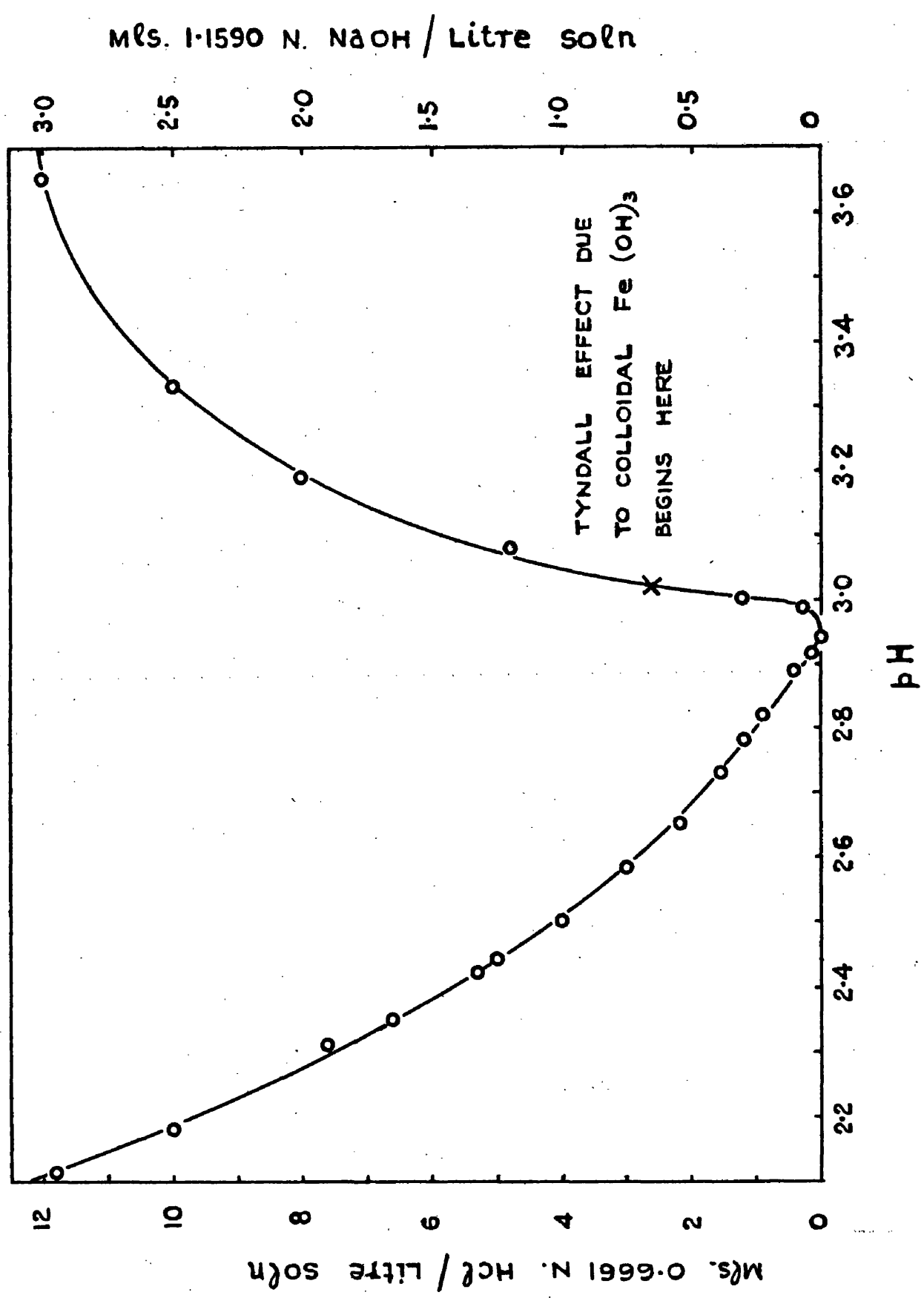
The two cells used are shown in Fig. 17. The larger, made entirely of quartz, had optically plane faces of 4 cm. diameter and an optical depth of 7.3 cm. The cell was filled to a suitable mark engraved on the side (128.3 ml.). The cell had a seat for a magnetic stirrer and a B 40 socket top into which could be fitted a dip-type conductivity cell.

The smaller cell, used for the actinometer solution, was constructed by cementing two 4 cm. diameter quartz end-pieces on to a length of wide bore glass tubing. The cell was of 3 cm. optical depth, 4 cm. diameter and 30 ml. capacity. The cell had two side arms for introducing the solution.

Reaction Technique.

All photolyses of ferric chloride solutions were carried out in the large cell since stirring was necessary to maintain homogeneity. In any run, four 10 ml. samples for ferrous analysis were withdrawn at 15 sec. intervals. The exact

FIG. 18



procedure was to irradiate for 15 seconds, close the shutter and remove the sample, and then open the shutter for another 15 seconds and so on until a total of four samples had been withdrawn after 60 seconds of irradiation. The decrease in volume of the solution was taken into account when calculating the number of moles of ferrous ion formed.

The small cell was filled with the actinometer solution and irradiated for 20 secs. after which the solution was thoroughly shaken and a 2 ml. sample withdrawn for analysis. The light energy was determined each time the lamp was used. The ferrous ion was estimated colorimetrically with 2-2' dipyridyl as previously described (page 56).

#### Preparation of Ferric Chloride Solutions.

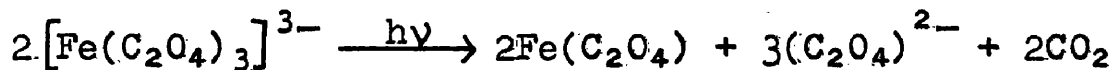
The  $1.3 \times 10^{-3}$  M ferric chloride solutions were prepared from the  $\text{FeCl}_3 \cdot 6\text{H}_2\text{O}$  melt in the usual manner. A solution in water had a pH of 2.94. For lower pH values, the ferric chloride was added to appropriately dilute solutions of hydrochloric acid, while for increased pH values sodium hydroxide was employed. The graph in Fig. 18 relates the pH to the volume of 0.666 N hydrochloric acid or 1.590 N sodium hydroxide per litre of solution.

The solutions were prepared immediately before irradiation by adding 0.02566 ml. of ferric chloride melt to

128.3 ml. of water or solution (magnetically stirred) in the irradiation cell. In this way, the effect of hydrolysis occurring prior to irradiation was minimised.

Actinometry.

The use of potassium ferrioxalate as an actinometer was first reported by Parker<sup>107</sup> and later by Hatchard and Parker<sup>108</sup>. On exposure to light of wavelength less than about 490 m $\mu$ , solutions of the ferrioxalate ion undergo decomposition according to the equation



These authors have determined values of the quantum yield of this reaction under various conditions of temperature, concentration, etc., at the wavelengths of all the principal mercury lines between 254 and 578 m $\mu$ .

By determining the molar concentration of ferrous ion produced per unit of time by the radiation and knowing the quantum yield  $\phi$ , the energy absorbed by the solution is given by

$$I_a = \frac{\frac{d\text{Fe}}{dt}^{2+}}{\phi}$$

By measuring the light absorption fraction  $k$  of the solution, the total light energy  $I$  entering the solution can be calculated from

$$I = I_a / k$$

The actinometer solution employed in the present investigation consisted of 0.006 M potassium ferrioxalate in 0.1 N sulphuric acid. Pure potassium ferrioxalate was prepared by mixing 3 volumes of 1.5 M A.R. potassium oxalate with 1 volume of 1.5 M A.R. ferric chloride with vigorous stirring. The precipitated potassium ferrioxalate was recrystallised three times from warm water and the (green) crystals dried in an oven at 45°C. The composition corresponded to  $K_3Fe(C_2O_4)_3 \cdot 3H_2O$ . The whole procedure was carried out in the dark room.

RESULTS.

I Calculation of the Total Light Energy of the Irradiating Beam.

The initial rates of photoreduction of  $1.3 \times 10^{-3}$  M ferric chloride solutions were studied using the unfiltered radiation from the 250 watt MED compact source mercury vapour lamp. For an evaluation of the quantum yield of the reaction a knowledge of the total light energy of the irradiating (polychromatic) beam was necessary. This was calculated from actinometric measurements (a) with filtered 'monochromatic' light of wavelength 365/6 m $\mu$  and (b) with the polychromatic light, as follows.

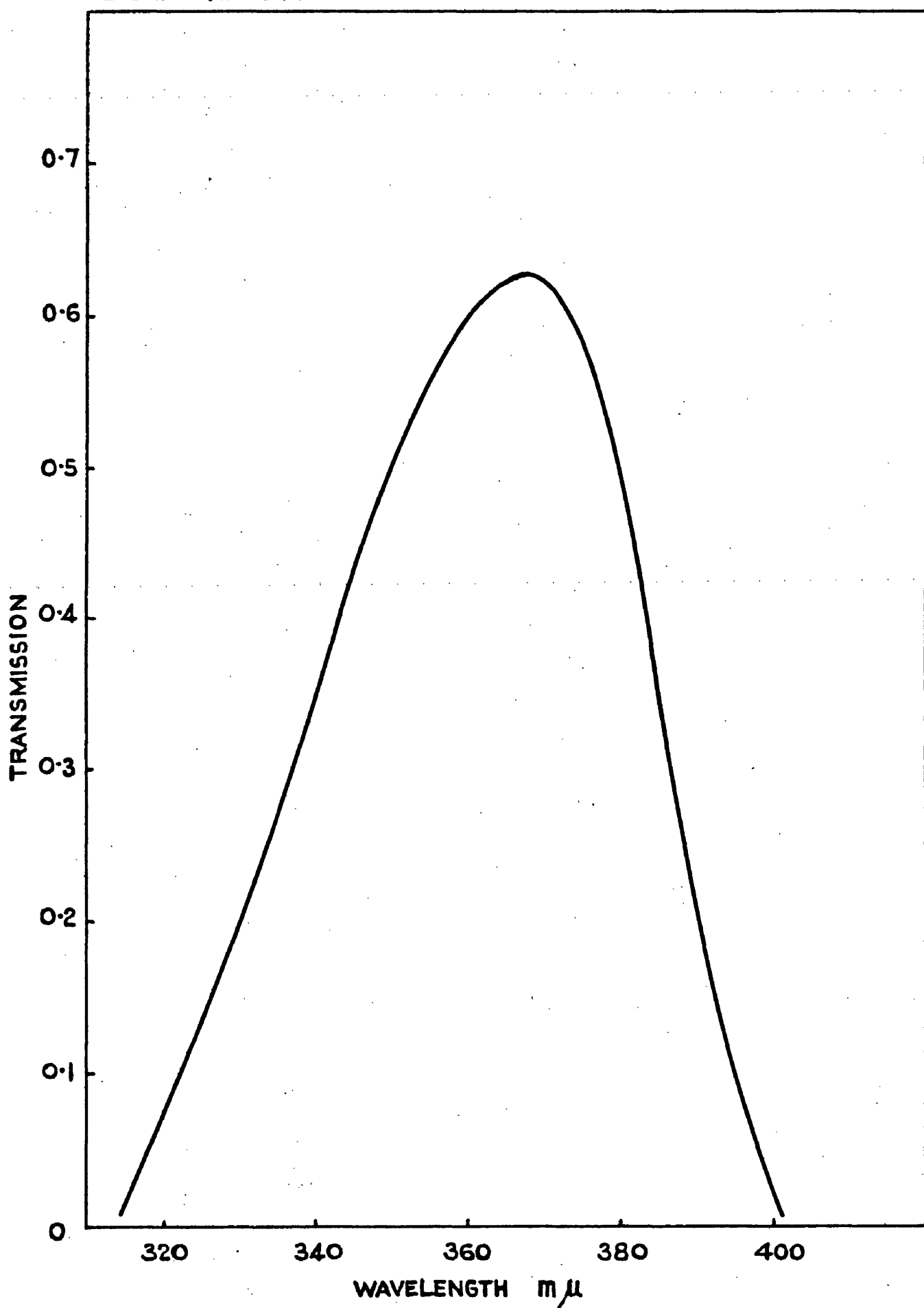
(a) Measurements with monochromatic light of wavelength

365/6 m $\mu$ .

In the initial experiments with light of wavelength 365/6 m $\mu$ , isolated by 2 cm. of 10% w/v copper sulphate solution and 2 mm. of Chance Glass OX 1, about fifty determinations of the light energy were carried out before the change-over to polychromatic light. The actinometer solution was exposed to the light in the 3 cm. cell and the exposure timed with a stopwatch (1 rev. = 10 secs.). A specimen calculation is shown below.

**FIG.19**

TRANSMISSION CURVE FOR 2 CM 10% Cu SO<sub>4</sub> SOLN  
+ 2 MM. CHANCE GLASS OXI MEASURED AGAINST  
2 CM WATER



Volume of solution = 30 ml.

Exposure time = 40 secs.

By analysis, the concentration of  $\text{Fe}^{2+}$  produced =  $1.93 \times 10^{-4}$  M

$$\begin{aligned}\text{No. of moles of } \text{Fe}^{2+} \text{ produced} &= \frac{1.93 \times 10^{-4} \times 30}{1000} \\ &= \underline{\underline{5.79 \times 10^{-6}}}\end{aligned}$$

$$\begin{aligned}\frac{d\text{Fe}^{2+}}{dt} &= \frac{5.79 \times 10^{-6} \times 60}{40} \\ &= \underline{\underline{8.69 \times 10^{-6} \text{ mole/minute}}}.\end{aligned}$$

I, the light energy entering the cell, =  $\frac{d\text{Fe}^{2+}}{dt} / k\phi$

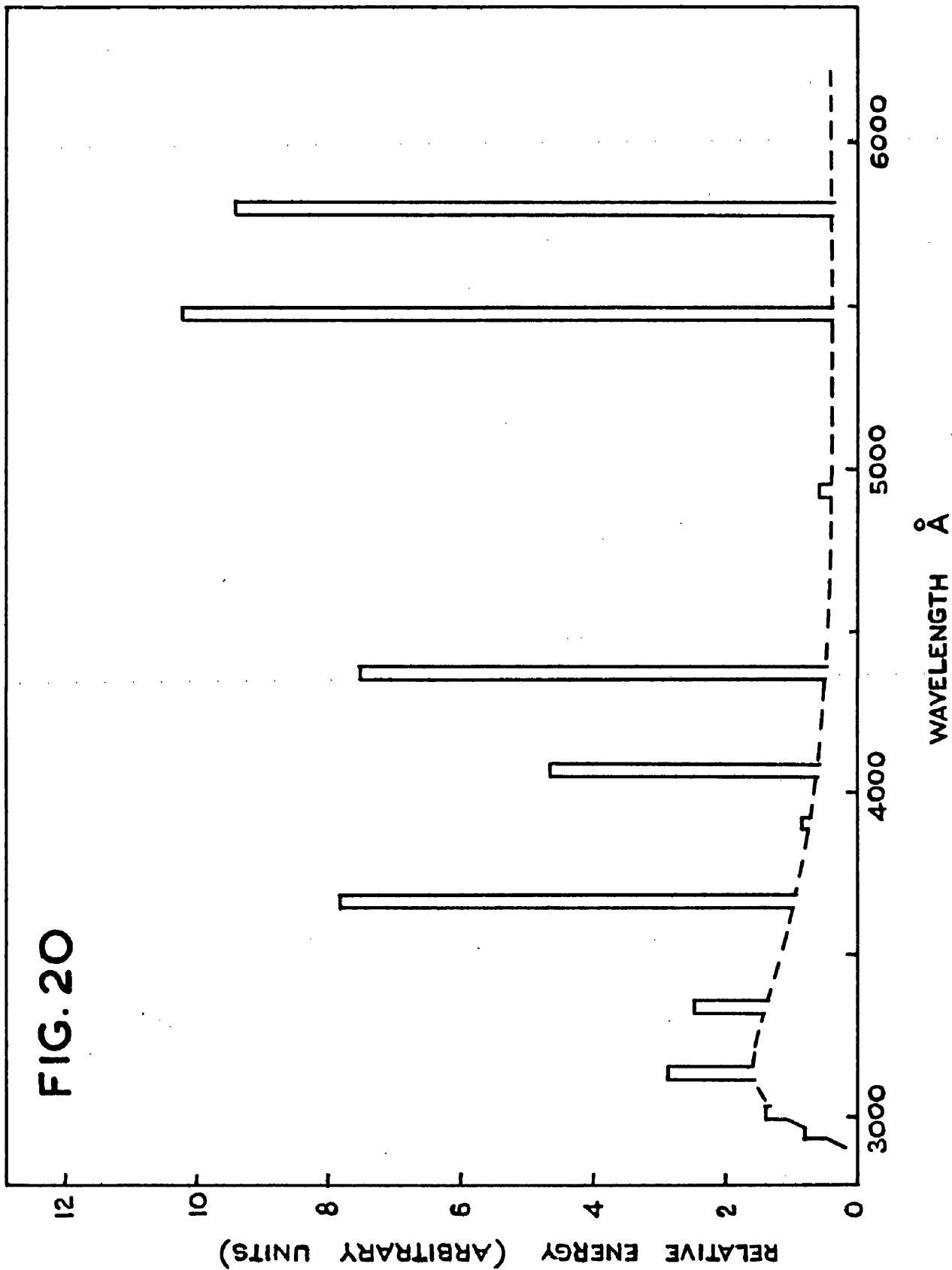
For light of  $365/6 \mu$ , Parker's value of  $\phi = 1.21$ , and for 3 cm. of actinometer solution, k the absorption fraction = 1 (obtained from Fig. 21)

$$I = \frac{8.69 \times 10^{-6}}{1.21} = \underline{\underline{7.20 \times 10^{-6} \text{ Einsteins / minute}}}.$$

The average value (over fifty readings) of the light energy entering the cell was  $7.24 \times 10^{-6} \text{ E / min.}$

The transmission curve of the copper sulphate - Chance Glass filter system is shown in Fig. 19. The transmission values were measured in a Unicam SP 600 spectrophotometer using a strip of Chance Glass OX 1 in conjunction with a

**FIG. 20**



2 cm. cell filled with the 10% copper sulphate solution. The value of the transmission at  $365/6 \text{ m}\mu$ , obtained from Fig. 19, is 0.625. Hence the energy of the light of wavelength  $365/6 \text{ m}\mu$  actually emitted by the lamp, i.e. unfiltered

$$\begin{aligned} &= \frac{7.24 \times 10^{-6}}{0.625} \\ &= \underline{\underline{1.16 \times 10^{-5} \text{ E / minute}}} \end{aligned}$$

In Fig. 20 is reproduced a graph kindly supplied by the General Electric Co., Ltd., showing the relative energy values in arbitrary units of all the principal lines emitted by the lamp, the dotted curve being an approximate indication of the background radiation. Now since the absolute value of the  $365/6 \text{ m}\mu$  line is known ( $1.16 \times 10^{-5} \text{ E/min.}$ ), the absolute value of the total energy (in the irradiating beam) emitted by the lamp can be obtained by dividing  $1.16 \times 10^{-5} \text{ E/min.}$  by the relative energy value (R.E. = 7.90) of the  $365/6 \text{ m}\mu$  line in the arbitrary units given in the graph and multiplying the result by the total relative energy value of all the lines ( $\sum \text{R.E.} = 49.10$ ).

$$\begin{aligned} \text{i.e.. Total Energy} &= \frac{1.16 \times 10^{-5} \times \sum(\text{R.E.})}{(\text{R.E.})_{365/6}} \\ &= \underline{\underline{7.20 \times 10^{-5} \text{ E / minute.}}} \end{aligned}$$

This is the energy of the polychromatic irradiating beam and is calculated to check the value obtained from the measurements with polychromatic light.

(b) Measurements with Polychromatic Light.

Each time a run was carried out with the polychromatic light, the ferrous ion produced per minute in the actinometer solution was determined in a manner similar to that described for the light of wavelength 365/6 m $\mu$ .

In the calculation of the total light energy, two difficulties arise viz., the quantum yield  $\phi$  and the light absorption factor k for the actinometer solution both vary with the wavelength of the light.

In general, if  $I_1, I_2, I_3, I_4, \dots$  are the energy values of the absorbed radiation at a series of wavelengths and  $\phi_1, \phi_2, \phi_3, \phi_4, \dots$  are the quantum yields of the resultant reaction, then the average value  $\phi_{av}$  of the quantum yield is given by

$$\phi_{av} = \frac{\phi_1 I_1 + \phi_2 I_2 + \phi_3 I_3 + \dots}{I_1 + I_2 + I_3 + \dots} \quad \frac{\sum \phi I}{\sum I}$$

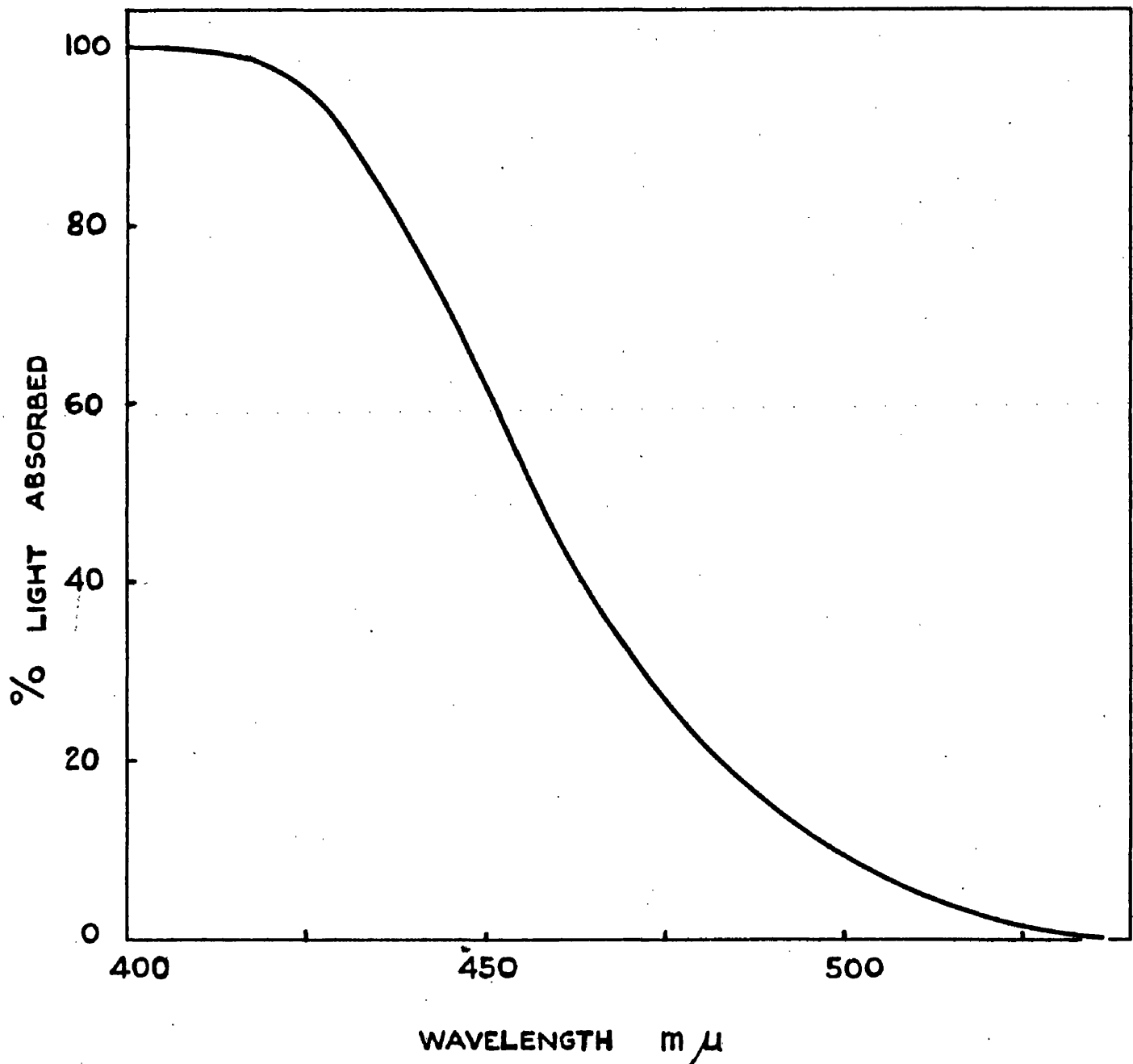
In the present case,  $I = k(R.E.)a$

where,  $k$  = the light absorption fraction for 3 cm. of actinometer solution at any particular wavelength.

(R.E.) = the relative energy value of the radiation

**FIG. 21**

ABSORPTION CURVE FOR 3 CM OF 0.006 M  
POTASSIUM FERRIOXALATE IN 0.1 N  $H_2SO_4$



a = the factor converting relative energy values  
into absolute energy values.

For the actinometer solution,

$$\phi_{av} = \frac{\sum \phi k(R.E.) a}{\sum k(R.E.) a} = \frac{\sum \phi k(R.E.)}{\sum k(R.E.)}$$

Values of (R.E.) are obtained from Fig. 20 while values of  $\phi$  are given by Hatchard and Parker. Values of k are obtained from the absorption curve for 3 cm. of actinometer solution, shown in Fig. 21. The data relating to the calculation of  $\phi_{av}$  are shown in Table 13.

TABLE 13

Wavelength(mu)	$\phi$	(R.E.)	k	k.(R.E.)	$\phi.k.(R.E.)$
492	0.88	0.6	0.14	0.1	0.1
436	1.11	7.6	0.94	7.1	7.9
405	1.14	4.7	1.0	4.7	5.4
392	1.15	0.9	1.0	0.9	1.0
365/6	1.21	7.9	1.0	7.9	9.6
334	1.23	2.5	1.0	2.5	3.1
313	1.24	2.9	1.0	2.9	3.6
297/302	1.24	2.2	1.0	<u>2.2</u> <u>28.3</u>	<u>2.7</u> <u>33.4</u>

$$\therefore \phi_{av} = \frac{33.4}{28.3} = 1.18$$

Beyond 492 m $\mu$ , k drops to zero at 540 m $\mu$ , so that the next intense line at 546 m $\mu$  is not absorbed. Now since the ferrous ion produced =  $5.24 \times 10^{-5}$  mole/min., the polychromatic light energy absorbed by the actinometer solution

$$= \frac{5.24 \times 10^{-5}}{1.18} = \underline{\underline{4.44 \times 10^{-5} \text{ E/minute.}}}$$

This value represents only that part of the total light energy which is absorbed by the actinometer solution, and corresponds to a relative energy value of 28.3 ( $\sum k(R.E.)$ ). The total energy of the irradiating beam corresponds (see Fig. 20) to a relative energy value of 49.1 ( $\sum(R.E.)$ ). Hence the total energy of the irradiating beam

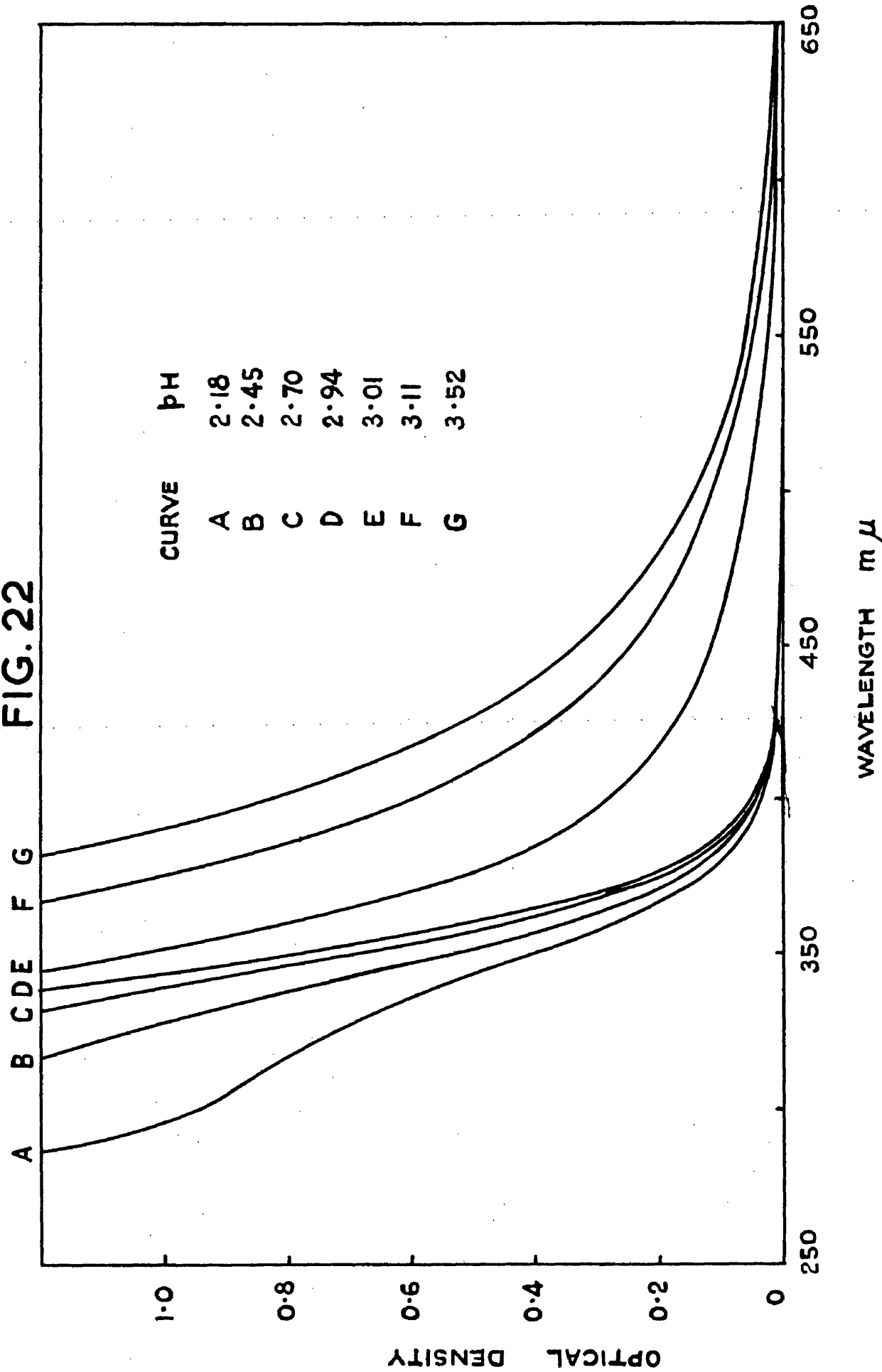
$$= \frac{4.44 \times 10^{-5} \times \sum(R.E.)}{\sum k.(R.E.)}$$

$$= \frac{4.44 \times 10^{-5} \times 49.1}{28.3}$$

$$= \underline{\underline{7.71 \times 10^{-5} \text{ E / minute.}}}$$

This value is slightly higher than the value  $7.20 \times 10^{-5}$  E/min. calculated in the previous section from measurements with the filtered light of wavelength 365/6 m $\mu$ . A possible explanation is that the previous calculation takes no account of the continuous radiation between the principal lines and which is possibly significant between 300 and 400 m $\mu$ . This

FIG. 22



error will be corrected to some extent in the latter calculation where the actinometer solution absorbs all the radiation in that region.

The value of the total energy of the unfiltered irradiating beam will therefore be taken as  $7.71 \times 10^{-5}$  E / minute. The energy of the beam at the lower intensity i.e. with the nickel screen in position, is  $7.71 \times 10^{-5} \times 0.374$   
=  $2.88 \times 10^{-5}$  E / minute.

## II Calculation of the Light Energy Absorbed by the Ferric Chloride Solutions during Irradiation.

The extent to which light is absorbed by  $1.3 \times 10^{-3}$  M ferric chloride solutions varies with pH and absorption curves (from optical density measurements) can easily be obtained for pH values up to 2.94. Above this value, however, secondary hydrolysis takes place rapidly, colloidal ferric hydroxide appears and it is not readily possible to say to what extent the light is absorbed or scattered, since both of these factors contribute to the optical density as measured in a spectrophotometer.

Fig. 22 shows the optical density curves (1 cm. cells) obtained for  $1.3 \times 10^{-3}$  M ferric chloride solutions at various pH's while Fig. 23 shows the calculated absorption

FIG. 23

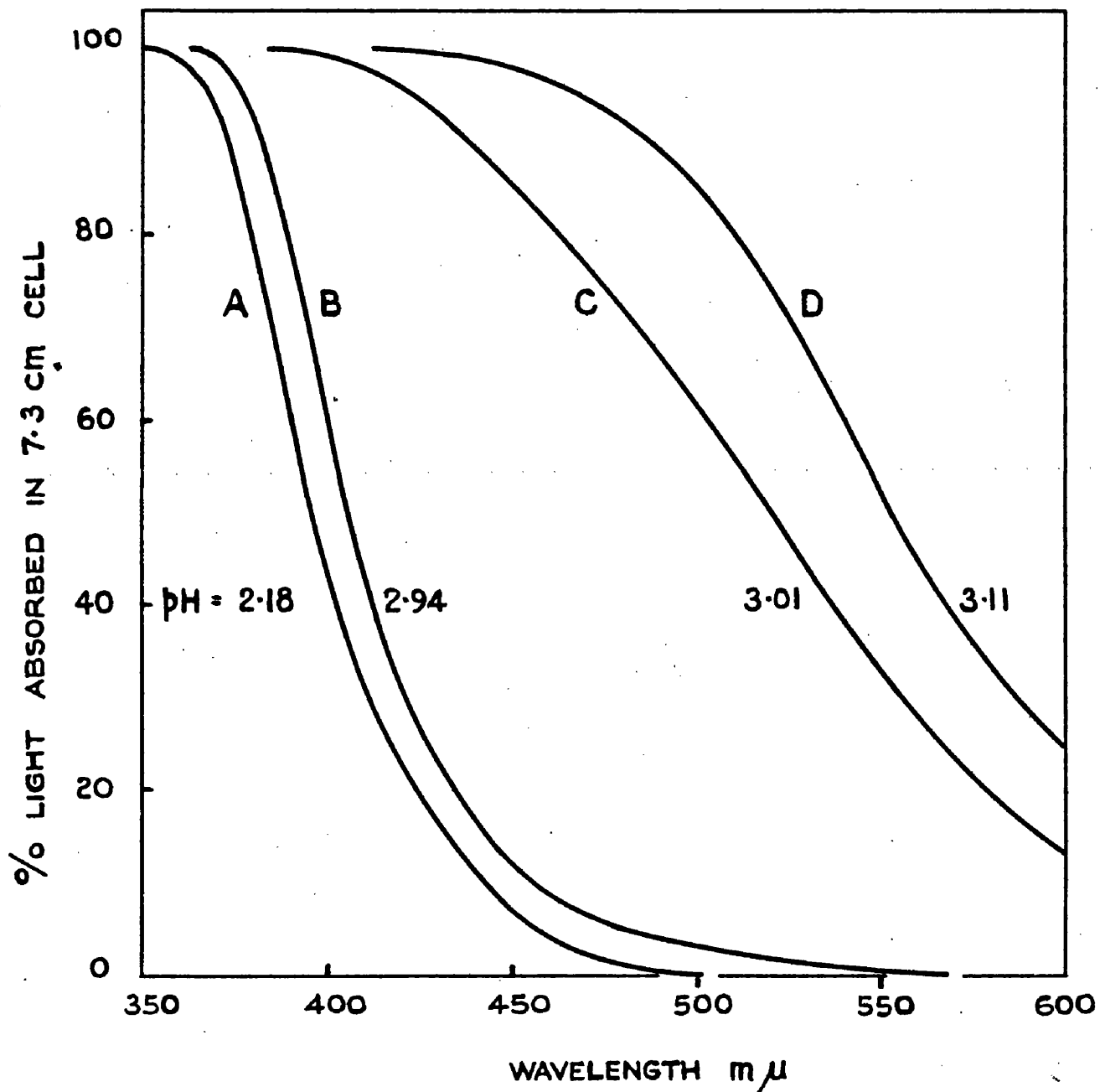
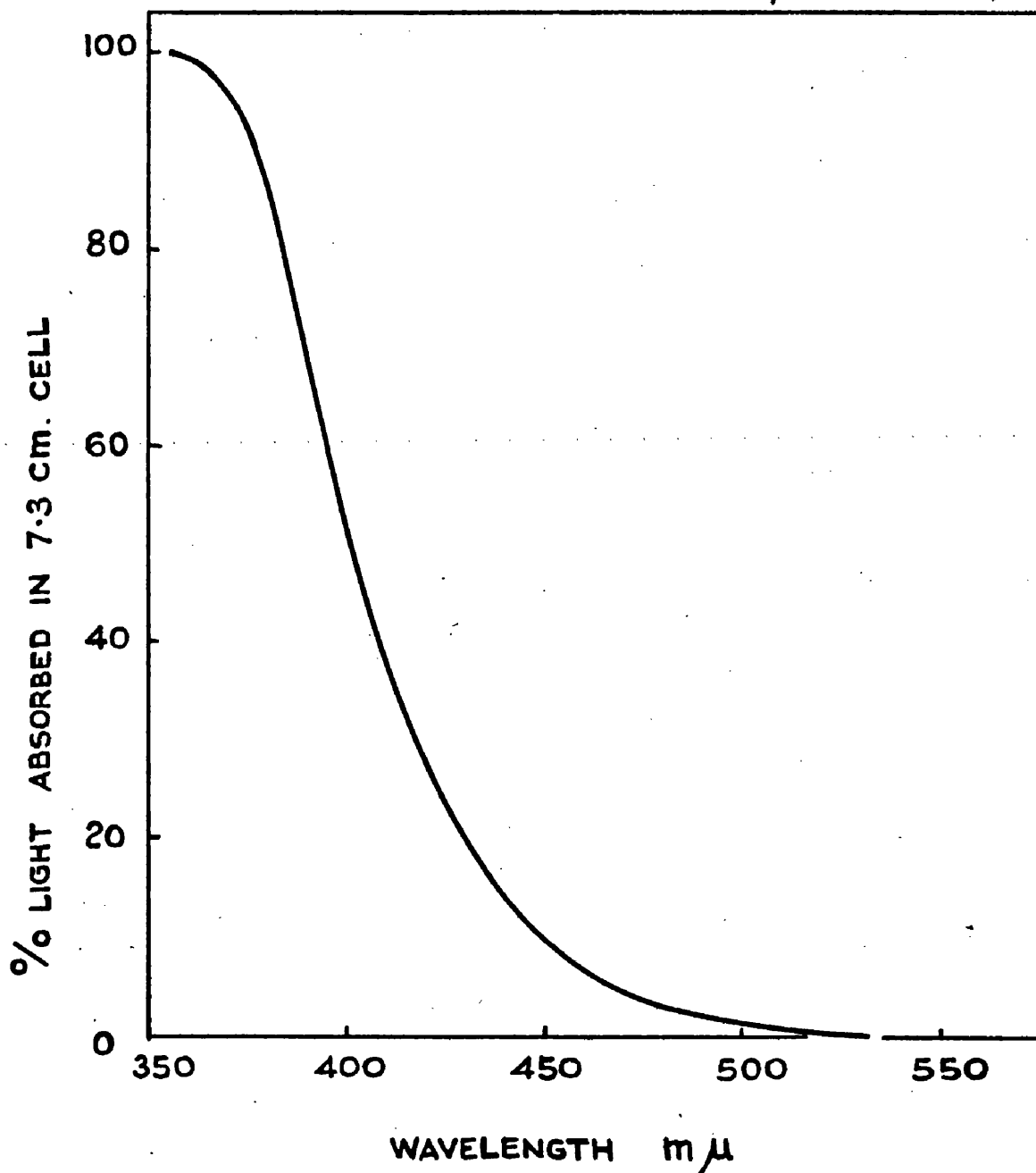


FIG. 24

AVERAGE ABSORPTION CURVE FOR  $1.3 \times 10^{-3}$  M  
FERRIC CHLORIDE SOLUTIONS OF pH 2.18 - 2.94



curves for 7.3 cm. (the path length of the large cell) of  $1.3 \times 10^{-3}$  M ferric chloride solution at four pH values between 2.18 and 3.11. In solutions of pH above 2.94, the hydrolysis taking place during the optical density measurements gave rise to curves such as C and D in Fig. 23, showing higher absorption values than would otherwise have been obtained. For this reason, no attempt was made to calculate the light energy absorbed by these solutions.

The absorption curves of all solutions from pH 2.18 to 2.94 lie within the curves A and B (Fig. 23) which were considered close enough to permit the assumption of an average absorption curve to facilitate the calculation. This average absorption curve is shown in Fig. 24. The fraction of the total light energy absorbed by these solutions can now be calculated from the light absorption fraction k obtained from Fig. 24, and the relative energy values from Fig. 20. The data are given in Table 14.

TABLE 14

Wavelength (m $\mu$ )	(R.E.)	k	k.(R.E.)
297	0.8	1.00	0.80
302	1.4	1.00	1.40
313	2.9	1.00	2.90
334	2.5	1.00	2.50
365/6	7.9	0.98	7.75
392	0.9	0.65	0.60
405	4.7	0.44	2.05
436	7.6	0.16	1.20
492	0.6	0.02	0.01
546	10.3	0	0
577/9	<u>9.5</u> <u>49.1</u>	0	<u>0</u> <u>19.2</u>

Fraction of the total light energy absorbed by the  
irradiated ferric chloride solutions =  $\frac{\sum k.(R.E.)}{\sum (R.E.)}$

$$= \frac{19.2}{49.1} = \underline{0.39}$$

Hence the light energy absorbed by  $1.3 \times 10^{-3}$  M ferric chloride  
solutions in the pH range 2.18 to 2.94, during irradiation

$$= 0.39 \times 7.71 \times 10^{-5} E / \text{minute.}$$

$$= \underline{3.01 \times 10^{-5} E / \text{minute.}}$$

The corresponding value at the lower light intensity

$$= 0.39 \times 2.88 \times 10^{-5}$$

$$= \underline{1.13 \times 10^{-5} \text{ E / minute.}}$$

### III Initial Rates of Photoreduction of $1.3 \times 10^{-3} \text{ M Ferric Chloride Solutions in the pH Range } 2.10 - 3.70$

In this series of experiments, the initial rate of reduction was determined at each pH first at the high intensity and then, after insertion of the nickel screen, at the lower intensity. A typical calculation was as follows :-

$$[\text{FeCl}_3] = 1.3 \times 10^{-3} \text{ M} \quad \text{pH} = 2.94 \quad \text{Temperature} = 20^\circ\text{C}$$

$$\text{Total energy of the irradiating beam} = 7.84 \times 10^{-5} \text{ E / min.}$$

$$\text{Initial volume of solution} = 128.3 \text{ ml.}$$

10 ml. withdrawn for analysis at 15 second intervals.

Time sec.	Extinction	$[\text{Fe}^{2+}] \text{ M} \times 10^5$	Moles $\text{Fe}^{2+}$ formed $\times 10^7$	$[\text{Fe}^{2+}] \text{ M} \times 10^7$ corrected for samples withdrawn
15	0.024	0.280	3.60	3.60
30	0.041	0.478	5.65	5.93
45	0.058	0.681	7.39	8.15
60	0.077	0.904	8.98	10.42

FIG. 25

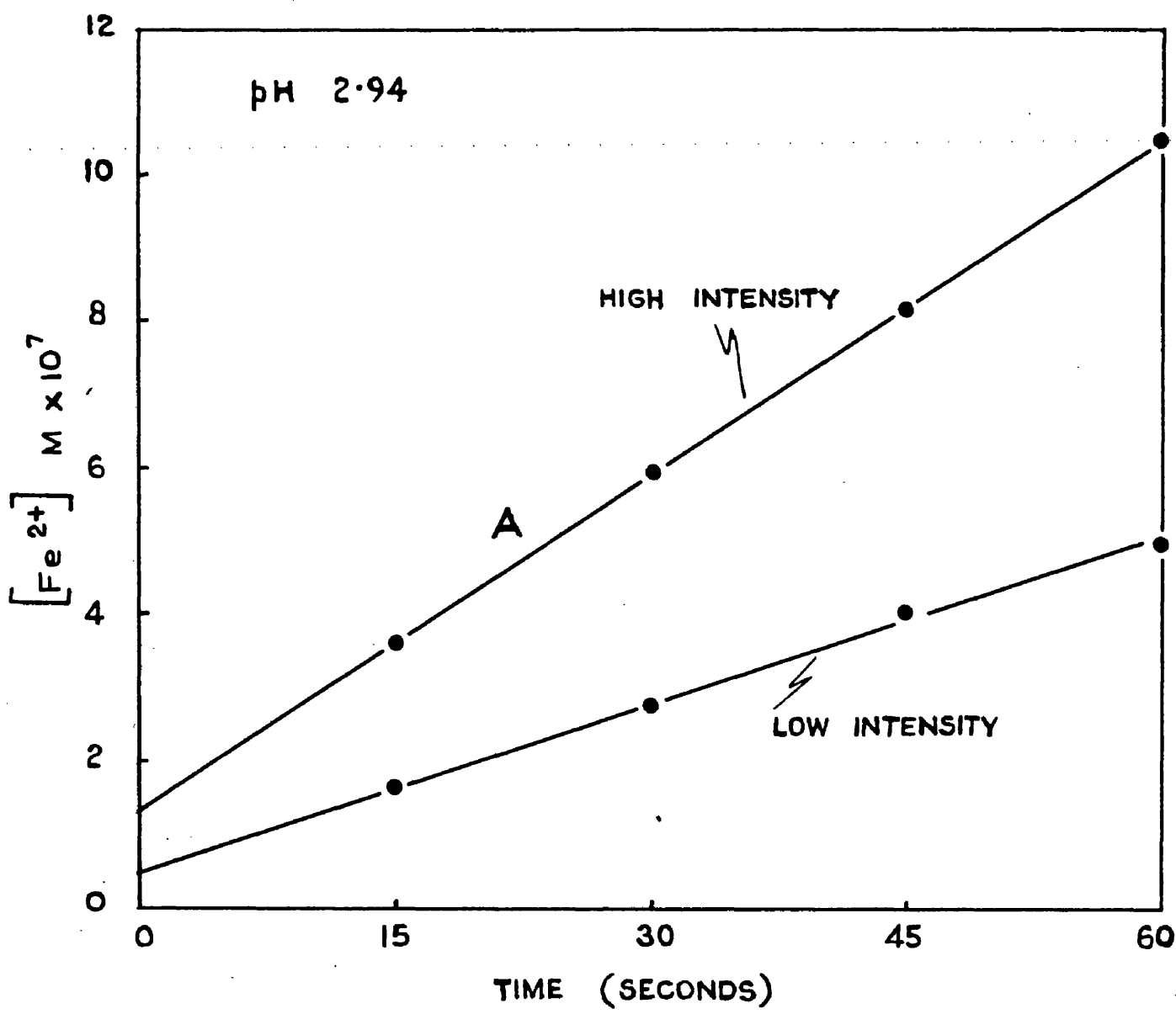
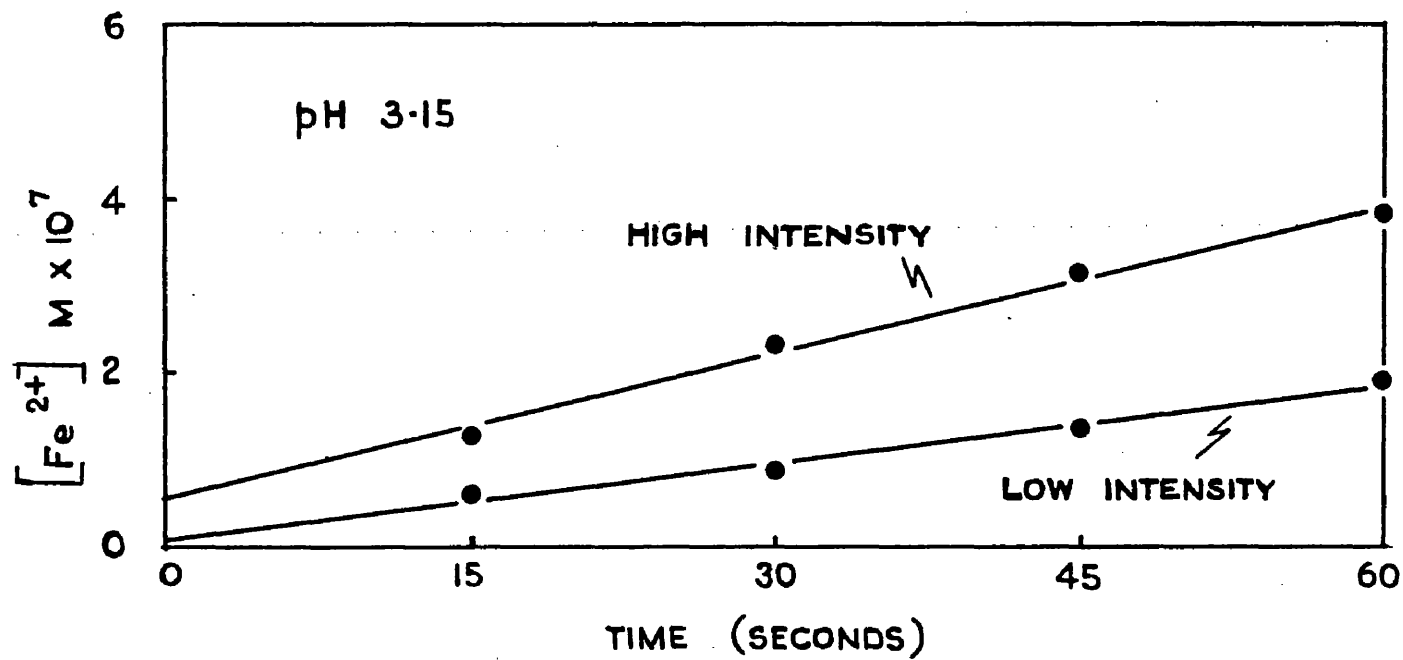


Fig. 25 shows the plot of ferrous ion formed, against time at two pH values, the points for the line marked 'A' at pH 2.94 being those calculated above. In drawing these and similar graphs, the same procedure was adopted throughout namely, the best straight line was drawn through the four points. At either light intensity, at any pH, the four points always lie fairly closely on a straight line which intersects the vertical ordinate above the origin. This is not due to ferrous ion initially in the solution because a blank estimation was always carried out, but could be explained by the photo-oxidation by ferric ion in the first seconds of irradiation, of traces of organic impurities in the water. The initial rate of reduction,  $\frac{d\text{Fe}^{2+}}{dt}$  corresponding to the above calculation was found from graph A, Fig. 25 to be  $9.12 \times 10^{-7}$  mole / minute.

The energy values of the irradiating beam at the two intensities were found to vary from day to day within  $\pm 7\%$  of the average values of  $7.71 \times 10^{-5}$  and  $2.88 \times 10^{-5}$  E / min. calculated on page 112. This variation was taken into account when plotting reduction rates against pH by a direct proportion correction of the rate values to the values expected for the average light energy. For example, a reduction rate of  $9.12 \times 10^{-7}$  mole/min. at a light energy of  $7.84 \times 10^{-5}$  E/min. would become  $8.96 \times 10^{-7}$  mole/min. at the

**FIG. 26**

EFFECT OF pH AND LIGHT INTENSITY ON THE INITIAL RATE OF FERROUS ION FORMATION

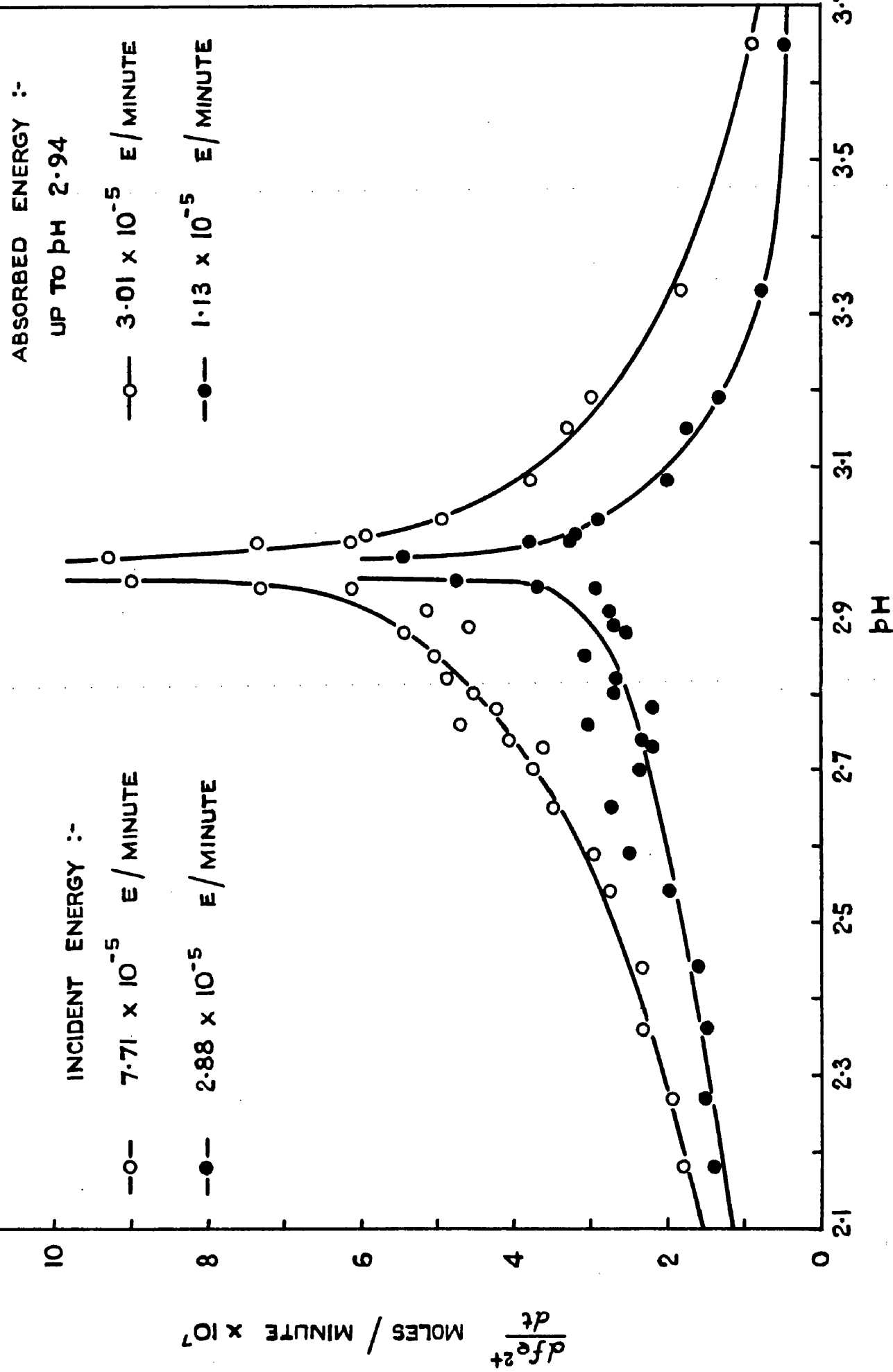


FIG. 27

QUANTUM YIELDS

ENERGY OF ABSORBED RADIATION :-

$$A \quad 1.13 \times 10^{-5} \text{ E / MINUTE}$$

$$B \quad 3.01 \times 10^{-5} \text{ E / MINUTE}$$

6

5

4

3

2

1

0

QUANTUM YIELD  $\times 10^2$

pH

3.0

2.8

2.6

2.4

2.2

A

B

- - -

average light energy of  $7.71 \times 10^{-5}$  E / min. Although  $\frac{d\text{Fe}^{2+}}{dt}$  is not proportional to the light energy, the error incurred in assuming direct proportionality is considered to be negligible.

Fig. 26 shows the initial rates of ferrous ion formation plotted against pH at the two intensities. At either intensity, the rate reaches a maximum in the region of pH 2.9.

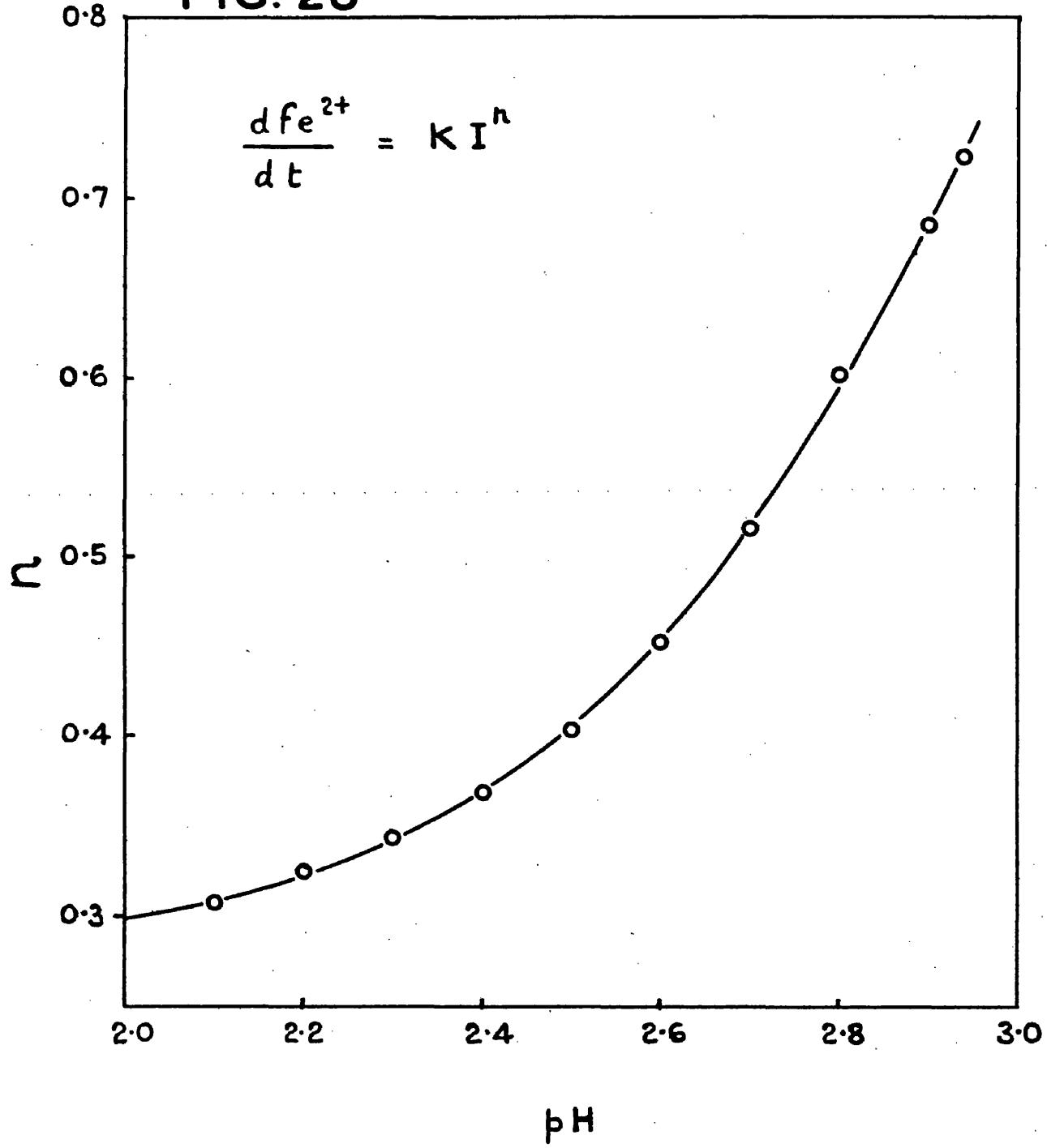
#### IV Quantum Yields.

$$\text{The quantum yield } \phi = \frac{\frac{d\text{Fe}^{2+}}{dt}}{kI} / kI$$

$kI$ , the energy absorbed by the solution, has the values  $3.01 \times 10^{-5}$  E/min. and  $1.13 \times 10^{-5}$  E/min. at the high and low intensities respectively (calculated on page 114), while smoothed values for  $\frac{d\text{Fe}^{2+}}{dt}$  are obtained from Fig. 26.

The plot of quantum yield against pH at the two intensities is shown in Fig. 27. For reasons stated previously, it is impossible with accuracy to calculate quantum yields at pH values greater than 2.94. It must be noted that these are only average quantum yields, since the absorbed light varies in wavelength from 300 to 500  $\mu$ , and it is quite possible, if the quantum yield varies appreciably with wavelength, that they are the average of widely differing values.

**FIG. 28**



The quantum yield at any pH, increases with decreasing light intensity, the maximum value at the higher intensity being 0.05 at pH 2.94.

## V The Effect of Light Intensity

For a photochemical reaction with homogeneous light, the reaction velocity is, in general, given by :-

$$\frac{dc}{dt} = K \cdot I^n$$

where  $I$  is the intensity of the absorbed light or the energy of the absorbed light if the cross-sectional area of the irradiating beam remains constant, and  $K$  and  $n$  are constants depending upon pH.

This equation can only be applied to non-homogeneous light if, on altering the intensity, all the wavelengths are modified in the same proportion. By using a nickel screen this condition is fulfilled. Hence :-

$$\frac{dFe^{2+}}{dt} = K \cdot I^n$$

Values for  $\frac{dFe^{2+}}{dt}$  and  $I$ , the energy absorbed, may be obtained from Fig. 26 enabling  $n$  and  $K$  to be evaluated at various pH's. Fig. 28 shows  $n$  plotted against pH in the pH range 2.1 to 2.94. The value of  $n$  is of interest since it indicates the dependence of the reaction rate on light intensity at any particular pH.

## DISCUSSION.

### The Effect of pH on Photoreduction.

Fig. 26 shows that the initial rate of reduction increase steadily with increasing pH in the pH range 2.10 to 2.90 and then much more rapidly to reach a maximum between 2.94 and 2.98; thereafter, the reduction rate decreases as the pH is increased from 2.98 to 3.70.

The increase (shown in Fig. 1) in the concentrations of the light absorbing species  $\text{FeOH}^{2+}$  and  $\text{Fe(OH)}_2^+$  as the pH of the solution is raised from 2.10 to 2.90 almost certainly accounts for the increase in the rate of photoreduction in this pH range. It would appear that the decrease in the rate of photoreduction as the pH rises above 2.98 is associated with the formation of colloidal ferric hydroxide.

On the other hand, the very rapid increase in the rate of reduction as the pH increases from 2.90 to 2.94 cannot be accounted for by an increase in the concentrations of the absorbing species since reference to Fig. 1 shows that the concentration of  $\text{Fe(OH)}_2^+$  does not increase particularly rapidly in this range while the concentration of  $\text{FeOH}^{2+}$  actually decreases. It was observed that solutions in this pH region, while initially colourless, became yellowish-brown during the first minute of irradiation, indicating the formation of colloidal ferric hydroxide. This did not occur if

the solutions were kept in the dark, nor did it occur in solutions of pH below 2.90. It is therefore suggested that the rapid increase in the photo-activity of solutions in the region of pH 2.94 might be attributed to a sudden increase in the concentration of  $\text{Fe}(\text{OH})_2^+$  and possibly of  $\text{FeOH}^{2+}$  at the onset of hydrolysis. This initiation of the hydrolysis by light and its relation to the photoreduction are investigated in Part 4.

#### The Effect of Light Intensity.

Fig. 28 indicates that the effect of light intensity on the initial rate of reduction increases with increasing pH in the pH range 2.10 to 2.94. For example, at pH 2.90 where  $n = 0.69$ , a 10-fold increase in the light intensity would cause a 5-fold increase in the rate of reduction, whereas at pH 2.10 where  $n = 0.30$ , a similar increase in the light intensity would only cause a 2-fold increase in the reaction rate.

#### The Quantum Yield.

Fig. 27 shows that the quantum yield of ferrous ion formation increases with increasing pH in the pH range 2.10 to 2.94 and at any particular pH increases with decreasing light intensity. The maximum value of the quantum yield obtained at the lower intensity was approximately 0.05.

A value of 0.05 for the quantum yield of ferrous ion formation has also been calculated by Evans, Santappa and Uri<sup>61</sup> from a study of the photopolymerization of acrylonitrile initiated by  $\text{FeOH}^{2+}$  at wavelengths between 300 and 400 m $\mu$ , and by Bates, Evans and Uri<sup>67</sup> from an investigation of the photo-oxidation of benzoic acid by  $\text{FeOH}^{2+}$  with light of wavelength 365 m $\mu$ .

Since oxygen is produced according to the equation



it follows that  $\phi_{\text{O}_2} = \frac{1}{4}\phi_{\text{Fe}^{2+}} = 0.0125$ .

---

PART 4.

THE EFFECT OF LIGHT ON THE HYDROLYSIS.

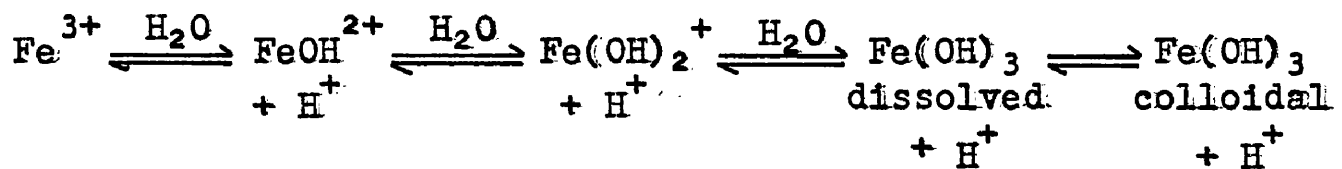
## INTRODUCTION

Ferric chloride being the salt of a strong acid and a weak base, immediately hydrolyses when dissolved in water to give an acid solution. This primary hydrolysis is followed, in not too concentrated solutions, by a much slower secondary hydrolysis which may take anything from a few moments to several months for completion, depending on conditions such as temperature, concentration, etc. During this secondary hydrolysis there is a decrease in pH accompanied by the appearance of the reddish - brown colour of colloidal ferric hydroxide which may ultimately precipitate out.

This secondary hydrolysis has been the object of a number of investigations since the end of the last century, the earlier ones being excellently reviewed by Mellor<sup>109</sup>. There was a wide divergence in the explanations put forward by these early investigators and it was Lamb and Jacques<sup>76</sup> who first attempted to quantitatively relate their experimental data to a proposed mechanism. They investigated the phenomenon by means of conductivity, colorimetric and electrometric measurements and confirmed the previously observed increase in the speed of the hydrolysis with increasing dilution and temperature, and the retarding effect of acids such as hydrochloric and nitric. An induction period prior

to hydrolysis was apparent at ferric concentrations of 0.0013 M and higher.

The explanation suggested was that as soon as the ferric salt dissolves, a rapid reversible hydrolysis ensues giving rise to a number of hydrolysis products, but in particular to a dilute but supersaturated solution of ferric hydroxide (see page 30).



The slow coagulation of ferric hydroxide to the colloidal state was proposed as the controlling step in the reaction, the rate of hydrolysis being proportional to the degree of supersaturation in solution of the undissociated ferric hydroxide. Much of the work relating to the hydrolysis of ferric iron solution has been mentioned in Part I.

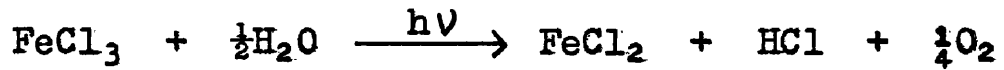
At the beginning of this century, Moore<sup>110</sup>, in a spectrophotometric investigation, found that light had no effect on the initiation of the hydrolysis of ferric iron solutions. However, subsequent work by Bhatnager<sup>111</sup>, Zocher and Heller<sup>112</sup>, and Heller<sup>113</sup>, suggested that although light is not active in the initiation of the

hydrolysis, it does accelerate the coagulation of the ferric hydroxide once formed.

Purdon,<sup>75</sup> in the course of experiments on the photoreduction of ferric chloride, observed that a reddish-brown colour formed during U.V. irradiation, whereas another portion of the same solution standing in the dark at the same temperature remained colourless. He attributed the brown colour to colloidal ferric hydroxide and concluded that light initiates and accelerates the hydrolysis (already mentioned on page 119). This effect was observed even if the solutions were irradiated for short periods only (up to one hour) and then thermostated in the dark. Purdon suggested that the accelerating action of light on the hydrolysis might be due to the reaction  $\text{Fe}^{2+} + \text{H}_2\text{O}_2$ , the environment of the freshly produced ferric ion being such that complete hydrolysis takes place.

In this section of the present investigation, the effect of oxygen, hydrogen peroxide, and glucose on the dark hydrolysis of ferric chloride and ferric-ferrous chloride solutions was studied. The ferric-ferrous chloride solutions contained ferric chloride, ferrous chloride and hydrochloric acid in concentrations such that

[Iron] =  $1.3 \times 10^{-3}$  M and [FeCl<sub>2</sub>] = [HCl], the aim being to produce in the dark, conditions identical to those arising during irradiation :-



The effects of glucose and hydrogen peroxide on the light hydrolysis of ferric chloride were also studied.

EXPERIMENTAL

The preparation of  $1.3 \times 10^{-3}$  M ferric chloride solution has been described in Part 2. The ferric-ferrous chloride-hydrochloric acid solutions were prepared by adding the required quantity of ferric chloride melt to a solution of equal concentrations of ferrous chloride and hydrochloric acid to give a final solution in which the total iron concentration was  $1.3 \times 10^{-3}$  M. For this purpose, a stock solution of ferrous chloride in hydrochloric acid such that  $[FeCl_2] = [HCl]$  i.e.  $[Cl^-] / [Fe^{2+}] = 3/1$  was prepared as follows.

Iron sponge was dissolved in A.R. hydrochloric acid in the proportion  $[Cl^-] / [Iron]$  slightly under 3/1 and the solution diluted with water to one litre, care being taken to eliminate oxygen both from the water and from the atmosphere above the solution. The total chloride concentration was estimated by titration with silver nitrate and the total iron by oxidation to ferric by hydrogen peroxide and titration with titanous chloride. A calculated volume of hydrochloric acid solution of suitable strength was then added to increase the  $[Cl^-] / [Iron]$  ratio to 3/1. Finally, the ferrous ion was estimated colorimetrically by 2-2' dipyridyl. The analysis was:-

[Ferrous Ion] = 0.1707 M

[Ferric Ion] = 0.0015 M [Chloride Ion] = 0.5182 M

[Total Iron] = 0.1722 M

$$[\text{Chloride}] / [\text{Total Iron}] = 3.010/1$$

Although the total iron concentration remained constant, the ferric ion concentration increased slowly with time at the expense of the ferrous by atmospheric oxidation, so that the solution had to be standardised periodically.

When it was required to have hydrogen peroxide or glucose present, up to 10 ml. of a concentrated stock solution were added to the irradiation or hydrolysis flask prior to the addition of the iron solution.

#### Materials.

Iron Sponge. The spectrographically standardised iron sponge was supplied by Johnson Matthey and Co., Ltd.

Hydrogen Peroxide. The hydrogen peroxide was 86% unstabilised, supplied by Laporte.

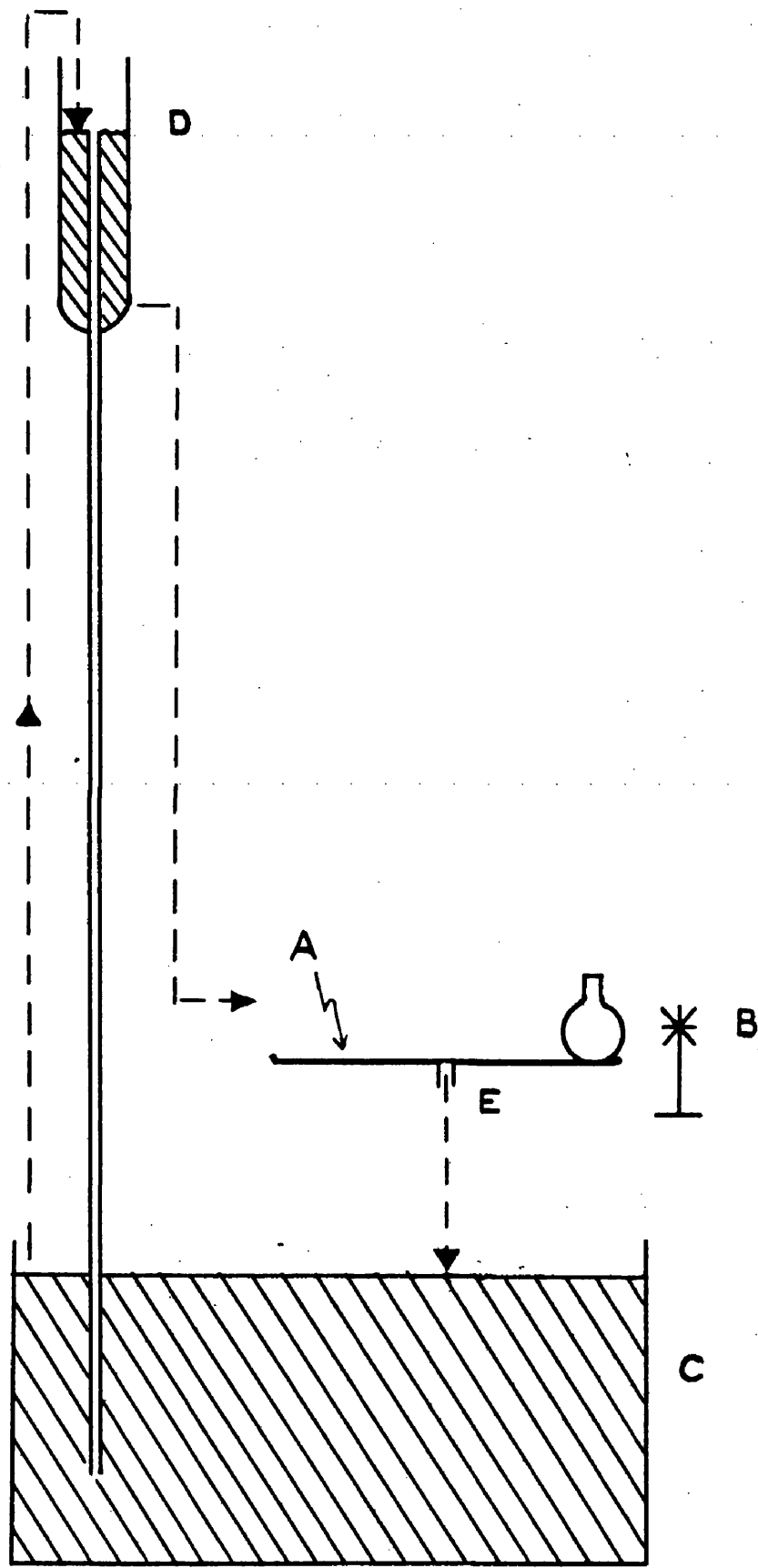
For the various other solutions, A.R. materials were always used if obtainable.

#### Measurement of Secondary Hydrolysis.

All the solutions investigated were initially colourless. The onset and development of secondary

**FIG. 29**

**IRRADIATION APPARATUS**



hydrolysis, resulting in the appearance of a gradually deepening reddish-brown colour due to colloidal ferric hydroxide, was followed by measuring the increase in optical density in a Unicam S.P. 600 Spectrophotometer at wavelength 440 m $\mu$ . 4 cm. cells were used at the beginning of a run until an optical density of about 0.8 was reached, when these cells were replaced by 2 cm. cells, the appropriate cell correction factor being applied to correlate the measurements.

Experiments on the dark hydrolysis were performed in a dark-room illuminated by Kodak OB Safelights (lime yellow). The solutions were kept in quickfit conical flasks thermostated at 20°C ( $\pm 0.05^\circ$ ), the samples being withdrawn by pipette.

#### Irradiation Apparatus.

An outline of the apparatus is shown in Fig. 29. A is a stainless steel table, 45 cm. in diameter, constructed to hold round its circumference eight 250 ml. B 34 quickfit pyrex flasks and rotated by an electric motor through a reduction gear, the speed (4 to 5 r.p.m.) being controlled by a variable resistance. The flasks were thus carried at regular intervals past a 500 watt UVS 500 Hanovia mercury arc lamp B situated 4 cm. from the table.

To maintain the solutions at 20°C, water was pumped from a large thermostat tank C to a constant head device D, from which it fell through six nozzles situated round the table on to the flasks. The nozzles were so arranged that on leaving one flask, the jet immediately fell on to the next, assuring an efficient use of the cooling water and minimising splashing. The water drained from the table through its hollow driving shaft E back into the tank below. With this arrangement the temperature of the solutions in the flasks rose by not more than 0.4°C in seven hours.

Each flask was filled to a 200 ml. mark engraved on the side and stoppered during the run, samples being withdrawn by pipette. To ensure that each flask transmitted the same amount of light, 200 ml. portions of a  $1.3 \times 10^{-3}$  M ferric chloride solution were simultaneously irradiated in the flasks and the hydrolysis followed. Since identical hydrolysis curves were obtained in each case, it was assumed that for the purpose of this investigation, the flasks had equal transmission values.

RESULTS.

The products of the photochemical reduction of  $1.3 \times 10^{-3}$  M ferric chloride solutions at pH 2.94 are (a) ferric ion (b) ferrous ion (c) possibly hydrogen peroxide decomposing to water and (d) oxygen, and in an investigation into the action of light on hydrolysis, the effects of all these must be considered. The hydrolysis of solutions with ferrous ion concentrations greater than  $4 \times 10^{-4}$  M was not studied since this is approximately the limiting concentration arising from photoreduction. Hydrogen peroxide concentrations are expressed in normalities on account of the stoichiometry  $\text{Fe}^{2+} \equiv \frac{1}{2} \text{H}_2\text{O}_2$ .

pH Measurements on Ferrous-Ferric Iron Solutions.

pH Measurements were carried out with the Cambridge pH meter described in Part 2. The solutions were prepared from the ferric chloride melt and the stock ferrous chloride-hydrochloric acid solution. The  $[\text{Fe}^{3+}] / [\text{Fe}^{2+}]$  ratio was varied but the total iron concentration kept constant at  $1.3 \times 10^{-3}$  M and the total chloride at  $3.9 \times 10^{-3}$  M. The pH values found at 20°C are given in Table 15. It is evident that variation of the ratio  $[\text{Fe}^{3+}] / [\text{Fe}^{2+}]$  has very little effect on the pH of the systems.

**FIG. 30**  
HYDROLYSIS IN THE LIGHT AND IN THE DARK

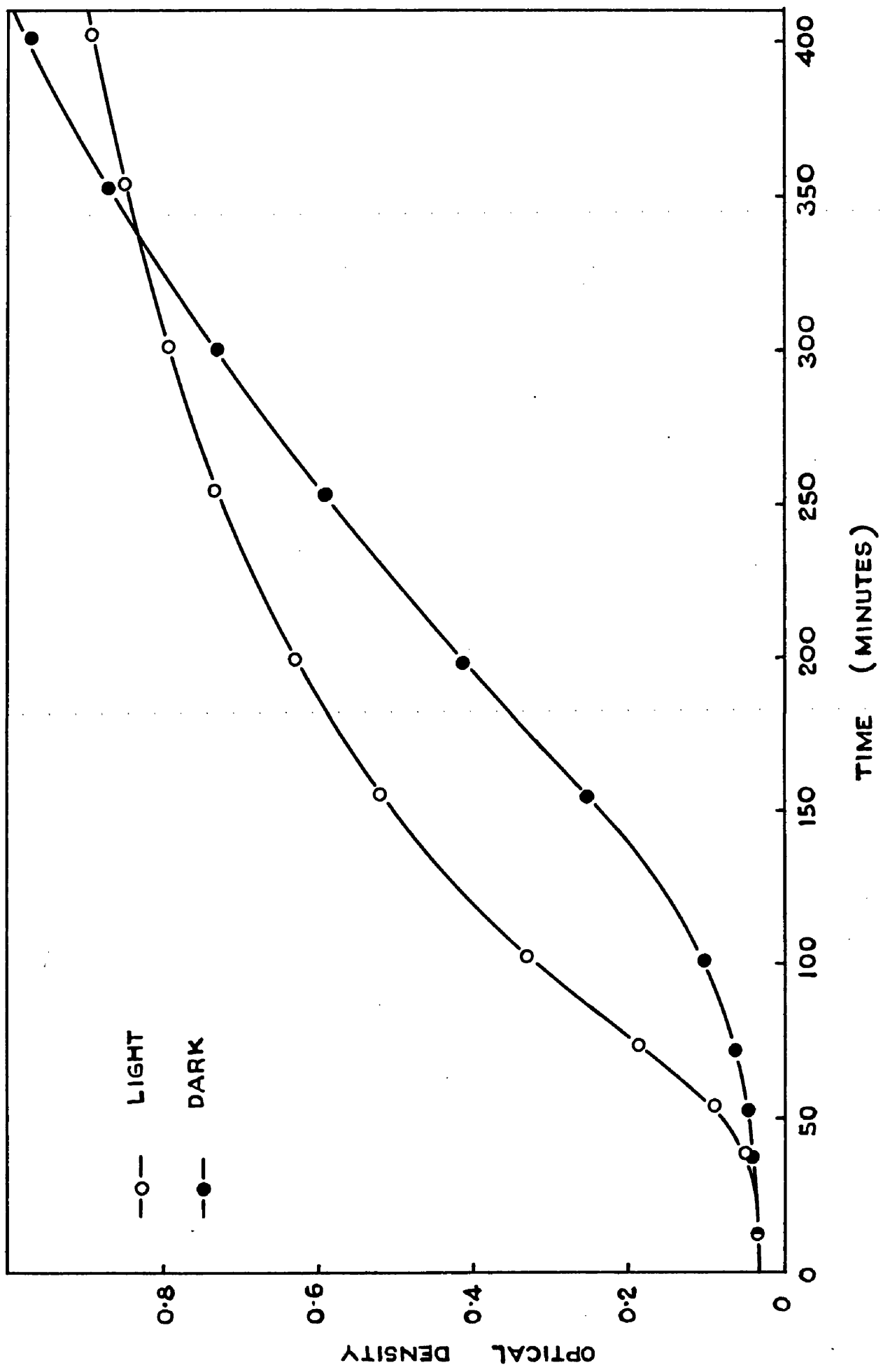


TABLE 15

$[\text{Fe}^{3+}] \text{M} \times 10^3$	$[\text{Fe}^{2+}] \text{ M} \times 10^3$	$[\text{HCl}] \text{M} \times 10^3$	pH
1.30	0	0	2.94
0.67	0.63	0.63	2.93
0	1.30	1.30	2.92

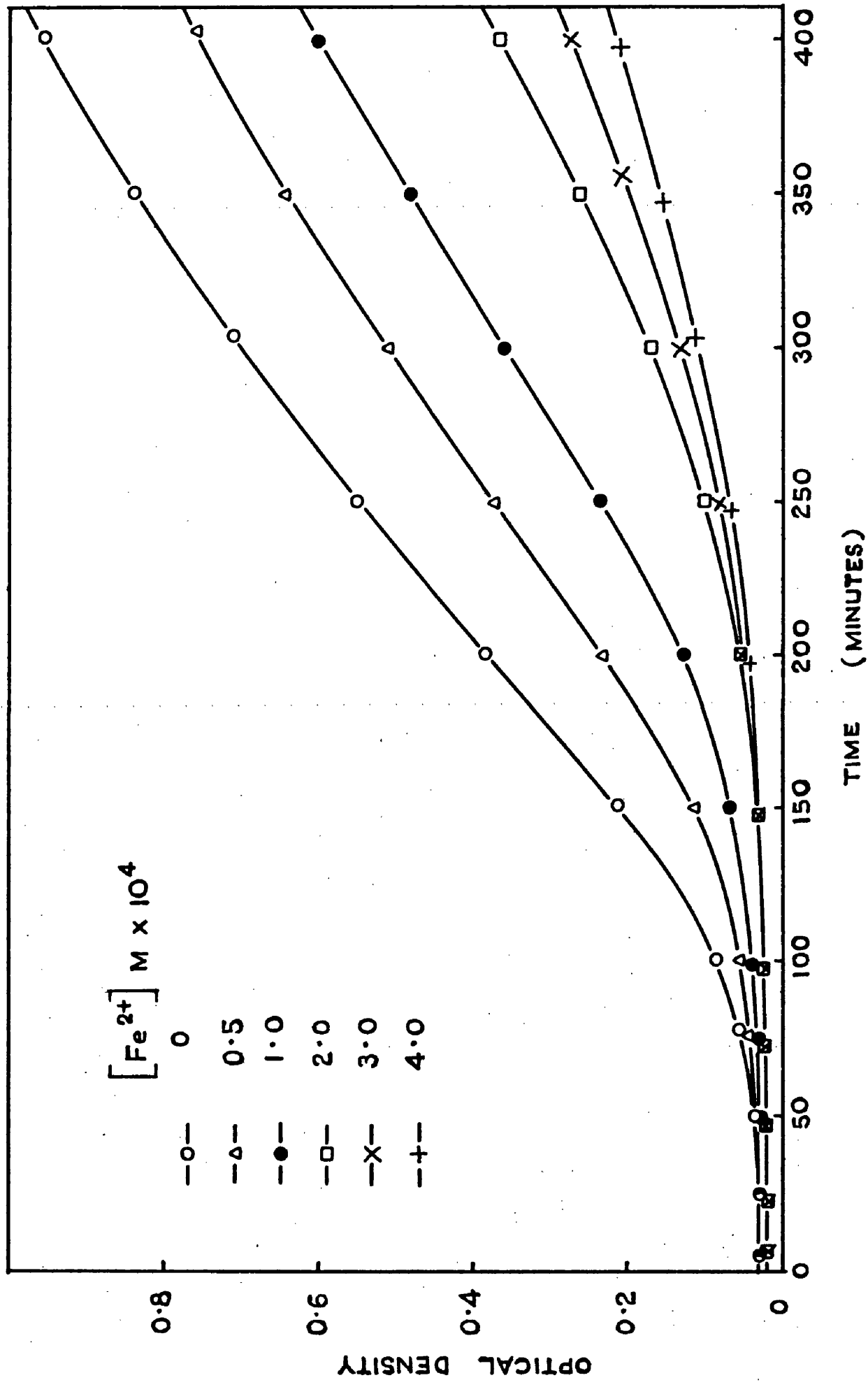
In any future reference to adjustments in the proportion of ferrous ion in a solution, it should be understood that the concentration of hydrochloric acid was appropriately adjusted so that  $[\text{Fe}^{2+}] = [\text{HCl}]$

The Dark and Light Hydrolysis of Ferric Chloride Solution.

The typical dark and light hydrolysis curves for  $1.3 \times 10^{-3}$  M ferric chloride solution, shown in Fig.30, illustrate the pronounced accelerating effect of light on the hydrolysis. However, although the exposed solution shows an initial boosting of the hydrolysis, the dark solution catches up and surpasses it due to the fact that photoreduction in the exposed solution leaves less ferric iron to hydrolyse and, in fact, Purdon has calculated that the percentage difference in the maximum optical densities (not shown in Fig.30) is equal to the percentage reduction of the ferric iron. The pH of a  $1.3 \times 10^{-3}$  M ferric chloride solution was found to drop

FIG. 31

THE HYDROLYSIS OF FERROUS - FERRIC IRON SOLUTIONS



from 2.94 to 2.74 after six hours' irradiation.

### THE DARK HYDROLYSIS.

#### I. The Hydrolysis of Ferrous-Ferric Iron Solutions.

In the solutions studied, the total iron concentration was  $1.3 \times 10^{-3}$  M. From the results, shown in Fig. 31, it is evident that the greater the ferrous ion concentration the longer is the initiation period before hydrolysis and the smaller is the extent of hydrolysis at any time.

#### II. The Effect of Oxygen in Ferric Chloride Solutions.

400 ml. of distilled water was boiled in each of two 500 ml. flasks which were then thermostated at 20°C. The water in one was allowed to cool under an atmosphere of nitrogen ('white spot') and in the other under an atmosphere of oxygen, both gases having been previously scrubbed with water. About ten minutes before the addition of the ferric chloride, the oxygen was bubbled through the water to saturate it. The requisite amount of ferric chloride melt was added to each to give two  $1.3 \times 10^{-3}$  M ferric chloride solutions, one saturated with oxygen and the other oxygen free. The hydrolysis curves for the two solutions were found to be identical,

showing that oxygen has no effect. The curve is similar to the dark hydrolysis curve shown in Fig.30.

### III. The Effect of Oxygen in Ferrous-Ferric Iron Solutions.

The solutions were prepared in the same way as explained above using ferric chloride melt and the stock ferrous chloride-hydrochloric acid solution. The investigation was carried out at two ferrous ion concentrations:-  $0.05 \times 10^{-3}$  M and  $0.17 \times 10^{-3}$  M. Oxygen was found to have no effect on the hydrolysis in either case.

### IV. The Effect of Hydrogen Peroxide in Ferric Chloride Solutions.

The hydrolysis of  $1.3 \times 10^{-3}$  M ferric chloride solutions was measured with hydrogen peroxide concentrations of 0.1, 0.5, 2.0, 4.0,  $\times 10^{-4}$  N. The hydrogen peroxide was found to have no effect, each curve being similar to the dark hydrolysis curve shown in Fig.30.

### V. The Effect of Hydrogen Peroxide in Ferrous-Ferric Iron Solutions.

The effect on the hydrolysis of increasing hydrogen peroxide concentrations in solutions of constant initial

**FIG. 32**

THE EFFECT (ON HYDROLYSIS) OF THE OXIDATION OF FERROUS IRON

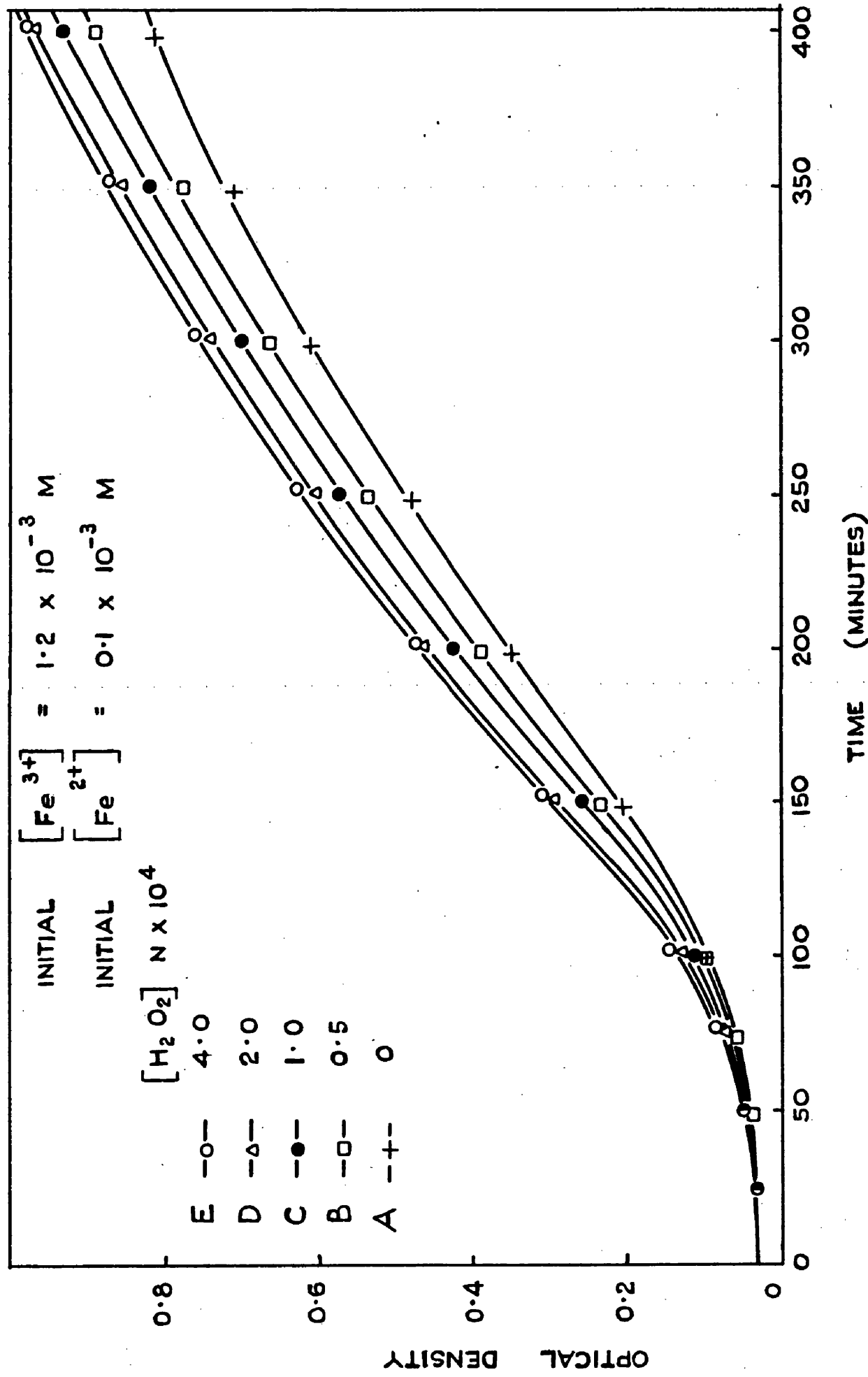
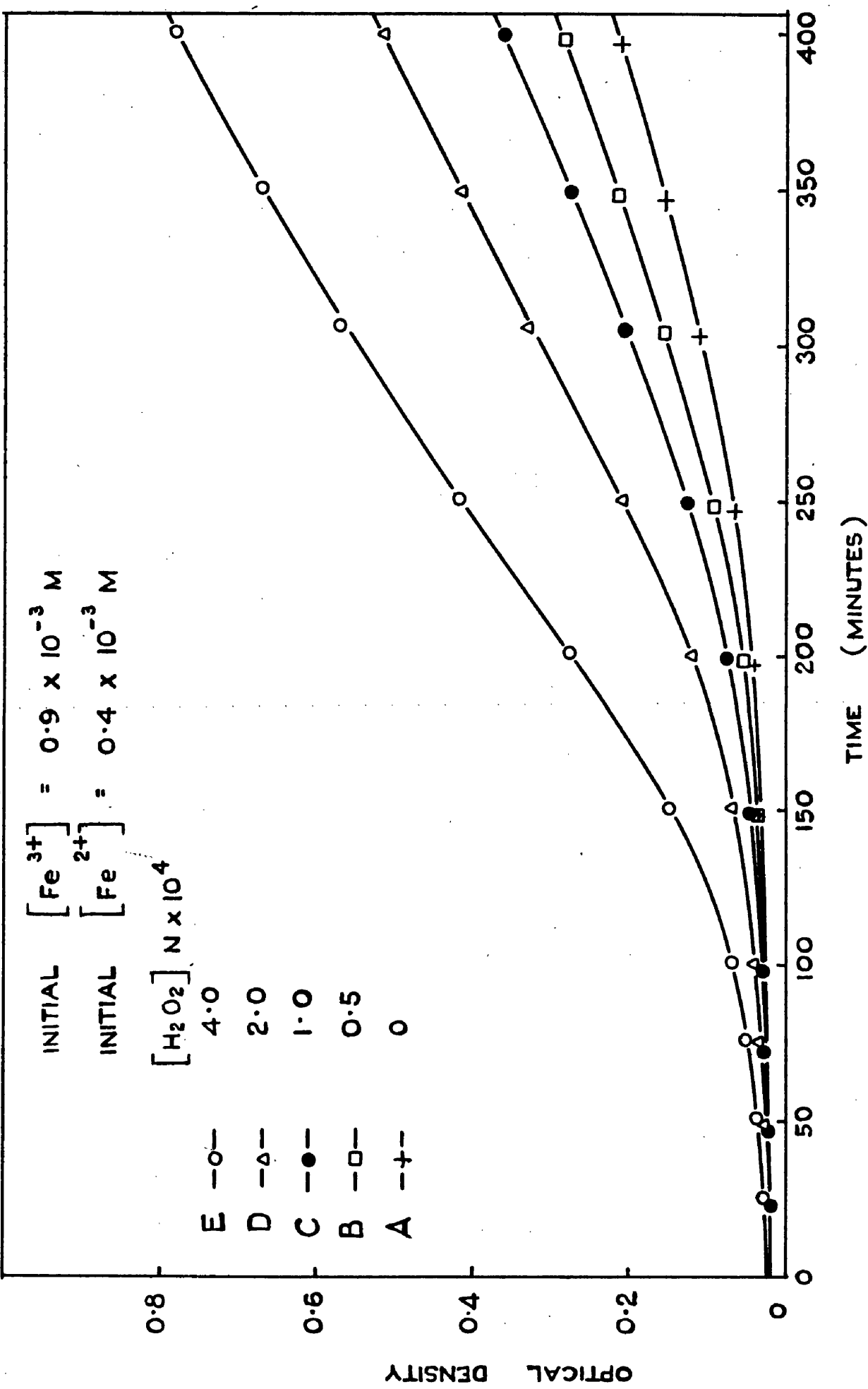


FIG. 33

THE EFFECT (ON HYDROLYSIS) OF THE OXIDATION OF FERROUS IRON



ferrous ion concentration, was investigated at two ferrous ion concentrations. The dark hydrolysis curves are plotted in Figs. 32 and 33, and Tables 16 and 17, showing the initial hydrogen peroxide concentrations and percentage ferrous ion oxidised, are given below.

TABLE 16 (Fig. 32)

$$[\text{Ferrous}] = 1 \times 10^{-4} \text{ M.} \quad [\text{Ferric}] = 1.2 \times 10^{-3} \text{ M.}$$

Curve	Initial [H <sub>2</sub> O <sub>2</sub> ] N × 10 <sup>4</sup>	After 5 hrs. [Fe <sup>2+</sup> ] M × 10 <sup>5</sup>	% Fe <sup>2+</sup> oxidised
A	0	10.00	0
B	0.5	6.05	39.5
C	1.0	3.22	67.8
D	2.0	0.65	93.5
E	4.0	0.12	98.8

TABLE 17 (Fig. 33)

$$[\text{Ferrous}] = 4 \times 10^{-4} \text{ M} \quad [\text{Ferric}] = 0.9 \times 10^{-3} \text{ M}$$

Curve	Initial [H <sub>2</sub> O <sub>2</sub> ] N × 10 <sup>4</sup>	After 5 hrs. [Fe <sup>2+</sup> ] M × 10 <sup>4</sup>	% Fe <sup>2+</sup> oxidised
A	0	4.00	0
B	0.5	3.52	12.1
C	1.0	3.06	23.5
D	2.0	2.20	45.1
E	4.0	0.81	79.6

From the results in Table 16 and Fig. 32 it is evident that the more ferrous ion oxidised the greater is the subsequent hydrolysis, the limit being the complete oxidation of the ferrous ion when the dark hydrolysis curve in Fig. 30 for  $1.3 \times 10^{-3}$  M ferric chloride solution is obtained. The results in Table 17 and Fig. 33 follow the same pattern although the extent of hydrolysis is lower on account of the greater ferrous ion concentration.

#### VI. The Effect of Glucose in Ferric Chloride Solutions.

$1.3 \times 10^{-3}$  M ferric chloride solutions containing [Iron] / [Glucose] molar ratios of 4, 5, 20, 50, 100, 250/1 were investigated but it was found that in each case the glucose had no effect on the hydrolysis. The curves were similar to the dark hydrolysis curve shown in Fig. 30.

#### THE LIGHT HYDROLYSIS.

##### I. The Effect of Hydrogen Peroxide in Ferric Chloride Solutions.

Hydrogen peroxide was found to have a retarding action on the light hydrolysis of  $1.3 \times 10^{-3}$  M ferric chloride solutions, a typical set of hydrolysis curves for hydrogen peroxide concentrations up to  $1 \times 10^{-4}$  N

FIG. 34

THE EFFECT OF HYDROGEN PEROXIDE ON THE LIGHT HYDROLYSIS

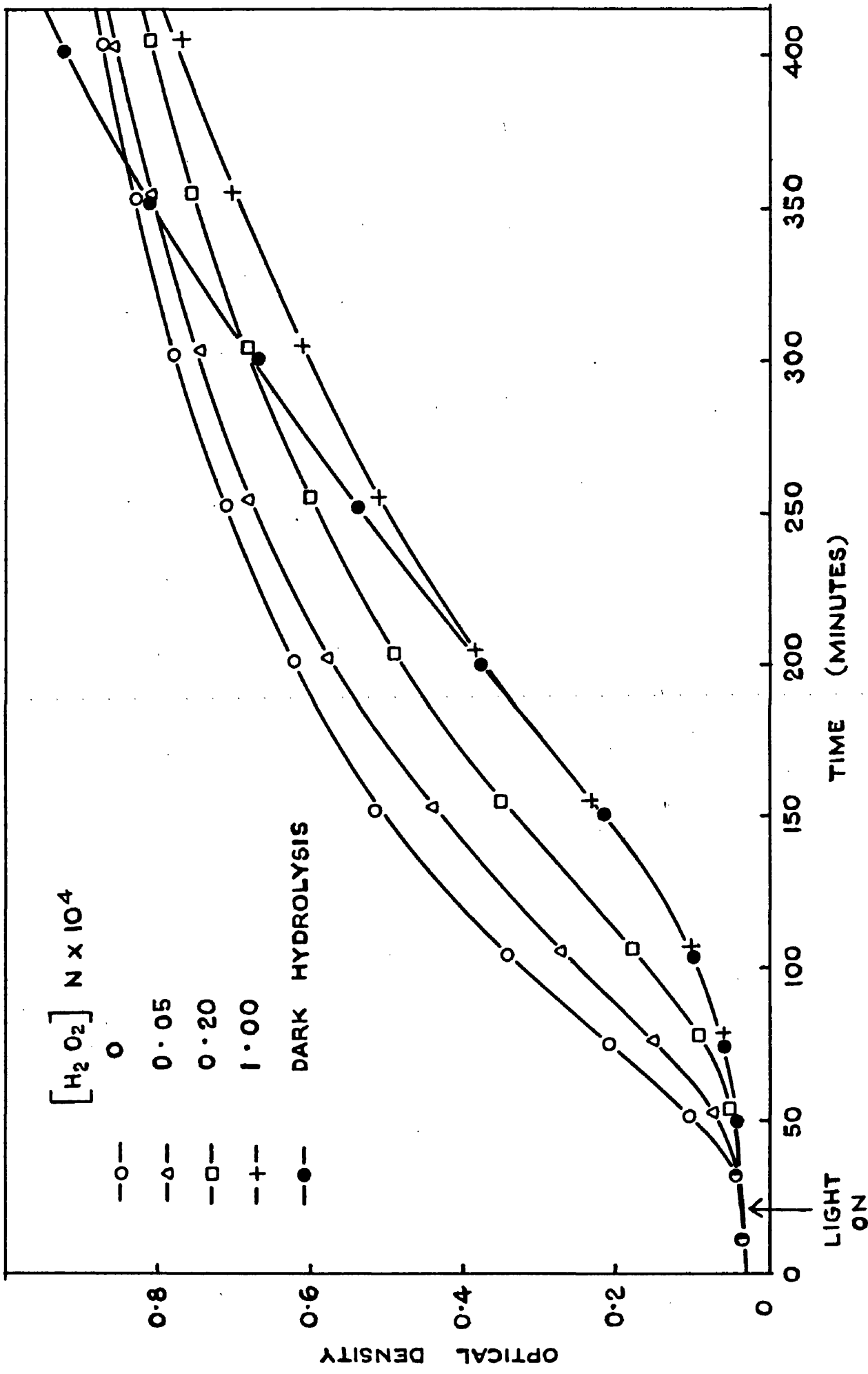
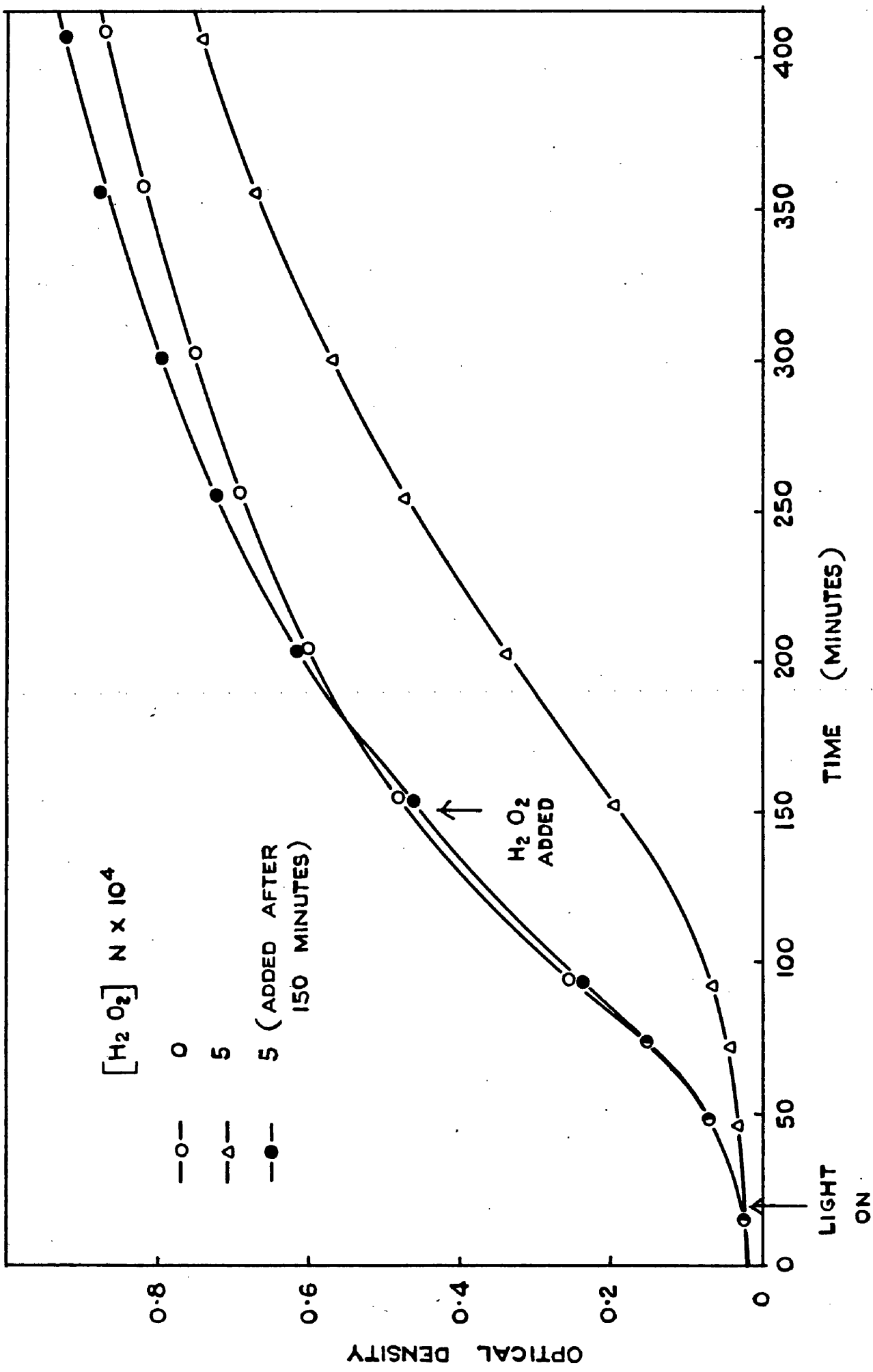


**FIG. 35**

THE EFFECT OF ADDING HYDROGEN PEROXIDE DURING LIGHT HYDROLYSIS



being given in Fig.34. Increase in the hydrogen peroxide concentration above  $1 \times 10^{-4}$  N was found to produce no further increase in the retarding effect.

The effect of adding hydrogen peroxide to a ferric chloride solution in the course of hydrolysis is shown in Fig.35. There is a slight acceleration of the hydrolysis on the addition of the hydrogen peroxide which carries the curve above that for the solution with no peroxide.

### III. The Effect of Glucose in Ferric Chloride Solutions.

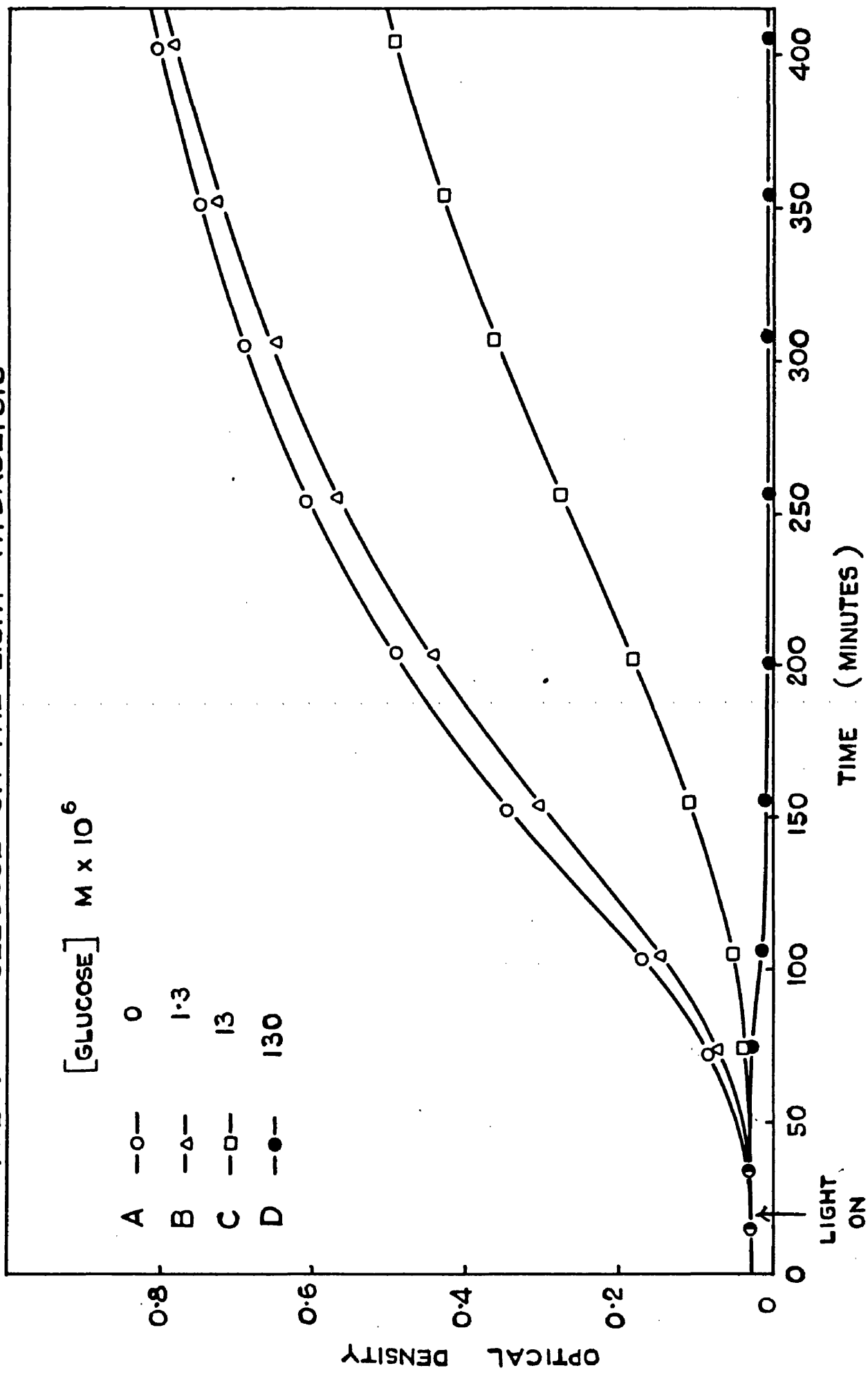
It was observed that glucose retarded the light hydrolysis, the greater its concentration, the greater the retardation, the limit being when no hydrolysis took place at all. The results are plotted in Fig.36 from which it may be seen that a glucose concentration of  $1.3 \times 10^{-4}$  M completely prevented any hydrolysis. The concentrations of ferrous ion in the solutions after 5 hours' irradiation are given in Table 18.

TABLE 18.

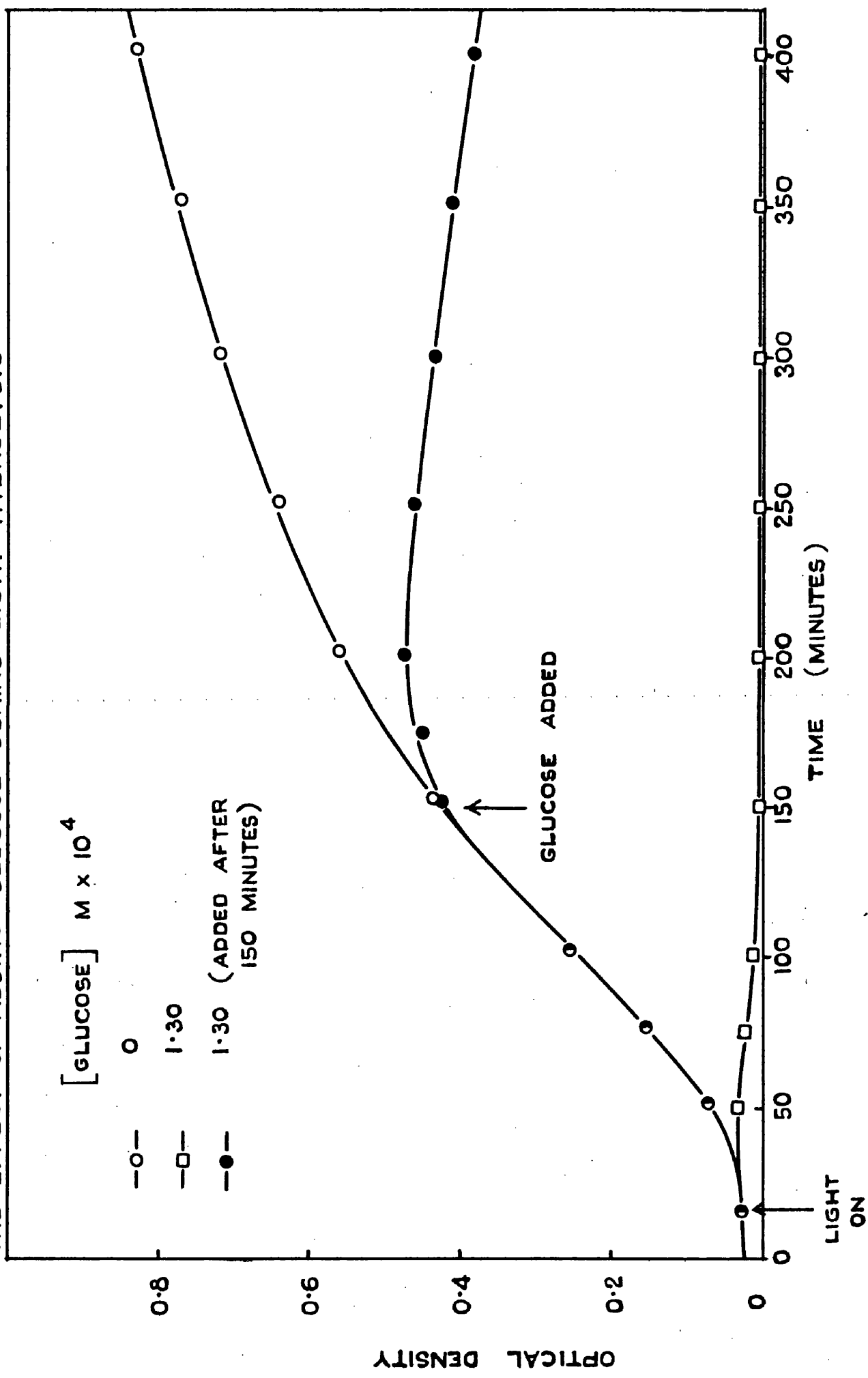
Curve	[Glucose] M	[Ferrous] M $\times 10^4$
A	0	1.95
B	$1.3 \times 10^{-6}$	2.00
C	$1.3 \times 10^{-5}$	3.25
D	$1.3 \times 10^{-4}$	11.80*

**FIG. 36**

**THE EFFECT OF GLUCOSE ON THE LIGHT HYDROLYSIS**



**FIG. 37**  
**THE EFFECT OF ADDING GLUCOSE DURING LIGHT HYDROLYSIS**

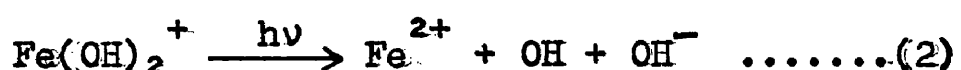
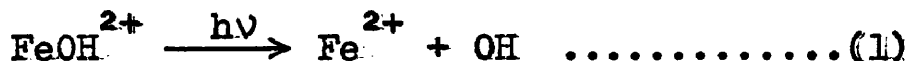


\* Nearly complete reduction.

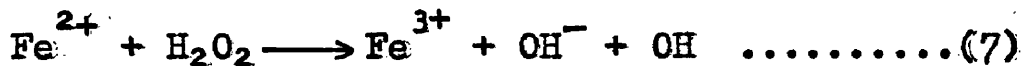
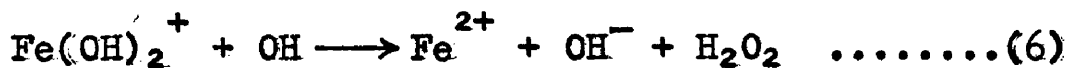
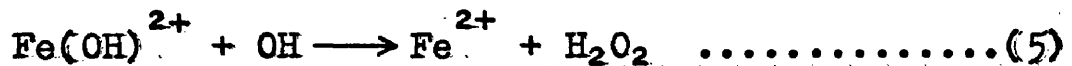
Fig. 37 illustrates the effect of adding glucose to a ferric chloride solution in the course of hydrolysis. The hydrolysis slows down until finally the solution begins to "dehydrolyse" and the optical density slowly decreases.

## DISCUSSION

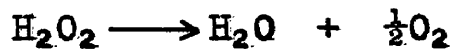
The following reaction scheme (see page 96) is accepted as describing the photoreduction of the ferric iron under the conditions of the present investigation :-



## Formation of hydrogen peroxide :-



## Decomposition of hydrogen peroxide by iron catalysis :-



If an organic substrate, e.g. glucose, is added to the system then the reaction



takes place.

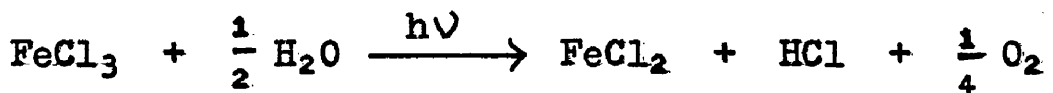
(A). pH Measurements on Ferrous-Ferric Iron Solutions.

In these solutions,  $[\text{Total Iron}] = 1.3 \times 10^{-3} \text{ M}$  and  $[\text{FeCl}_2] = [\text{HCl}]$ .

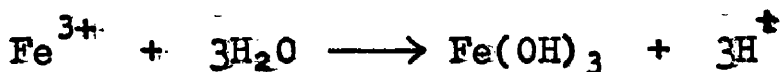
It was observed that when the iron concentration of the solution varied from entirely ferric to entirely ferrous, the pH only dropped from 2.94 to 2.92. The excellent agreement of the latter value with that of 2.89 calculated for a  $1.3 \times 10^{-3} \text{ M}$  solution of hydrochloric acid in water indicates that in the solution  $[\text{FeCl}_2] = [\text{HCl}] = 1.3 \times 10^{-3} \text{ M}$ , the presence of the ferrous chloride does not significantly alter the pH, i.e. the ferrous ion is not significantly hydrolysed.

It is, of course, purely fortuitous that a  $1.3 \times 10^{-3} \text{ M}$  ferric chloride solution hydrolyses to such an extent that the pH (2.94) is almost the same as that (2.92) of a  $1.3 \times 10^{-3} \text{ M}$  solution of ferrous chloride and hydrochloric acid, and it is for this reason that the pH of the ferrous-ferric chloride solutions is virtually independent of the  $[\text{Fe}^{2+}] / [\text{Fe}^{3+}]$  ratio. It can therefore be concluded that no change in the pH occurs under the conditions of the present investigation as a result purely of the photoreduction of ferric chloride

solution by the reaction:-



The drop in pH from 2.94 to 2.74 after 6 hours' irradiation of a  $1.3 \times 10^{-3}$  M ferric chloride solution must therefore be attributed to secondary hydrolysis:-



Note:- The light and dark hydrolysis of a  $1.3 \times 10^{-3}$  M ferric chloride solution, illustrated in Fig.30, will be referred to as the standard light hydrolysis and the standard dark hydrolysis respectively.

(B). The Hydrolysis of Ferrous-Ferric Iron Solutions.

The lowering of the amount of hydrolysis (Fig.31) as the ratio  $[\text{Fe}^{3+}] / [\text{Fe}^{2+}]$  in the solutions decreases is explained by the decreasing amount of ferric ion left to hydrolyse. The increase in the hydrolysis (Figs.32 and 33) of solutions initially containing  $1 \times 10^{-4}$  and  $4 \times 10^{-4}$  M ferrous ion, resulting from the whole or partial oxidation of the ferrous ion, must therefore be due to the increasing in situ of the ratio  $[\text{Fe}^{3+}] / [\text{Fe}^{2+}]$ . The important feature, however, is that the hydrolysis of the oxidised

solution never rises above the standard dark hydrolysis curve. It may be concluded therefore, that the boost in hydrolysis of ferric iron solutions cannot be due to the occurrence of the reaction  $\text{Fe}^{2+} + \text{H}_2\text{O}_2$  in any suggested mechanism of the photolytic reduction of ferric to ferrous iron.

(C). The Hydrolysis of Ferric Chloride Solutions.

1. The dark hydrolysis.

It has been observed that neither oxygen nor hydrogen peroxide have any effect on the standard dark hydrolysis which suggests that the boost in the hydrolysis by light is not the result of interaction of either of these products of photoreduction with ferric ion.

2. The light hydrolysis in the presence of hydrogen peroxide.

The effect of hydrogen peroxide on the light hydrolysis is very puzzling. Fig. 34 shows that initially added hydrogen peroxide retards the light hydrolysis while Fig. 35 shows that hydrogen peroxide added after  $2\frac{1}{2}$  hours when hydrolysis is well under way, slightly accelerates it causing the curve to rise above that for the standard light hydrolysis. It is suggested that the accelerating effect of hydrogen peroxide added after hydrolysis has commenced (by which time there will be an appreciable concentration

of ferrous ion) is analogous to the increase in the hydrolysis caused by the addition of hydrogen peroxide to the ferrous-ferric iron solutions (Figs. 32 and 33) and can therefore be explained by the oxidation of all or part of the photoproduced ferrous ion to produce an increase in the amount of ferric ion available for hydrolysis.

The retardation of the light hydrolysis by initially added hydrogen peroxide, however, is much more difficult to explain. The shapes of the curves in Fig. 34 suggest that the hydrogen peroxide retards the initiation of hydrolysis but that once started, the hydrolysis proceeds in a manner similar to the standard light hydrolysis, i.e. as if the hydrogen peroxide had never been added. The retarding effect of the hydrogen peroxide will of course decrease as the latter decomposes and the greater retarding effect in solutions of higher initial hydrogen peroxide concentration is probably to be attributed to the corresponding increase in the time required for its decomposition.

It was observed (page 136) that the retarding effect on the light hydrolysis reached a maximum in the region of  $[H_2O_2] = 1 \times 10^{-4} N$ , that is, the addition of hydrogen peroxide in concentrations of the order of  $10^{-4} N$  does not

initially retard the light hydrolysis below the rate of standard dark hydrolysis. The initial coincidence of the curves will be seen in Fig. 34.

It is evident that any ferrous ion formed photochemically will immediately be oxidised as long as a significant concentration of hydrogen peroxide remains in solution and, if anything, this might have been expected to accelerate the light hydrolysis as in the case of hydrogen peroxide added after  $2\frac{1}{2}$  hours. It must be noted however, that in the latter instance hydrolysis had actually commenced, whereas initially added peroxide appears to delay its initiation.

The retarding effect of hydrogen peroxide on the light hydrolysis cannot be due to ferric-hydrogen peroxide complexes because (a) hydrogen peroxide does not affect the dark hydrolysis and (b) the retarding effect reaches its maximum in solutions in which the molar ratio of  $[H_2O_2] / [Fe^{3+}]$  is only 1/26.

Although no adequate explanation of the effect of hydrogen peroxide on the light hydrolysis has been found, it seems quite definite that the accelerating effect of light on the hydrolysis is not due to the reaction  
 $Fe^{2+} + H_2O_2$ .

3. Light hydrolysis in the presence of glucose.

The retarding effect of glucose on the light hydrolysis (Figs. 36 and 37) may be due to its competition with  $\text{Fe}^{2+}$  for the OH radicals produced by the primary reactions (1) and (2) (page 138). The reaction



will result in a reduced back oxidation of the  $\text{Fe}^{2+}$  ion by reaction (3). Ferrous ion formation will thus proceed until either all the ferric ion is reduced or the glucose is all oxidised by reaction (8). The extent of light hydrolysis will therefore depend on the amount of iron remaining in the ferric state and the results shown in Figs. 36 and 37 can be explained on this basis.

Glucose has no effect on the dark hydrolysis.

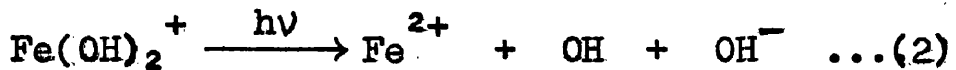
The Mechanism of the Acceleration of the Hydrolysis by Light.

From the foregoing results and discussion it appears that the reactions of  $\text{H}_2\text{O}_2$  or  $\text{O}_2$  with  $\text{Fe}^{2+}$  or  $\text{Fe}^{3+}$  do not directly account for the boost in the hydrolysis by light.

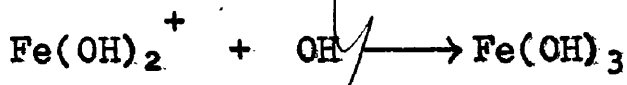
Lamb and Jacques<sup>76</sup> have shown that all solutions of ferric chloride less concentrated than 0.1M are supersaturated with respect to ferric hydroxide. This is in accordance with the observation that the  $1.3 \times 10^{-3}$  M

ferric chloride solutions employed throughout this entire study were very delicately poised with regard to hydrolysis, i.e. secondary hydrolysis with the formation of colloidal  $\text{Fe(OH)}_3$  always seemed imminent from the moment the solutions were prepared. It is therefore reasonable to suggest that any reaction which leads to the production of ferric hydroxide nuclei on which dissolved ferric hydroxide could deposit, would initiate the hydrolysis.

It has been suggested (page 96) that the two light absorbing reactions in the present system are :-



Reaction (2) is seen to produce  $\text{OH}^-$  ions which are unlikely to be removed by the back reaction  $\text{Fe}^{2+} + \text{OH} + \text{OH}^-$  since this would involve termolecular collisions. It is therefore suggested that in solutions of pH 2.94 in which  $\text{Fe(OH)}_2^+$  has been shown (Part 1) to absorb about 25% of the absorbed light, the sudden production, by irradiation, of  $\text{OH}^-$  ions by reaction (2) could then lead to



The resulting increase in the concentration of dissolved ferric hydroxide would break down the supersaturation and

provide the nuclei which initiate the hydrolysis.

This mechanism could account for the observed accelerating effect of light on the hydrolysis of  $1.3 \times 10^{-3}$  M ferric chloride solutions.

---

PART 5

THE DECOMPOSITION OF HYDROGEN PEROXIDE IN  
 $1.3 \times 10^{-3}$  M FERRIC IRON SOLUTIONS.

## INTRODUCTION

The mechanism of the iron catalysed decomposition of hydrogen peroxide has been fully discussed in the General Introduction to this thesis.

Barb et al<sup>32</sup> have found that the decomposition is first order with respect to the hydrogen peroxide concentration in ferric nitrate solutions, at temperatures from 25° to 45°C at pH's 2.3 and lower, in which the  $[H_2O_2]/[Fe^{3+}]$  ratio is greater than unity. When this ratio is reduced to between unity and 0.002, the decomposition becomes 1.5 order and by varying the hydrogen peroxide concentration these authors found that the change in order is a function not of the amount of reaction, but of the peroxide concentration. This is in agreement with the results of Andersen<sup>37</sup> who observed that with lower  $[H_2O_2]/[Fe^{3+}]$  ratios the reaction order appears to be higher than first. In both of these investigations acid was added to the solutions to suppress the hydrolysis of the ferric ion.

The present investigation is chiefly concerned with the decomposition of hydrogen peroxide solutions at pH 2.94 and temperature 20°C catalysed by  $1.3 \times 10^{-3}$  M ferric ion which hydrolyses during the reaction. The ferric salts employed were chloride and nitrate.

EXPERIMENTAL

Preparation of Solutions.

The hydrogen peroxide was 86% unstabilised supplied by Laporte, a stock solution of suitable strength being prepared with distilled water.

The  $1.3 \times 10^{-3}$  M ferric chloride solutions were prepared as before, by adding the supercooled melt to distilled water or dilute hydrochloric acid solution if lower pH's were required. For the preparation of ferric nitrate solutions,  $\text{Fe}(\text{NO}_3)_3 \cdot 9\text{H}_2\text{O}$  was employed, but since its melting point is comparatively high at  $50^\circ\text{C}$  it was not possible to supercool it to  $20^\circ\text{C}$ . Sufficient distilled water (determined by trial and error) was therefore added to the melt just to prevent its resolidifying at  $20^\circ\text{C}$  and this solution added to the water in a manner similar to that for the ferric chloride melt to give a  $1.3 \times 10^{-3}$  M ferric nitrate solution. A ferric nitrate solution thus prepared was found to have the same pH as a  $1.3 \times 10^{-3}$  M ferric chloride solution, viz. 2.94.

Reaction Technique.

The reaction mixture was made by immediately adding

the freshly prepared ferric iron solution to a small volume (up to 10 ml.) of the stock hydrogen peroxide solution in a 750 ml. quickfit conical flask which was then stoppered and thermostated at 20°C. 10 ml. samples were withdrawn by pipette at 5 minute intervals, timed with a stopwatch, and run into conical flasks containing 5 ml. of 3N sulphuric acid to stop the reaction. This was done in such a manner that the pipette was half empty when the stopwatch hand passed the 5 minute mark.

The hydrogen peroxide contents were determined by titration with standard potassium permanganate solution, a 10 ml. burette, smallest subdivision 0.02 ml., being used. In cases where the titration was greater than 10 ml., the burette was refilled rather than use a larger size. On the basis of the titration results the concentration of non-decomposed hydrogen peroxide at the various times was calculated. The  $3.9 \times 10^{-3}$  M chloride ion in the ferric chloride solutions did not interfere with the titration.

As far as possible, all work was carried out in the darkroom illuminated by the Kodak OB safelights.

#### THEORY

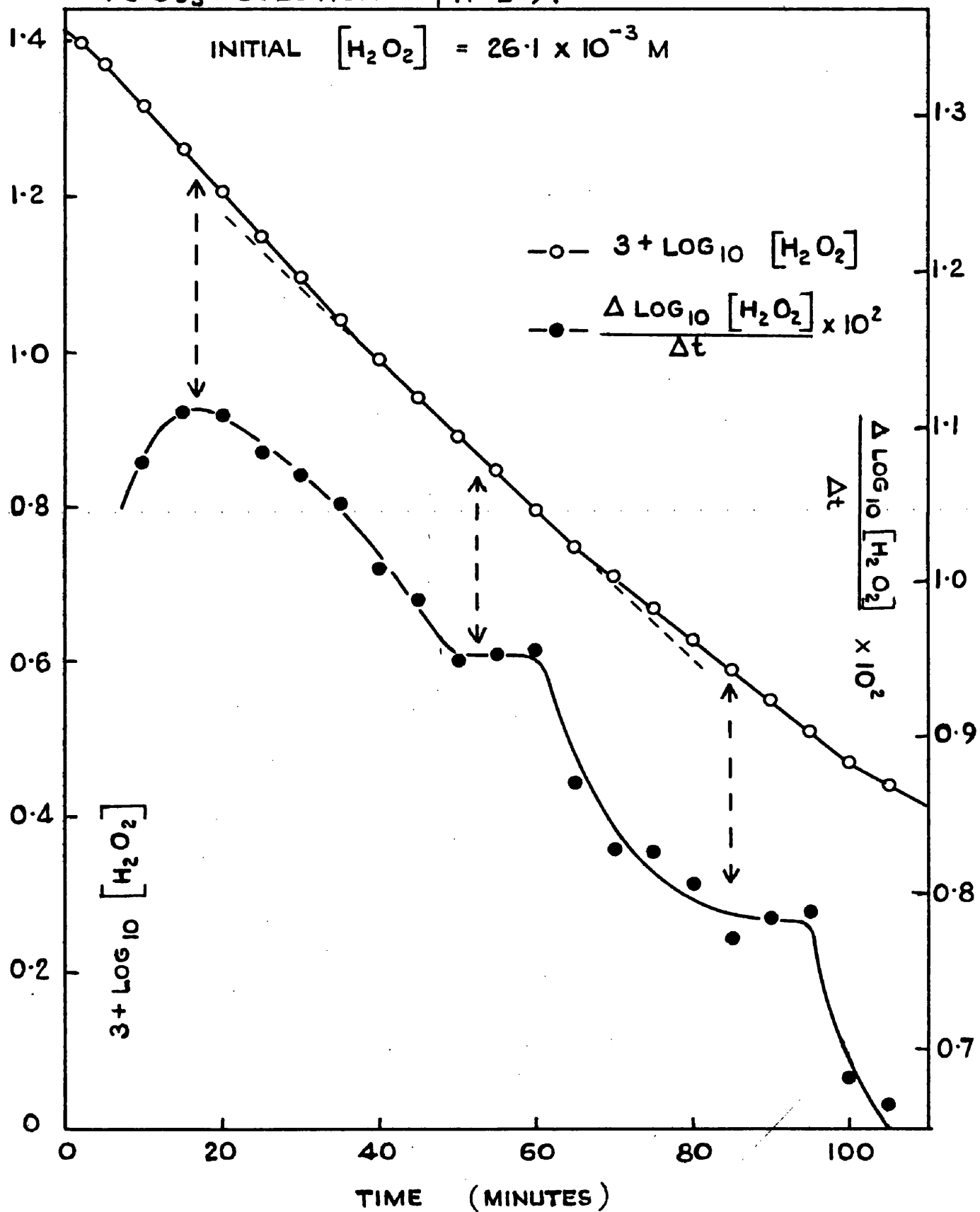
A first order reaction can be expressed by the equation

$$\frac{kt}{2.303} = \log_{10} a - \log_{10} x$$

where k is the rate constant, a is the initial concentration of reactant and x the concentration after time t. The rate constant may be determined by plotting  $\frac{kt}{2.303}$  against  $\log_{10} x$ , when  $\frac{k}{2.303}$  is the gradient of the line so obtained.

**FIG. 38**

DECOMPOSITION OF  $\text{H}_2\text{O}_2$  IN 0.0013 M  
 $\text{FeCl}_3$  SOLUTIONS pH 2.94



RESULTS

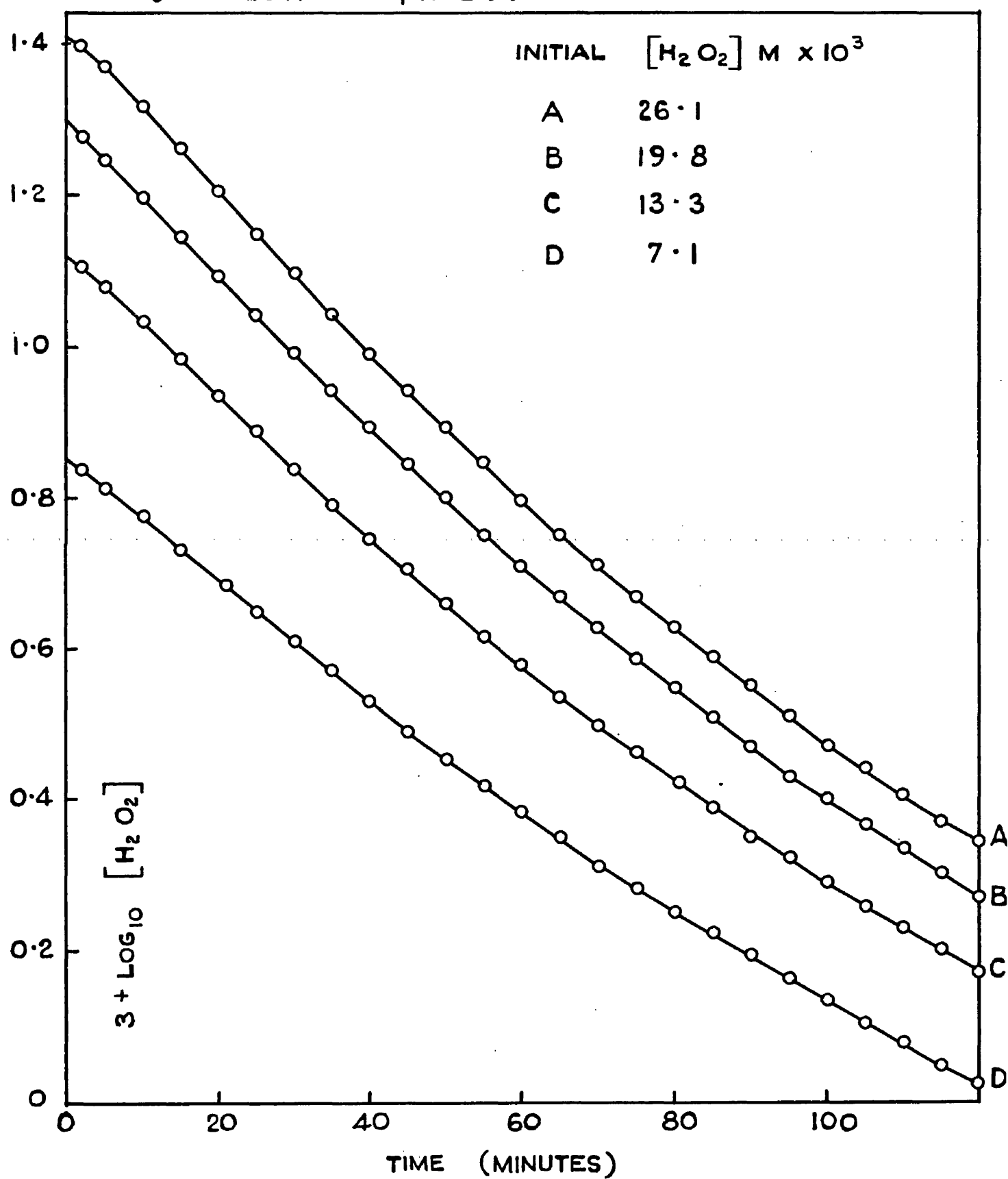
(1) Ferric Chloride Catalysis.

The decomposition of hydrogen peroxide catalysed by  $1.3 \times 10^{-3}$  M ferric chloride at  $20^\circ\text{C}$  and pH 2.94 was investigated at four different initial hydrogen peroxide concentrations. When, in the first case, for a peroxide concentration of  $26.1 \times 10^{-3}$  M,  $\log_{10}[\text{H}_2\text{O}_2]$  was plotted against time, the graph appeared to fall into three fairly distinct straight sections as shown in Fig. 38. In order to verify this, gradients at five minute intervals along the plot  $\log_{10}[\text{H}_2\text{O}_2]$  against time were calculated from the experimental results by subtracting from each value of  $\log_{10}[\text{H}_2\text{O}_2]$  the one ten minutes after it to give an average gradient at the point between the two. This procedure will be clear from the figures in the following table.

Time	$3 + \log_{10}[\text{H}_2\text{O}_2]$	$\log_{10}[\text{H}_2\text{O}_2]_1$ - $\log_{10}[\text{H}_2\text{O}_2]_2$	$\frac{\Delta \log_{10}[\text{H}_2\text{O}_2]}{\Delta t} \times 10^3$
....	.....	.....	.....
25	1.1501	0.1086	10.86
30	1.0969	0.1071	10.71
35	1.0430	0.1052	10.52
40	0.9917	0.1010	10.10
45	0.9420	0.0990	9.90
....	.....	.....	.....

**FIG. 39**

DECOMPOSITION OF  $\text{H}_2\text{O}_2$  IN 0.0013 M.  
 $\text{FeCl}_3$  SOLUTIONS pH 2.94



Gradients were calculated in this manner rather than by subtracting successive values in order to give a greater degree of smoothing. The plot of  $\frac{\Delta \log_{10} [H_2O_2]}{\Delta t}$  against time (hereafter referred to as the gradient plot) is also shown in Fig. 38 from which it is seen that the sections in the  $\log_{10} [H_2O_2]$  plot correspond with the inflexions in the gradient plot. The scatter of the points in the gradient plot is due to the experimental error being of a magnitude almost comparable to the small differences in the  $\Delta \log_{10} [H_2O_2]$  values. Results for times above 100 minutes are ignored since the titrations fell below 2 ml. at this point, and the error (max. 0.04 ml.) became significant. This phenomenon was observed at the other three peroxide concentrations for which the gradient plots were found to be similar to that shown in Fig. 38. The  $\log_{10} [H_2O_2]$  plots for the four concentrations are shown in Fig. 39.

The values of the rate constant  $k_r$ , calculated from the gradient of the initial straight section of each  $\log_{10} [H_2O_2]$  plot, are given in Table 19.

**FIG. 40**

DECOMPOSITION OF  $\text{H}_2\text{O}_2$  IN 0.0013 M  
 $\text{FeCl}_3$  SOLUTIONS pH 2.53

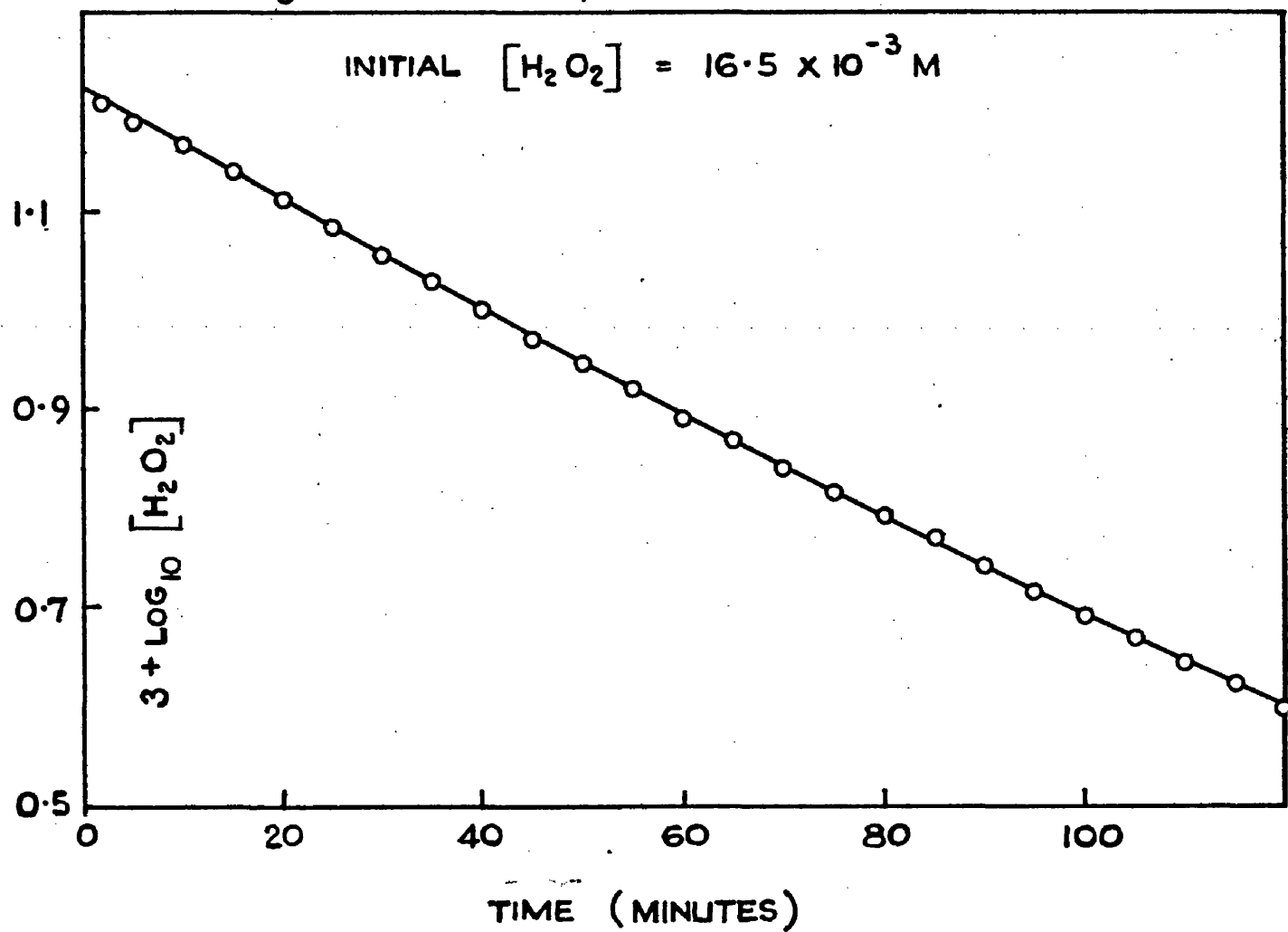


TABLE 19

Initial [H <sub>2</sub> O <sub>2</sub> ] M x 10 <sup>3</sup>	k x 10 <sup>3</sup> litre mole <sup>-1</sup> min. <sup>-1</sup>
26.1	4.82
19.8	4.46
13.3	4.31
7.1	3.71

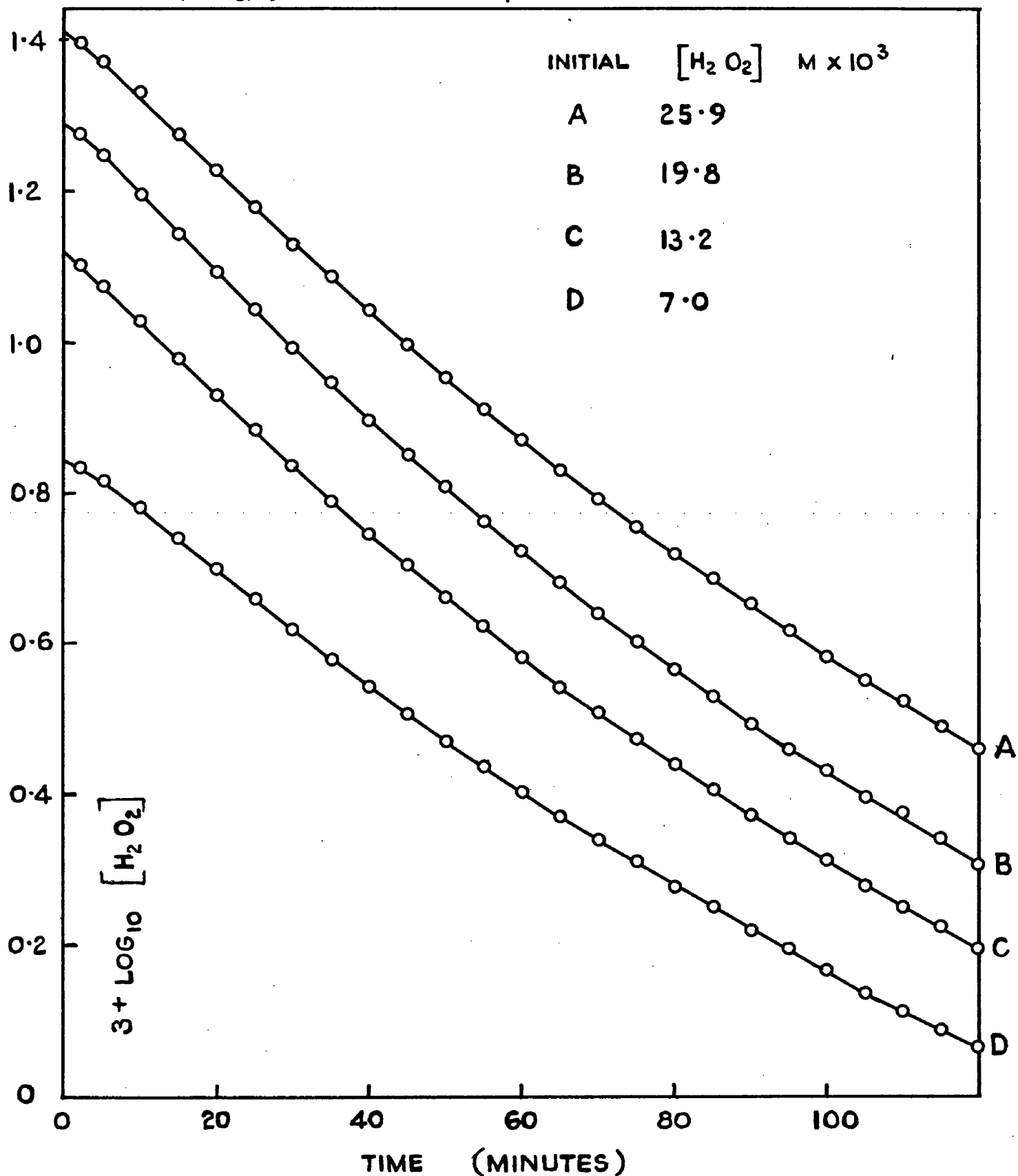
It is seen that the initial rate constant increases slowly with increasing peroxide concentration.

Fig.40 shows the log<sub>10</sub> [H<sub>2</sub>O<sub>2</sub>] plot for the decomposition of  $16.5 \times 10^{-3}$  M hydrogen peroxide catalysed by  $1.3 \times 10^{-3}$  M ferric chloride at pH 2.53. Due to the slower rate of decomposition at this pH it is not possible to observe any definite indication of segmentation, and since the points of the gradient plot (not shown) are rather scattered for the same reason, no conclusion can be drawn. The initial value of the rate constant k is  $2.43 \times 10^{-3}$  litre mole<sup>-1</sup> min.<sup>-1</sup>. It should be noted that no secondary hydrolysis of the iron took place during the reaction.

#### (2). Ferric Nitrate Catalysis.

The decomposition of hydrogen peroxide catalysed by  $1.3 \times 10^{-3}$  M ferric nitrate at 20°C and pH 2.94 was investigated at approximately the same peroxide concentrations

**FIG. 41**  
 DECOMPOSITION OF  $\text{H}_2\text{O}_2$  IN 0.0013 M  
 $\text{Fe}(\text{NO}_3)_3$  SOLUTIONS pH 2.94



as for the ferric chloride. The  $\log_{10} [H_2O_2]$  plots are shown in Fig.41, the gradient plots being similar to that for ferric chloride shown in Fig.38, are not shown. The initial rate constants are listed in Table 20.

TABLE 20

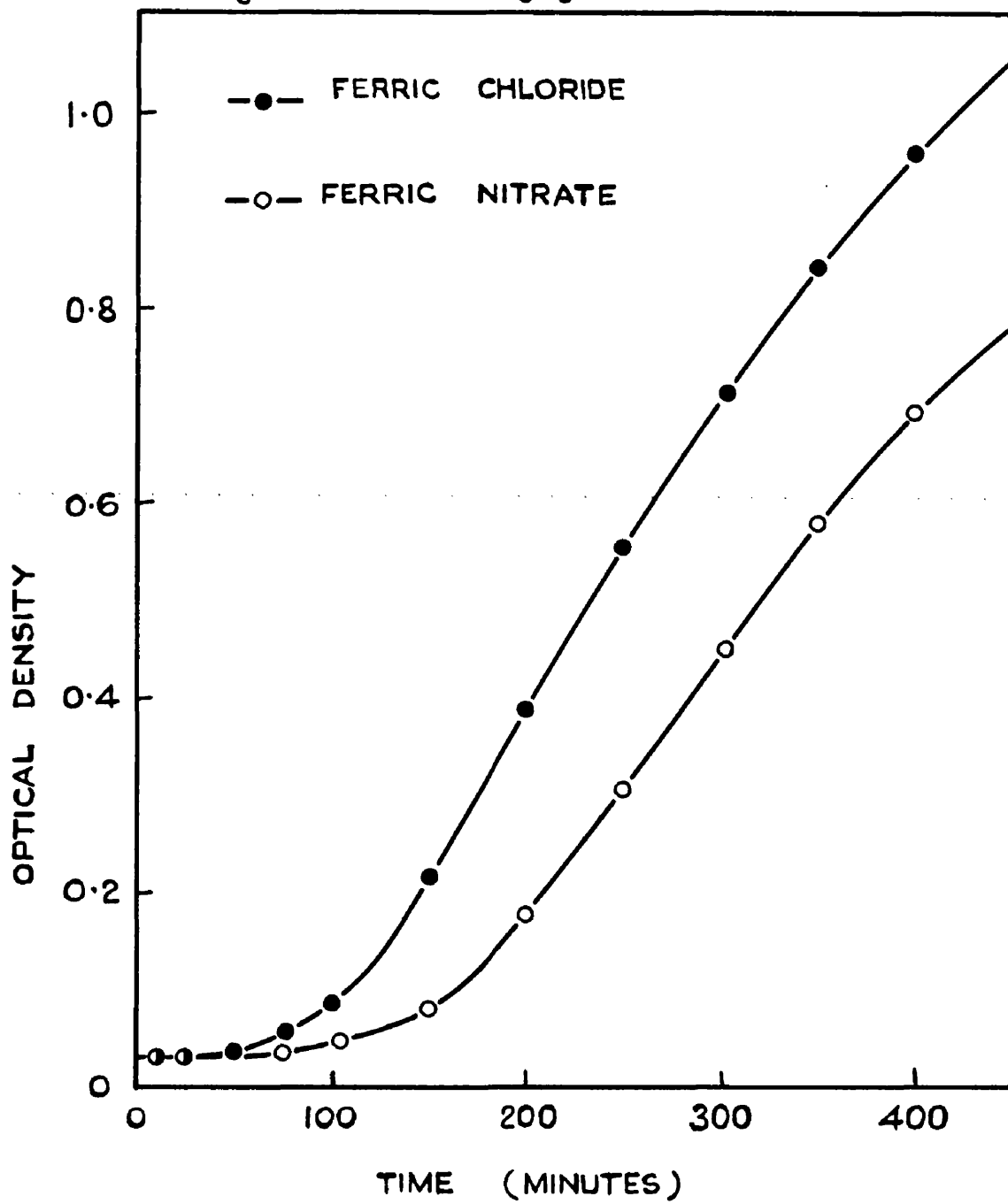
Initial $[H_2O_2] M \times 10^3$	$k \times 10^3$ litre mole $^{-1}$ min. $^{-1}$
25.9	4.19*
19.8	4.43
13.2	4.31
7.0	3.55

\* This result appears to be out of place, but it is not considered important.

It can be seen that while the results are of the same magnitude as those for the ferric chloride, the sections in the  $\log_{10} [H_2O_2]$  plot are not quite so well defined although there seems to be no doubt that they do exist.

Finally, the hydrolysis curves for  $1.3 \times 10^{-3} M$  ferric chloride and ferric nitrate are shown in Fig.42, the ferric nitrate hydrolysing somewhat more slowly than the ferric chloride.

**FIG. 42**  
THE DARK HYDROLYSIS OF 0.0013 M  
 $\text{FeCl}_3$  AND  $\text{Fe}(\text{NO}_3)_3$  SOLUTIONS



## DISCUSSION

Under the conditions of the present investigation, the decomposition of hydrogen peroxide has been shown to take place in a sequence of first order steps of decreasing rates. Since the molar ratio of  $[H_2O_2] / [Fe^{3+}]$  did not fall below unity, even at the end of the first 100 minutes of the reaction, a first order decomposition is in agreement with the results of Barb *et al.*<sup>32</sup>

The gradient plot in Fig.38 indicates that there is an induction period in the first ten minutes of the decomposition during which the rate increases to its maximum value. This might possibly be attributed to the breaking down of complexes formed by the hydrogen peroxide with the ferric ion.

Comparison of Figs.39 and 41 shows that the hydrogen peroxide decomposes slightly faster in solutions of ferric chloride than in those of ferric nitrate. Therefore, since Fig.42 shows that the solutions of ferric chloride hydrolyse faster than those of ferric nitrate, it is suggested that the segmentation of the  $\log_{10} [H_2O_2]$  plot might be due in some way to the changing nature of the catalyst as a result of hydrolysis.

This segmentation in the plot of  $\log_{10}[\text{H}_2\text{O}_2]$  against time was previously observed by Good<sup>114</sup> working with similar concentrations of ferric chloride solution.

---

BIBLIOGRAPHY.

1. Taylor, Trans. Faraday Soc., 1925, 21, 560.
2. Steacie, "Atomic and Free Radical Reactions", Reinhold Publishing Corporation, New York, 2nd. Edition, 1954.
3. Waters, "The Chemistry of Free Radicals", Oxford University Press, London, 1948.
4. Uri, Chem. Rev., 1952, 50, 375.
5. Chemical Society Special Publication No. 9, 1957.
6. Semenov, "Some Problems in Chemical Kinetics and Reactivity", Princeton University Press, New Jersey, 1958.
7. Bonhoeffer and Haber, Z.physik. Chem., 1928, A137, 263.
8. Farkas, Goldfinger and Haber, Naturwiss., 1929, 17, 674.
9. Haber, Naturwiss., 1931, 19, 450.
10. Bonhoeffer and Reichhardt, Z.physik.Chem., 1928, A139, 75.
11. Urey, Dawsey and Rice, J. Amer. Chem. Soc., 1929, 51, 1371.
12. Oldenberg, J. Chem. Physics, 1935, 3, 266.
13. Oldenberg and Reike, ibid., 1938, 6, 169, 439.  
ibid., 1939, 7, 487.
14. Bates, ibid., 1933, 1, 457.  
Hinshelwood and Williamson, "The Reaction between Hydrogen and Oxygen", Oxford, 1934.
15. Weiss, Trans. Faraday Soc., 1935, 31, 668.
15. Bates and Salley, J. Amer. Chem. Soc., 1933, 55, 110.

16. Hinshelwood, Proc. Roy. Soc. A, 1946, 188, 1.  
Lewis and von Elbe, J. Chem. Physics, 1942, 10, 366.
17. Geib and Harteck, Ber., 1932, 65, 1551.
18. Bodenstein and Schenk, Z. physik. Chem., 1933, B20, 420.
19. Farkas and Sachsse, ibid., 1934, B27, 111.
20. Minkoff, Faraday Soc. Discussions, 1947, 2, 151.
21. Gray, Trans. Faraday Soc., 1959, 55, 408.
22. Helms and Klemm, Z. anorg. Chem., 1939, 241, 97.
23. Kassatochkin, Compt. rend. Acad. Sci. U.R.S.S.,  
1945, 47, 193.
24. Kassatochkin and Kotov, J. Chem. Physics, 1936, 4, 458.
25. Haber and Weiss, Proc. Roy. Soc. A, 1934, 147, 332.
26. Weiss, Trans. Faraday Soc., 1935, 31, 668.
27. Evans, Hush and Uri, Quart. Rev., 1952, 6, 186.
28. Bray and Gorin, J. Amer. Chem. Soc., 1932, 54, 2124.
29. Medalia and Kolthoff, J. Polymer Sci., 1949, 4, 377.
30. Uri, Faraday Soc. Discussions, 1950, 8, 207.
31. Barb, Baxendale, George and Hargrave,  
Trans. Faraday Soc., 1951, 47, 462.
32. idem, ibid., p. 591.
33. George, Faraday Soc. Discussions, 1947, 2, 196.
34. Agar and Dainton, ibid., 1947, 2, 218.

35. Barb, Baxendale, George and Hargrave,  
Nature, 1949, 163, 692.
36. Weiss and Humphrey, ibid., 1949, 163, 691.
37. Andersen, Acta Chem. Scand., 1948, 2, 1.
38. Christiansen and Andersen, ibid., 1950, 4, 1538.
39. Weiss, Experientia, 1951, 7, 135.
40. Uri, "L. Farkas Memorial Vol.", Research Council of  
Israel, p. 193.
41. Evans and Uri, Nature, 1950, 166, 602.
42. Cahill and Taube, J. Amer. Chem. Soc., 1952, 74, 2312.
43. Abel, Monatsh., 1956, 87, 375.
44. Koefoed, Acta Chem. Scand., 1955, 9, 283.
45. Jones, Kitching, Tobe and Wynne-Jones,  
Trans. Faraday Soc., 1959, 55, 79.
46. Kremer and Stein, ibid., 1959, 55, 959.
47. Orgel, Quart. Rev., 1954, 8, 422.
48. Franck and Scheibe, Z. physik. Chem., 1928, A139, 22.
49. Franck and Haber, Sitzber. preuss. Akad. Wiss., 1931, 250.
50. Farkas and Farkas, Trans. Faraday Soc., 1938, 34, 1113.
51. Fromherz and Lih, Z. physik. Chem., 1931, A153, 321.  
Doehlmann and Fromherz, ibid., 1934, A171, 353.  
Fromherz and Lih, ibid., 1933, A167, 103.  
Fromherz and Walls, ibid., 1936, A178, 29.

52. Rabinowitch, Rev. Mod. Phys., 1942, 14, 112.
53. Potterill, Walker and Weiss, Proc. Roy. Soc. A,  
1936, 156, 561.
54. Dain and Kachan, Doklady Akad. Nauk., S.S.S.R.  
1948, 61, 471.
55. Dainton and James, Symposium on the Mechanism of  
Electron Transfer Reactions, Paris, 1951.
56. Rabinowitch and Stockmayer,  
J. Amer. Chem. Soc., 1942, 64, 335.
57. Kiss, Abraham and Hegedus, Z. anorg. Chem., 1940, 244, 98.
58. Evans and Uri, Trans. Faraday Soc., 1949, 45, 224.
59. Evans and Uri, J. Soc. Dyers Colourists, 1949, 65, 709.
60. Evans and Uri, Nature, 1949, 164, 404.
61. Evans, Santappa and Uri, J. Polymer Sci., 1951, 7, 243.
62. Dainton and Tordoff, Trans. Faraday Soc., 1957, 53, 666.
63. Draper, Phil. Mag., 1857, 14, 161.
64. Baur, Z. Elektrochem., 1919, 25, 102.
65. Ross, J. Amer. Chem. Soc., 1906, 28, 790.
66. Prasad and Limayl, J. Indian Chem. Soc.,  
1933, 10, 91, 101.
67. Bates, Evans and Uri, Nature, 1950, 166, 869.
68. Bates and Uri, J. Amer. Chem. Soc., 1953, 75, 2754.
69. Baxendale and Magee, Trans. Faraday Soc., 1955, 51, 205.

70. Korsunovskii, Zhur. Fiz. Khim., 1957, 31, 2351.
71. Weiss and Porret, Nature, 1937, 119, 1019.
72. Heidt and Smith, J. Amer. Chem. Soc., 1948, 70, 2476.
73. Evans and Uri, Symposium No. 5, "Carbon Dioxide Fixation and Photosynthesis", Soc. for Experimental Biology, Sheffield, 1950. p. 130.
74. Weiss, ibid., p. 143.
75. Purdon, Ph.D. Thesis, Glasgow, 1956.
76. Lamb and Jacques, J. Amer. Chem. Soc., 1938, 60, 967, 1215.
77. Bray and Hershey, ibid., 1934, 56, 1889.
78. Brosset, Svensk. kem. Tidskr., 1941, 53, 434.
79. Olson and Simonson, J. Chem. Physics, 1949, 17, 348, 1322.
80. Siddall and Vosburgh, J. Amer. Chem. Soc., 1951, 73, 4270.
81. Hedstrom, Arkiv. Kemi., 1953, 6, 1.
82. Biedermann and Sillen, ibid., 1953, 5, 424.
83. Milburn and Vosburgh, J. Amer. Chem. Soc., 1955, 77, 1352.
84. Mulay and Selwood, ibid., 1955, 77, 2693.
85. Olerup, Svensk. kem. Tidskr., 1943, 55, 324.
86. Gamlen and Jordan, J., 1953, 1435.
87. Connick and Tsao, J. Amer. Chem. Soc., 1954, 76, 5311.
88. Connick, Hepler, Hugus, Kury, Latimer and Tsao, ibid., 1956, 78, 1827.

89. Milburn, ibid., 1957, 79, 537.
90. Perrin, J. 1959, 1710.
91. Brosset, Naturwiss., 1941, 29, 455.
92. Brosset, Diss., Stockholm, 1942.
93. Arden, J., 1951, 350.
94. Badoz-Lambling, Bull. Soc. Chim. France, 1950, 552.
95. Lindstrand, Diss., Lund, 1939.
96. Lister and Rivington, Canad. J. Chem., 1955, 33, 1603.
97. Glickman, Dain and Kutsaya, Zhur. Fiz. Chim.,  
1948, 22, 906.
98. Sutton, Nature, 1952, 169, 71.
99. Hersch, ibid., 1952, 169, 792.  
(to Mond Nickel Co., Ltd.) Brit. Pat. No.707,323.
100. Pamphlet entitled "Baker-Hersch Dissolved Oxygen Meter",  
issued by the Baker Platinum Division, Engelhard  
Industries, Ltd., England.
101. Kaye and Laby, "Tables of Physical and Chemical  
Constants", Longmans, Green & Co., 11th. Edn., p. 137.
102. v. Stackelberg and v. Freyhold, Z. Elektrochem.,  
1940, 46, 120.
103. Heyrovsky, "Polarographie", Springer, Vienna, 1941, p.106
104. West and Dean, Ind. Eng. Chem. Anal. Ed.,  
1945, 17, 686.

105. Tian, Compt. rend., 1913, 156, 1063.  
Granath, Phys. Review, 1929, 34, 1046.  
Goodeve and Stein, Trans. Faraday Soc., 1931, 27, 193.
  106. Lewis, J. Chem. Educ., 1958, 35, 87.
  107. Parker, Proc. Roy. Soc. A, 1953, 220, 104.
  108. Hatchard and Parker, ibid., 1956, 235, 518.
  109. Mellor, 'A Comprehensive Treatise on Inorganic and Theoretical Chemistry', Vol. XIX, Longmans, Green & Co., N.Y., 1935, pp. 59 - 65.
  110. Moore, Phys. Review, 1901, 12, 163.
  111. Bhatnager, Zeit. Phys., 1929, 56, 692.
  112. Zocher and Heller, Z. anorg. Chem., 1930, 186, 75.
  113. Heller, Compt. rend., 1934, 199, 723.
  114. Good, Unpublished Work, Glasgow, 1953.
-